SUPPLEMENTARY DATA

Cognitive Impairment after Aneurysmal Subarachnoid Hemorrhage: Temporal Patterns and Electrophysiological Risk Stratification

Kun Yang, Peng Liu, Oxana Semyachkina-Glushkovskaya, Mingchang Li, Yuxiang Yan, Hongqi Zhang

SUPPLEMENTARY DATA

Cognitive Impairment after Aneurysmal Subarachnoid Hemorrhage: Temporal Patterns and Electrophysiological Risk Stratification

Contents

Supplementary. Details of Materials and Methods

Study design and population

This secondary analysis used data from a single-center prospective cohort [1]. The parent study was registered in the Chinese Clinical Trial Registry (ChiCTR1900028096). It enrolled adults aged 18–80 years with aSAH or UIA who were admitted to Xuanwu Hospital between November 2019 and November 2021. aSAH was confirmed by head computed tomography (CT) or lumbar puncture, and aneurysms were confirmed by digital subtraction angiography. Patients with UIA had no previous neurological disease and served as controls without aneurysm rupture. Written informed consent was obtained from all participants, and the ethics committee of Xuanwu Hospital approved both the parent study and this secondary analysis.

At baseline in-hospital, we recorded demographic details, aneurysm location and laterality, clinical severity scores (Hunt–Hess, modified Fisher), the discharge modified Rankin Scale (mRS) score, and markers of early brain injury when available. All aneurysm repair procedures, including surgical clipping and endovascular treatment, were performed under general anesthesia. Because anesthetic exposure may influence perioperative cognition, the use of a uniform anesthetic modality across UIA and aSAH minimized confounding in between-group comparisons. A standardized neuropsychological battery (Auditory Verbal Learning Test [AVLT], Boston Naming Test [BNT], Clock Drawing Test [CDT], Mini-Mental State Examination [MMSE]) was administered during hospitalization. Ancillary testing included structural and resting-state MRI, ERP, and plasma and CSF biomarkers within 2 weeks of admission when feasible.

Outcome definitions

Cognitive status was reassessed once between 7 and 24 months after hospital discharge (mean, 18.1 months) by trained neuropsychologists using the Montreal Cognitive Assessment (MoCA). Consistent with normative recommendations, one point was added for participants with ≤12 years of education. The primary cognitive endpoint was first-detected CI during follow-up, defined a priori as an education-adjusted MoCA score <26 at the 7–24-month follow-up assessment. Because cognition was assessed once after discharge, this endpoint represents follow-up detection rather than the exact biological onset of cognitive impairment. Accordingly, our primary survival analyses were conducted with interval-censored methods. Participants without CI at follow-up were considered right-censored observations in Cox/Kaplan–Meier analyses. Secondary outcomes included baseline domain-specific cognitive scores, which were used as candidate predictors, and exploratory analyses of domain changes from baseline to follow-up.

Predictor variables and missing-data patterns

Candidate predictors comprised sociodemographic variables (age, sex, education), aneurysm location and laterality, clinical severity (Hunt–Hess, modified Fisher, discharge mRS, World Federation of Neurological Surgeons [WFNS] grade), baseline neuropsychological scores, and multimodal biomarkers (MRI metrics, ERP features, plasma and CSF Aβ/tau concentrations). Not all participants underwent all ancillary tests; the approximate availability was n=87 for MRI, n=170 for ERP, n=92 for plasma biomarkers, and n=47 for CSF biomarkers. We enumerated the observed missing-data patterns and defined pattern-specific sub-cohorts. Patterns with <10 events were excluded a priori. For each retained pattern, we report sample size, number of events, the candidate predictor set, and the events-per-parameter ratio.

Statistical analysis

Statistical analysis for pragmatic multimodal prediction modeling

Prediction modeling was performed in the aSAH subgroup only. The analytic objective was to predict whether a patient would be classified as having cognitive impairment at follow-up using baseline or early-available predictors obtained during the index hospitalization. The prediction pipeline was designed as an aSAH-only, resource-aware, binary prediction framework. It used prespecified predictor schemes to reflect different levels of real-world data availability. The primary binary prediction framework had four main steps. First, six resource-stratified predictor schemes were specified. Second, one scheme-level strategy was retained after structured screening. Third, the aSAH cohort was used for model development with bootstrap optimism correction. Fourth, temporal internal validation was reserved as a secondary same-center drift assessment.

After restriction to the aSAH cohort and exclusion of records with missing follow-up cognitive status, 125 patients were available for binary prediction modeling. The binary outcome indicated follow-up-detected CI under the primary definition of education-adjusted MoCA <26. In the analysis dataset, the variable censor was coded as 1 for follow-up-detected CI and 0 for no CI, yielding 67 events and 58 non-events (event rate, 0.536). A temporal split indicator (test) was available and used for secondary temporal internal validation.

Prespecified predictor schemes

Six predictor schemes were defined a priori to reflect progressively richer data environments:
Scheme A, core clinical variables only;
Scheme B, core clinical variables plus baseline cognitive measures;
Scheme C, core clinical variables plus plasma biomarkers;
Scheme D, core clinical variables plus ERP-derived features;
Scheme E, core clinical variables plus MRI-derived features; and
Scheme F, core clinical variables plus CSF biomarkers. The core clinical pool consisted of early available variables, namely age, sex, years of education, Hunt–Hess grade, Fisher grade, aneurysm location, side, admission mRS, and admission WFNS. Candidate cognitive, blood, ERP, MRI, and CSF variables were grouped into separate blocks and were only used within the corresponding scheme.

For the scheme-based modeling stage, the full 13 × 7 selector–learner grid was implemented within each prespecified scheme. This stage was designed as structured screening to compare candidate feature-selection and learning strategies under each data-availability scenario. The seven supervised learners were logistic regression, naive Bayes, neural network, random forest, support vector machine, XGBoost, and ridge regression. The 13 feature-selection techniques were LASSO, elastic net, RFE, PCA, Boruta, mutual information, Pearson correlation, Spearman correlation, Kendall rank correlation, ANOVA F-test, variance thresholding, forward selection, and no feature selection. For each selector–learner combination, out-of-fold predicted probabilities were generated using cross-validation within the scheme-specific cohort. After screening, a retained scheme-level strategy was frozen and used for bootstrap optimism correction, gate-based assessment, and temporal internal validation. No further selector–learner reselection was conducted in the temporal internal validation cohort.

SUPPLEMENTARY DATA

Missing-data handling

Missing data were handled within each scheme rather than across the entire multimodal dataset. This approach allowed imputation to address item-level missingness among measured predictors. It also preserved true differences in modality availability. For the primary analysis, missing values were imputed using a scheme-specific simple imputation strategy: continuous variables were replaced by the median of the corresponding scheme cohort, and categorical variables were replaced by the mode. Predictors with all values missing, zero variance, or residual unresolved missingness after imputation were excluded from the modeling matrix. This approach was applied separately within each scheme and, for temporal validation, the imputation map was derived in the development subset and then applied unchanged to the temporal subset.

A sensitivity-analysis framework for multiple imputation was also implemented. Multiple imputed datasets were generated within each scheme using an iterative chained-equation style algorithm (Iterative Imputer) with posterior sampling. Continuous values were modeled using Bayesian ridge regression. Categorical variables were rounded back to the nearest observed category. Each imputed dataset was modeled separately, and the resulting predicted probabilities were averaged across imputations. This sensitivity analysis was intended to assess the robustness of model performance to the primary simple-imputation strategy. Structural non-availability of a modality, such as the absence of MRI, ERP, or CSF acquisition, was not imputed across schemes.

Model fitting

For each fixed feature panel, model fitting used internal hyperparameter tuning by stratified K-fold cross-validation. The number of folds was adapted to the smallest class size to avoid invalid partitions. Class imbalance was accommodated by balanced class weights or, where applicable, a scheme-specific scale_pos_weight defined as the ratio of non-events to events. Logistic regression was fit with L2 penalization using the liblinear solver. Neural networks were fit as multilayer perceptrons with standardized inputs and a small grid over hidden-layer size and L2 regularization. Random forest, support vector machine, XGBoost, and ridge classifier were available in the broader scheme-level pipeline. All models were implemented in Python using scikit-learn, xgboost, numpy, pandas, statsmodels, and pyreadstat.

For a binary learner with predictors X_i, the target $Y_i \in \{0,1\}$denoted follow-up cognitive impairment status. For logistic-type models, the linear predictor can be written as

$$\text{logit}\{P(Y_i = 1 \mid X_i)\} = \beta_0 + \sum_{j=1}^{p} \beta_j X_{ij}.$$

The retained predictors differed by scheme and scenario model, but the evaluation framework was uniform across all models. For multiple imputation sensitivity analyses, if $m$imputed datasets were fit, the pooled predicted probability for participant $i$was

$$\bar{p}_i = \frac{1}{m}\sum_{k=1}^{m} p_i^{(k)}.$$

Performance evaluation

Model discrimination was quantified using the area under the receiver-operating-characteristic curve (AUROC) and the area under the precision–recall curve (AUPRC). Overall accuracy of probabilistic predictions was summarized using the Brier score

$$\text{Brier} = \frac{1}{n}\sum_{i=1}^{n}(p_i - y_i)^2.$$

Apparent performance was first estimated on the scheme cohort used for model development. To account for overfitting in the primary analysis, performance was then corrected using bootstrap optimism correction. Specifically, for each bootstrap replicate $b = 1, \ldots, B$, a bootstrap sample was drawn from the development data, the full fixed strategy was refit in that bootstrap sample, and performance was evaluated both in the bootstrap sample and in the original sample. The optimism for metric $M$was defined as

$$\text{Optimism}_b(M) = M_{b,\text{boot}} - M_{b,\text{orig}},$$

and the optimism-corrected estimate was

$$M_{\text{corrected}} = M_{\text{apparent}} - \frac{1}{B}\sum_{b=1}^{B}\text{Optimism}_b\,(M).$$

This procedure was applied to AUROC, AUPRC, Brier score, and calibration slope. The number of bootstrap replicates was set to 200 in the current implementation. Separate bootstrap percentile confidence intervals were obtained for AUROC, AUPRC, and Brier score, generally using 1000 replicates. Calibration was assessed numerically using a logistic recalibration model in which the observed outcome was regressed on the logit of the predicted probability:

$$\text{logit}\{P(Y_i = 1)\} = \alpha + \beta\,\text{logit}(p_i).$$

The intercept αrepresents calibration-in-the-large and the slope βrepresents the calibration slope, with $\beta = 1$indicating ideal spread of predictions. Graphical calibration curves were generated using quantile-based binning of predicted risks.

Clinical utility was evaluated by decision curve analysis. For a threshold probability p_t, net benefit was calculated as

$$\text{NB}(p_t) = \frac{\text{TP}}{n} - \frac{\text{FP}}{n} \times \frac{p_t}{1 - p_t},$$

and was compared with the default strategies of treating all patients and treating none. Threshold-based diagnostic summaries were additionally reported at prespecified thresholds of 0.10, 0.15, 0.20, and 0.25, including sensitivity, specificity, positive predictive value, negative predictive value, accuracy, F1 score, and the proportion classified as high risk.

Benchmarking and model selection

Three clinically interpretable benchmark models were specified: a core clinical logistic model, a severity-only logistic model, and a baseline cognition-only logistic model. Benchmark models were evaluated using the same discrimination, Brier score, and bootstrap optimism-correction framework as the scheme-derived models. The final main-text scenario model was selected from the four pragmatic models according to optimism-corrected performance, prioritizing higher AUROC and AUPRC and lower Brier score.

Temporal internal validation

Temporal internal validation was treated as a secondary analysis. When a temporal split indicator was available, the scheme cohort was partitioned into a development subset (test = 1) and a later temporal subset (test = 2). The final fixed strategy determined in the main analysis was then refit in the development subset only, using the same selector, hyperparameters, and feature definitions, and evaluated in the temporal subset without further model reselection. Temporal validation metrics included AUROC, AUPRC, Brier score, and calibration slope, with bootstrap confidence intervals for AUROC.

Feature importance and visualization

For the final selected main model, feature importance was summarized using **permutation importance** based on mean AUROC decrease after repeated permutation of each predictor. The resulting ranking was visualized as a horizontal bar plot of mean AUROC drop. The final reporting package comprised a scheme-comparison figure, ROC curves for the four pragmatic scenario models, a pairwise AUROC comparison heatmap, calibration and decision-curve plots for the final model, a feature-importance figure, and accompanying performance tables.

Gate-based model selection framework

To ensure robustness beyond apparent performance, final model selection was performed using a prespecified multi-criterion gate framework integrating calibration, internal validation, and temporal validation.

1 Notation

Let:

- M_{dev}: performance in development (training) cohort
- M_{int}: performance in internal validation cohort
- M_{temp}: performance in temporal internal validation cohort

For discrimination:

$$\mathrm{AUC}_{\mathrm{dev}}, \mathrm{AUC}_{\mathrm{int}}, \mathrm{AUC}_{\mathrm{temp}}$$

For calibration:

$$\gamma_{\mathrm{boot}}$$

denotes the optimism-corrected calibration slope obtained from bootstrap resampling.

2 Gate 1: Calibration stability (primary gate)

Calibration was assessed using logistic recalibration:

$$\mathrm{logit}\{\Pr(Y = 1)\} = \alpha + \gamma \cdot \mathrm{logit}(\hat{p})$$

where:

- γ: calibration slope
- γ_{boot}: optimism-corrected slope

A model was considered to have acceptable calibration if:

$$\gamma_{\mathrm{boot}} \in [0.8,1.2]$$

Models with:

- $\gamma_{\mathrm{boot}} > 1.2$: underfitting (predictions too conservative)
- $\gamma_{\mathrm{boot}} < 0.8$: overfitting (predictions too extreme)

were excluded.

3 Gate 2: Internal validation discrimination and stability

Discrimination was evaluated using AUROC in the internal validation cohort.

Two conditions were required:

(1) Minimum discrimination:

$$\mathrm{AUC}_{\mathrm{int}} \geq 0.70$$

(2) Limited optimism (development → internal drop):

$$\Delta_{\mathrm{int}} = \mathrm{AUC}_{\mathrm{dev}} - \mathrm{AUC}_{\mathrm{int}} \leq 0.10$$

Models exceeding this drop were considered unstable and excluded.

4 Gate 3: Temporal validation robustness
Temporal internal validation was used as a same-center drift assessment rather than as evidence of external transportability.
Two conditions were required:
(1) Minimum temporal discrimination:

$$\mathrm{AUC}_{\mathrm{temp}} \geq 0.70$$

(2) Limited temporal performance drop:

$$\Delta_{\mathrm{temp}} = \mathrm{AUC}_{\mathrm{dev}} - \mathrm{AUC}_{\mathrm{temp}} \leq 0.10$$

S6.5 Final model selection rule
A candidate model was retained only if all three gates were satisfied:

$$\mathrm{PASS} = \begin{cases} 1, & \text{if Gate 1 \& Gate 2 \& Gate 3 satisfied} \\ 0, & \text{otherwise} \end{cases}$$

Among all candidate models:
- Models failing any gate were excluded
- If multiple models passed all gates, the model with the highest $\mathrm{AUC}_{\mathrm{temp}}$ was selected
- If no model passed all gates, no model was locked at the scheme level, and downstream derivation was performed

Pattern-submodel survival sensitivity analysis
The pattern-submodel survival analysis was conducted as a separate exploratory sensitivity analysis to examine whether the prognostic signals observed in the primary binary prediction framework were qualitatively consistent when time-to-detection information and observed modality-availability patterns were considered. This analysis was separate from the primary binary model-selection framework and did not contribute to ERP CP2 model selection or external validation. The primary model-selection framework remained the aSAH-only binary prediction analysis with bootstrap optimism correction and same-center temporal internal validation.

To develop prognostic models in the context of real-world missingness, we adopted the pattern submodel (PS) approach [2] as sensitive analysis. This approach has been proposed for prediction settings with structured missingness and may be useful when modality availability is informative [3]. In this study, the framework served as a sensitivity analysis rather than the primary model-selection strategy.

For each subcohort, we employed multiple algorithms. These included Cox proportional hazards models, LASSO-penalized Cox models, random survival forests, survival XGBoost, survival support-vector machines, and DeepSurv. Continuous predictors were standardized, and categorical variables were one-hot encoded. To avoid information leakage, only baseline measurements were permitted as predictors.

Hyperparameters were optimized using inner five-fold stratified cross-validation and grid or random searching. Model discrimination was quantified by calculating the Harrell's C-index and time-dependent area under the curve (AUC), which captures the local discriminative ability of baseline markers over time [4]. Model calibration was assessed via Brier scores and optimism-corrected calibration curves at 12 and 18 months; both the calibration slope and intercept were reported. When the calibration slope was <1, we applied uniform shrinkage to final coefficients.

SUPPLEMENTARY DATA

To evaluate clinical utility, we calculated net benefit across a range of threshold probabilities through decision curve analysis (DCA) [5]. Net benefit incorporates the trade-off between true positives and false positives, allowing comparison with default strategies of treating all or no patients. We applied bootstrap cross-validation to correct for overfitting and extended DCA to censored data following the methodology described by Vickers et al [6].

Analyses were conducted in R (version 4.3.2) using the *survival, riskRegression, pec, rms,* and *randomForestSRC* packages, and in Python (version 3.9) with *scikit-survival, xgboost, scikit-learn*, and *torch*. This study adhered to the STROBE guidelines for cohort studies [7] as well as the TRIPOD AI [8] statements for prediction model development and validation. A completed checklist is provided in the supplementary material.

References

[1] Liu P, Li R, Zhang T, Xu Y, Yang K, Li Y, et al. (2025). Multimodal assessment predicts cognitive impairment after aneurysmal subarachnoid hemorrhage: a prospective cohort study. Int J Surg, 111:1977-1987.

[2] Fletcher Mercaldo S, Blume JD (2020). Missing data and prediction: the pattern submodel. Biostatistics, 21:236-252.

[3] Sisk R, Sperrin M, Peek N, van Smeden M, Martin GP (2023). Imputation and missing indicators for handling missing data in the development and deployment of clinical prediction models: A simulation study. Stat Methods Med Res, 32:1461-1477.

[4] Bansal A, Heagerty PJ (2019). A comparison of landmark methods and time-dependent ROC methods to evaluate the time-varying performance of prognostic markers for survival outcomes. Diagn Progn Res, 3:14.

[5] Vickers AJ, van Calster B, Steyerberg EW (2019). A simple, step-by-step guide to interpreting decision curve analysis. Diagnostic and Prognostic Research, 3:18

[6] Vickers AJ, Cronin AM, Elkin EB, Gonen M (2008). Extensions to decision curve analysis, a novel method for evaluating diagnostic tests, prediction models and molecular markers. BMC Medical Informatics and Decision Making, 8:53.

[7] Von Elm E, Altman DG, Egger M, Pocock SJ, Gøtzsche PC, Vandenbroucke JP (2007). The Strengthening the Reporting of Observational Studies in Epidemiology (STROBE) statement: guidelines for reporting observational studies. Lancet, 370:1453-1457.

[8] Collins GS, Moons KGM, Dhiman P, Riley RD, Beam AL, Van Calster B, et al. (2024). TRIPOD+AI statement: updated guidance for reporting clinical prediction models that use regression or machine learning methods. Bmj, 385:e078378.

Supplemental table 1. Multimodal data availability and modality-combination use by groups.

Data setting	Total (N= 214)	UIA (n= 89)	aSAH (n=125)			
			Total	No CI (n=58)	CI (n=67)	P
MRI	87(40.65)	45(50.56)	42(33.6)	22	20	0.3402
ERP	170(79.44)	70(78.65)	100(80)	50	50	0.1065
Plasma	92(42.99)	38(42.7)	54(43.2)	26	28	0.7325
CSF	47(21.96)	0(0)	47(37.6)	24	23	0.417
MRI+ERP	71(33.18)	39(43.82)	32(25.60)	16	16	0.0678
MRI+Plasma	79(36.92)	38(42.70)	41(32.80)	21	20	0.7485

MRI+CSF	34(15.89)	0(0)	34(27.20)	19	15	0.3796
ERP+Plasma	76(35.51)	33(37.08)	43(34.40)	20	23	0.2006
ERP+CSF	39(18.22)	0(0)	39(31.20)	19	20	0.1091
Plasma+CSF	43(20.09)	0(0)	43(34.40)	22	21	0.7011

Cognitive status at follow-up (7–24 months, mean 18.1 months) was classified as No cognitive impairment (No CI) if the Montreal Cognitive Assessment (MoCA) score ≥26 (with +1 point for ≤12 years of education) or Cognitive impairment (CI) if the MoCA score <26. Entries are n (%) unless otherwise indicated.

UIA = unruptured intracranial aneurysm; aSAH = aneurysmal subarachnoid hemorrhage; MRI = magnetic resonance imaging; ERP = event-related potential; CSF = cerebrospinal fluid. MRI/ERP/CSF/plasma biomarkers were acquired within 2 weeks of admission when feasible. Percentages were calculated with the subgroup denominator. *P values for between-group comparisons. Note CSF sampling was only performed in the aSAH group.

SUPPLEMENTARY DATA

Supplemental Table 2 ERP availability, quality-control documentation, and operational burden.

Metric	Value / description
ERP available in total cohort	170/214 (79.4%)
ERP available in UIA	70/89 (78.7%)
ERP available in aSAH	100/125 (80.0%)
ERP available in aSAH CI	50/67 (74.6%)
ERP available in aSAH no CI	50/58 (86.2%)
ERP available in early period	65/75 (86.7%)
ERP available in temporal validation period	35/50 (70.0%)
ERP stimulus protocol	75-dB /ba/ stimulus; 500 ms; ISI 800–1200 ms; 450 trials
Approximate stimulus recording time	6–9 min, excluding preparation
Preprocessing	Average reference, 250 Hz resampling, 0.5–45 Hz filter, ICA ocular artifact correction, visual inspection, −200 to 800 ms epochs, >150 µV rejection, baseline correction

Detailed acquisition failure, retained-epoch distributions, and operator time were not systematically recorded as formal implementation endpoints. Therefore, feasibility metrics are reported descriptively and should not be interpreted as a complete implementation evaluation.

SUPPLEMENTARY DATA

Supplemental Table 3. Core clinical full selector–learner _all 91 candidates screening output.

selector	model	n_selected_features	oof_AUROC	oof_AUPRC	oof_Brier	oof_cal_intercept	oof_cal_slope	feature_stability	selected_features
LASSO	LogisticRegression	6	0.617858981	0.65826822	0.242240051	0.155678122	0.736605491	0.611111111	age, gender, mod_educationyear, H_H, Fisher, WFNS1n
LASSO	NaiveBayes	6	0.58389089	0.646500828	0.269232107	0.060390881	0.266797637	0.611111111	age, gender, mod_educationyear, H_H, Fisher, WFNS1n
LASSO	NeuralNetwork	6	0.544518785	0.597297848	0.319504191	0.10974395	0.054179175	0.611111111	age, gender, mod_educationyear, H_H, Fisher, WFNS1n
LASSO	RandomForest	6	0.569351518	0.582320216	0.25420306	0.090876578	0.325071332	0.611111111	age, gender, mod_educationyear, H_H, Fisher, WFNS1n
LASSO	SVM	6	0.529336078	0.559202317	0.255801058	0.125041854	0.112877284	0.611111111	age, gender, mod_educationyear, H_H, Fisher, WFNS1n
LASSO	XGBoost	6	0.508878024	0.572671095	0.293124856	0.136302164	0.091822364	0.611111111	age, gender, mod_educationyear, H_H, Fisher, WFNS1n
LASSO	RidgeRegression	6	0.601904272	0.653189069	0.239796435	0.070117137	1.2387971	0.611111111	age, gender, mod_educationyear, H_H, Fisher, WFNS1n
ElasticNet	LogisticRegression	6	0.610396294	0.673474283	0.239469729	0.146879027	1.094667214	0.62962963	age, gender, mod_educationyear, H_H, Fisher, WFNS1n
ElasticNet	NaiveBayes	6	0.577714874	0.636047595	0.273811121	0.07991884	0.232835855	0.62962963	age, gender, mod_educationyear, H_H, Fisher, WFNS1n
ElasticNet	NeuralNetwork	6	0.550694802	0.59383217	0.314299682	0.110511417	0.054072039	0.62962963	age, gender, mod_educationyear, H_H, Fisher, WFNS1n
ElasticNet	RandomForest	6	0.564462172	0.578782402	0.255297332	0.10040792	0.303227974	0.62962963	age, gender, mod_educationyear, H_H, Fisher, WFNS1n
ElasticNet	SVM	6	0.530880082	0.555995514	0.2569988	0.130149503	0.083018145	0.62962963	age, gender, mod_educationyear, H_H, Fisher, WFNS1n
ElasticNet	XGBoost	6	0.517241379	0.588714276	0.281665688	0.136533972	0.152408744	0.62962963	age, gender, mod_educationyear, H_H, Fisher, WFNS1n
ElasticNet	RidgeRegression	6	0.604734946	0.652294481	0.239604919	0.069507474	1.247441433	0.62962963	age, gender, mod_educationyear, H_H, Fisher, WFNS1n
RFE	LogisticRegression	6	0.543360782	0.603231329	0.246011922	0.135429628	0.802284471	0.571428571	gender, mod_educationyear, H_H, Fisher, mRSin, WFNS1n
RFE	NaiveBayes	6	0.530494081	0.581355377	0.293599239	0.131551257	0.111552054	0.571428571	gender, mod_educationyear, H_H, Fisher, mRSin, WFNS1n
RFE	NeuralNetwork	6	0.56755018	0.568677878	0.301886868	0.094528478	0.076956363	0.571428571	gender, mod_educationyear, H_H, Fisher, mRSin, WFNS1n
RFE	RandomForest	6	0.507848688	0.568855823	0.27376813	0.13465113	0.065388576	0.571428571	gender, mod_educationyear, H_H, Fisher, mRSin, WFNS1n

SUPPLEMENTARY DATA

RFE	SVM	6	0.456767885	0.496541797	0.260162512	0.282034673	-0.926756769	0.571428571	gender, mod_educationyear, H_H, Fisher, mRSin, WFNS1n
RFE	XGBoost	6	0.499099331	0.55460252	0.297720225	0.138888759	0.019998292	0.571428571	gender, mod_educationyear, H_H, Fisher, mRSin, WFNS1n
RFE	RidgeRegression	6	0.535898096	0.594199286	0.246840319	0.076186218	0.72945454	0.571428571	gender, mod_educationyear, H_H, Fisher, mRSin, WFNS1n
PCA	LogisticRegression	7	0.613998971	0.650616791	0.241989747	0.139349523	0.632733406	0.916666667	PC1, PC2, PC3, PC4, PC5, PC6, PC7
PCA	NaiveBayes	7	0.572825528	0.606125914	0.272148277	0.126302971	0.192112485	0.916666667	PC1, PC2, PC3, PC4, PC5, PC6, PC7
PCA	NeuralNetwork	7	0.58517756	0.613276936	0.334971171	0.090742941	0.071685672	0.916666667	PC1, PC2, PC3, PC4, PC5, PC6, PC7
PCA	RandomForest	7	0.615671642	0.63039031	0.237863693	0.038213298	0.825531243	0.916666667	PC1, PC2, PC3, PC4, PC5, PC6, PC7
PCA	SVM	7	0.496268657	0.543735079	0.262804437	0.178924751	-0.180222074	0.916666667	PC1, PC2, PC3, PC4, PC5, PC6, PC7
PCA	XGBoost	7	0.583118888	0.595852833	0.285109113	0.094204635	0.223756691	0.916666667	PC1, PC2, PC3, PC4, PC5, PC6, PC7
PCA	RidgeRegression	7	0.599073598	0.649882213	0.239240988	0.064060886	1.309024566	0.916666667	PC1, PC2, PC3, PC4, PC5, PC6, PC7
Boruta	LogisticRegression	1	0.577586207	0.651038917	0.244950337	0.144127061	1.441197019	1	age
Boruta	NaiveBayes	1	0.54130211	0.59380201	0.251209962	0.069923431	0.322643912	1	age
Boruta	NeuralNetwork	1	0.571667524	0.641805039	0.243942171	-0.019664419	0.828347688	1	age
Boruta	RandomForest	1	0.562017499	0.617067261	0.287202593	0.12543504	0.067033851	1	age
Boruta	SVM	1	0.489963973	0.562454243	0.250725946	0.191781988	-0.355811877	1	age
Boruta	XGBoost	1	0.568708183	0.607519177	0.273871851	0.120763964	0.201791575	1	age
Boruta	RidgeRegression	1	0.574755533	0.647144436	0.244163982	0.039014278	1.484928201	1	age
MutualInfo	LogisticRegression	6	0.577714874	0.657642753	0.241427574	0.092484373	0.909829691	0.714285714	age, H_H, location1, location2, mRSin, WFNS1n

SUPPLEMENTARY DATA

MutualInfo	NaiveBayes	6	0.508234689	0.579280353	0.30090968	0.132074472	0.056573988	0.714285714	age, H_H, location1, location2, mRSin, WFNS1n
MutualInfo	NeuralNetwork	6	0.570509521	0.628268342	0.313825748	0.03690999	0.107435008	0.714285714	age, H_H, location1, location2, mRSin, WFNS1n
MutualInfo	RandomForest	6	0.523417396	0.561696746	0.266340265	0.141424545	0.023136286	0.714285714	age, H_H, location1, location2, mRSin, WFNS1n
MutualInfo	SVM	6	0.55506948	0.566763746	0.254997465	0.077527891	0.272903609	0.714285714	age, H_H, location1, location2, mRSin, WFNS1n
MutualInfo	XGBoost	6	0.492923314	0.562611246	0.303755639	0.144818054	-0.002711797	0.714285714	age, H_H, location1, location2, mRSin, WFNS1n
MutualInfo	RidgeRegression	6	0.58260422	0.652417691	0.242616851	0.03716859	1.079956931	0.714285714	age, H_H, location1, location2, mRSin, WFNS1n
Pearson	LogisticRegression	6	0.610396294	0.675308495	0.237296416	0.116540442	1.000906191	0.642857143	mod_educationyear, H_H, age, WFNS1n, mRSin, Fisher
Pearson	NaiveBayes	6	0.562532167	0.631827752	0.281037264	0.119710089	0.184664011	0.642857143	mod_educationyear, H_H, age, WFNS1n, mRSin, Fisher
Pearson	NeuralNetwork	6	0.611940299	0.661194393	0.27940749	0.140857275	0.209717869	0.642857143	mod_educationyear, H_H, age, WFNS1n, mRSin, Fisher
Pearson	RandomForest	6	0.559444159	0.632972138	0.25366011	0.102694877	0.410466675	0.642857143	mod_educationyear, H_H, age, WFNS1n, mRSin, Fisher
Pearson	SVM	6	0.54387545	0.591241284	0.248360464	0.077018843	0.522427029	0.642857143	mod_educationyear, H_H, age, WFNS1n, mRSin, Fisher
Pearson	XGBoost	6	0.5249614	0.577224264	0.316866817	0.125300168	0.065796587	0.642857143	mod_educationyear, H_H, age, WFNS1n, mRSin, Fisher
Pearson	RidgeRegression	6	0.58389089	0.626382842	0.241834625	0.062186535	1.104634575	0.642857143	mod_educationyear, H_H, age, WFNS1n, mRSin, Fisher
Spearman	LogisticRegression	6	0.613355636	0.680347348	0.239866157	0.172032362	1.160470015	0.666666667	mod_educationyear, H_H, WFNS1n, age, mRSin, gender
Spearman	NaiveBayes	6	0.573468863	0.637130869	0.27752767	0.103348228	0.217612687	0.666666667	mod_educationyear, H_H, WFNS1n, age, mRSin, gender
Spearman	NeuralNetwork	6	0.541945445	0.607166609	0.296796685	0.111140058	0.124014073	0.666666667	mod_educationyear, H_H, WFNS1n, age, mRSin, gender
Spearman	RandomForest	6	0.521744725	0.563628355	0.277630269	0.136259968	0.095382797	0.666666667	mod_educationyear, H_H, WFNS1n, age, mRSin, gender
Spearman	SVM	6	0.480828616	0.546904144	0.257099877	0.155048652	-0.094927912	0.666666667	mod_educationyear, H_H, WFNS1n, age, mRSin, gender
Spearman	XGBoost	6	0.503474009	0.556091981	0.319203285	0.142095592	0.025588284	0.666666667	mod_educationyear, H_H, WFNS1n, age, mRSin, gender

SUPPLEMENTARY DATA

Spearman	RidgeRegression	6	0.615156974	0.66750528	0.240286593	0.079138421	1.40635453	0.666666667	mod_educationyear, H_H, WFNS1n, age, mRSin, gender
Kendall	LogisticRegression	6	0.613355636	0.680347348	0.239866157	0.172032362	1.160470015	0.666666667	mod_educationyear, H_H, WFNS1n, age, mRSin, gender
Kendall	NaiveBayes	6	0.573468863	0.637130869	0.27752767	0.103348228	0.217612687	0.666666667	mod_educationyear, H_H, WFNS1n, age, mRSin, gender
Kendall	NeuralNetwork	6	0.541945445	0.607166609	0.296796685	0.111140058	0.124014073	0.666666667	mod_educationyear, H_H, WFNS1n, age, mRSin, gender
Kendall	RandomForest	6	0.521744725	0.563628355	0.277630269	0.136259968	0.095382797	0.666666667	mod_educationyear, H_H, WFNS1n, age, mRSin, gender
Kendall	SVM	6	0.480828616	0.546904144	0.257099877	0.155048652	-0.094927912	0.666666667	mod_educationyear, H_H, WFNS1n, age, mRSin, gender
Kendall	XGBoost	6	0.503474009	0.556091981	0.319203285	0.142095592	0.025588284	0.666666667	mod_educationyear, H_H, WFNS1n, age, mRSin, gender
Kendall	RidgeRegression	6	0.615156974	0.66750528	0.240286593	0.079138421	1.40635453	0.666666667	mod_educationyear, H_H, WFNS1n, age, mRSin, gender
ANOVA_F	LogisticRegression	6	0.610396294	0.675308495	0.237296416	0.116540442	1.000906191	0.642857143	age, mod_educationyear, H_H, Fisher, mRSin, WFNS1n
ANOVA_F	NaiveBayes	6	0.562532167	0.631827752	0.281037264	0.119710089	0.184664011	0.642857143	age, mod_educationyear, H_H, Fisher, mRSin, WFNS1n
ANOVA_F	NeuralNetwork	6	0.660319094	0.731306572	0.255065288	0.132321289	0.270692518	0.642857143	age, mod_educationyear, H_H, Fisher, mRSin, WFNS1n
ANOVA_F	RandomForest	6	0.554297478	0.626656173	0.251359509	0.107741716	0.447023895	0.642857143	age, mod_educationyear, H_H, Fisher, mRSin, WFNS1n
ANOVA_F	SVM	6	0.54387545	0.591241284	0.248360464	0.077018843	0.522427029	0.642857143	age, mod_educationyear, H_H, Fisher, mRSin, WFNS1n
ANOVA_F	XGBoost	6	0.520329388	0.585213673	0.288572003	0.124004663	0.135687489	0.642857143	age, mod_educationyear, H_H, Fisher, mRSin, WFNS1n
ANOVA_F	RidgeRegression	6	0.58389089	0.626382842	0.241834625	0.062186535	1.104634575	0.642857143	age, mod_educationyear, H_H, Fisher, mRSin, WFNS1n
VarianceThreshold	LogisticRegression	9	0.607050952	0.67464642	0.239602976	0.149741235	1.084394905	1	age, gender, mod_educationyear, H_H, Fisher, location1, location2, mRSin, WFNS1n
VarianceThreshold	NaiveBayes	9	0.550437468	0.621534713	0.289616544	0.106165285	0.184358027	1	age, gender, mod_educationyear, H_H, Fisher, location1, location2, mRSin, WFNS1n
VarianceThreshold	NeuralNetwork	9	0.548378796	0.622574297	0.349559291	0.095207472	0.062695856	1	age, gender, mod_educationyear, H_H, Fisher, location1, location2, mRSin, WFNS1n
VarianceThreshold	RandomForest	9	0.572825528	0.589940045	0.255069954	0.101711918	0.300128248	1	age, gender, mod_educationyear, H_H, Fisher, location1, location2, mRSin, WFNS1n

SUPPLEMENTARY DATA

VarianceThreshold	SVM	9	0.516726711	0.537358723	0.264702244	0.149485273	-0.020105545	1	age, gender, mod_educationyear, H_H, Fisher, location1, location2, mRSin, WFNS1n
VarianceThreshold	XGBoost	9	0.508492023	0.562007312	0.310717283	0.13232697	0.055060649	1	age, gender, mod_educationyear, H_H, Fisher, location1, location2, mRSin, WFNS1n
VarianceThreshold	RidgeRegression	9	0.598044261	0.647960587	0.240626528	0.065335932	1.177308857	1	age, gender, mod_educationyear, H_H, Fisher, location1, location2, mRSin, WFNS1n
ForwardSelection	LogisticRegression	6	0.615285641	0.667748439	0.238018915	0.13419888	0.997282224	0.515873016	age, gender, mod_educationyear, Fisher, location1, WFNS1n
ForwardSelection	NaiveBayes	6	0.594956253	0.656009788	0.257149123	0.0621116	0.340756609	0.515873016	age, gender, mod_educationyear, Fisher, location1, WFNS1n
ForwardSelection	NeuralNetwork	6	0.65362841	0.675378359	0.276050254	0.160553027	0.173345645	0.515873016	age, gender, mod_educationyear, Fisher, location1, WFNS1n
ForwardSelection	RandomForest	6	0.51981472	0.595182956	0.257560982	0.11594597	0.248122446	0.515873016	age, gender, mod_educationyear, Fisher, location1, WFNS1n
ForwardSelection	SVM	6	0.488419969	0.551583969	0.258820701	0.168951316	-0.193545091	0.515873016	age, gender, mod_educationyear, Fisher, location1, WFNS1n
ForwardSelection	XGBoost	6	0.499485332	0.575744848	0.313654419	0.129523242	0.071472676	0.515873016	age, gender, mod_educationyear, Fisher, location1, WFNS1n
ForwardSelection	RidgeRegression	6	0.60370561	0.65450664	0.239759345	0.086335137	1.33685297	0.515873016	age, gender, mod_educationyear, Fisher, location1, WFNS1n
NoFeatureSelection	LogisticRegression	9	0.607050952	0.67464642	0.239602976	0.149741235	1.084394905	1	age, gender, mod_educationyear, H_H, Fisher, location1, location2, mRSin, WFNS1n
NoFeatureSelection	NaiveBayes	9	0.550437468	0.621534713	0.289616544	0.106165285	0.184358027	1	age, gender, mod_educationyear, H_H, Fisher, location1, location2, mRSin, WFNS1n
NoFeatureSelection	NeuralNetwork	9	0.548378796	0.622574297	0.349559291	0.095207472	0.062695856	1	age, gender, mod_educationyear, H_H, Fisher, location1, location2, mRSin, WFNS1n
NoFeatureSelection	RandomForest	9	0.572825528	0.589940045	0.255069954	0.101711918	0.300128248	1	age, gender, mod_educationyear, H_H, Fisher, location1, location2, mRSin, WFNS1n
NoFeatureSelection	SVM	9	0.516726711	0.537358723	0.264702244	0.149485273	-0.020105545	1	age, gender, mod_educationyear, H_H, Fisher, location1, location2, mRSin, WFNS1n
NoFeatureSelection	XGBoost	9	0.508492023	0.562007312	0.310717283	0.13232697	0.055060649	1	age, gender, mod_educationyear, H_H, Fisher, location1, location2, mRSin, WFNS1n
NoFeatureSelection	RidgeRegression	9	0.598044261	0.647960587	0.240626528	0.065335932	1.177308857	1	age, gender, mod_educationyear, H_H, Fisher, location1, location2, mRSin, WFNS1n

SUPPLEMENTARY DATA

Supplemental table 4. Core plus cognitive full selector–learner _all 91 candidates screening output.

selector	model	n_selected_features	oof_AUROC	oof_AUPRC	oof_Brier	oof_cal_intercept	oof_cal_slope	feature_stability	selected_features
LASSO	LogisticRegression	1	0.977483273	0.986576738	0.088560854	0.483648386	2.322693545	0.259259259	AVLT_Recognition
LASSO	NaiveBayes	1	0.981343284	0.989627726	0.036420291	-0.199267548	0.596217314	0.259259259	AVLT_Recognition
LASSO	NeuralNetwork	1	0.979284611	0.98772317	0.044114603	0.283958445	1.270985986	0.259259259	AVLT_Recognition
LASSO	RandomForest	1	0.993309315	0.994692295	0.029774801	0.20768427	1.41964471	0.259259259	AVLT_Recognition
LASSO	SVM	1	0.992151312	0.994006032	0.032019292	0.305915895	1.638732458	0.259259259	AVLT_Recognition
LASSO	XGBoost	1	0.994338652	0.994971182	0.028615144	0.059747297	1.384627497	0.259259259	AVLT_Recognition
LASSO	RidgeRegression	1	0.987261966	0.991719566	0.123930812	1.586917567	8.940441314	0.259259259	AVLT_Recognition
ElasticNet	LogisticRegression	9	0.965259907	0.981040483	0.069416922	0.301465757	1.488616977	0.420940171	AVLT_Immediate, AVLT_Recognition, AVLT_long_term_delay, AVLT_short_term_delay, BDS, FDS, H_H, VFT_in1, changyanchi_in
ElasticNet	NaiveBayes	9	0.978126608	0.987022099	0.047491675	-0.022294414	0.38165334	0.420940171	AVLT_Immediate, AVLT_Recognition, AVLT_long_term_delay, AVLT_short_term_delay, BDS, FDS, H_H, VFT_in1, changyanchi_in
ElasticNet	NeuralNetwork	9	0.954194545	0.972837035	0.072260892	-0.234154222	0.544776375	0.420940171	AVLT_Immediate, AVLT_Recognition, AVLT_long_term_delay, AVLT_short_term_delay, BDS, FDS, H_H, VFT_in1, changyanchi_in
ElasticNet	RandomForest	9	0.99871333	0.99892136	0.0270507	-0.871688601	6.164007856	0.420940171	AVLT_Immediate, AVLT_Recognition, AVLT_long_term_delay,

SUPPLEMENTARY DATA

									AVLT_short_term_delay, BDS, FDS, H_H, VFT_in1, changyanchi_in
ElasticNet	SVM	9	0.978383942	0.986890438	0.048753606	-0.243258626	1.326961419	0.420940171	AVLT_Immediate, AVLT_Recognition, AVLT_long_term_delay, AVLT_short_term_delay, BDS, FDS, H_H, VFT_in1, changyanchi_in
ElasticNet	XGBoost	9	0.996397324	0.996679518	0.023982563	0.289838721	1.53669875	0.420940171	AVLT_Immediate, AVLT_Recognition, AVLT_long_term_delay, AVLT_short_term_delay, BDS, FDS, H_H, VFT_in1, changyanchi_in
ElasticNet	RidgeRegression	9	0.988162635	0.991467573	0.122226875	0.826197004	7.636288647	0.420940171	AVLT_Immediate, AVLT_Recognition, AVLT_long_term_delay, AVLT_short_term_delay, BDS, FDS, H_H, VFT_in1, changyanchi_in
RFE	LogisticRegression	8	0.97632527	0.984072211	0.080388944	0.038838841	2.617899356	0.37995338	AVLT_Recognition, BDS, FDS, H_H, STTB_in1, VFT_in1, changyanchi_in, location2
RFE	NaiveBayes	8	0.952907874	0.969346833	0.089802438	-0.140737929	0.368313148	0.37995338	AVLT_Recognition, BDS, FDS, H_H, STTB_in1, VFT_in1, changyanchi_in, location2
RFE	NeuralNetwork	8	0.957025219	0.974623925	0.065578789	-0.311555275	0.719228174	0.37995338	AVLT_Recognition, BDS, FDS, H_H, STTB_in1, VFT_in1, changyanchi_in, location2
RFE	RandomForest	8	0.990735975	0.993177722	0.050973733	0.432902711	3.199842662	0.37995338	AVLT_Recognition, BDS, FDS, H_H, STTB_in1, VFT_in1,

									changyanchi_in, location2
RFE	SVM	8	0.963201235	0.974713235	0.072314373	-0.14284976	1.157628684	0.37995338	AVLT_Recognition, BDS, FDS, H_H, STTB_in1, VFT_in1, changyanchi_in, location2
RFE	XGBoost	8	0.983530623	0.98861216	0.040768466	-0.041671391	1.09816216	0.37995338	AVLT_Recognition, BDS, FDS, H_H, STTB_in1, VFT_in1, changyanchi_in, location2
RFE	RidgeRegression	8	0.966289243	0.977308321	0.137255203	-0.030671143	4.871377842	0.37995338	AVLT_Recognition, BDS, FDS, H_H, STTB_in1, VFT_in1, changyanchi_in, location2
PCA	LogisticRegression	19	0.931291817	0.94907228	0.128768997	0.222853966	2.355159832	1	PC1, PC2, PC3, PC4, PC5, PC6, PC7, PC8, PC9, PC10, PC11, PC12, PC13, PC14, PC15, PC16, PC17, PC18, PC19
PCA	NaiveBayes	19	0.859752959	0.902843461	0.144621609	0.332190623	0.330875089	1	PC1, PC2, PC3, PC4, PC5, PC6, PC7, PC8, PC9, PC10, PC11, PC12, PC13, PC14, PC15, PC16, PC17, PC18, PC19
PCA	NeuralNetwork	19	0.877766341	0.915994817	0.144802612	0.330563583	0.483009624	1	PC1, PC2, PC3, PC4, PC5, PC6, PC7, PC8, PC9, PC10, PC11, PC12, PC13, PC14, PC15, PC16, PC17, PC18, PC19
PCA	RandomForest	19	0.927045805	0.946929999	0.136945833	0.069142188	2.827721613	1	PC1, PC2, PC3, PC4, PC5, PC6, PC7, PC8, PC9, PC10, PC11, PC12, PC13, PC14, PC15, PC16, PC17, PC18, PC19
PCA	SVM	19	0.913278435	0.938834867	0.116536763	0.256040859	0.950356175	1	PC1, PC2, PC3, PC4, PC5, PC6, PC7, PC8, PC9, PC10, PC11, PC12, PC13, PC14,

									PC15, PC16, PC17, PC18, PC19
PCA	XGBoost	19	0.925373134	0.953003538	0.100980212	0.242266554	1.290896235	1	PC1, PC2, PC3, PC4, PC5, PC6, PC7, PC8, PC9, PC10, PC11, PC12, PC13, PC14, PC15, PC16, PC17, PC18, PC19
PCA	RidgeRegression	19	0.942871848	0.961294578	0.146210401	0.227704585	4.093653501	1	PC1, PC2, PC3, PC4, PC5, PC6, PC7, PC8, PC9, PC10, PC11, PC12, PC13, PC14, PC15, PC16, PC17, PC18, PC19
Boruta	LogisticRegression	8	0.963715903	0.980508689	0.059030764	0.353243761	1.185260726	0.759090909	AVLT_Immediate, AVLT_Recognition, AVLT_long_term_delay, AVLT_short_term_delay, BDS, BNT, CDT, FDS
Boruta	NaiveBayes	8	0.983530623	0.991480303	0.025742731	0.012452586	0.468140655	0.759090909	AVLT_Immediate, AVLT_Recognition, AVLT_long_term_delay, AVLT_short_term_delay, BDS, BNT, CDT, FDS
Boruta	NeuralNetwork	8	0.960627895	0.979595514	0.041841695	-0.00949166	0.553584118	0.759090909	AVLT_Immediate, AVLT_Recognition, AVLT_long_term_delay, AVLT_short_term_delay, BDS, BNT, CDT, FDS
Boruta	RandomForest	8	0.999871333	0.999780509	0.02460729	-221.4122523	1002.346922	0.759090909	AVLT_Immediate, AVLT_Recognition, AVLT_long_term_delay, AVLT_short_term_delay, BDS, BNT, CDT, FDS
Boruta	SVM	8	0.991765311	0.99357706	0.035351177	0.287438553	1.35540638	0.759090909	AVLT_Immediate, AVLT_Recognition, AVLT_long_term_delay,

									AVLT_short_term_delay, BDS, BNT, CDT, FDS
Boruta	XGBoost	8	0.996911992	0.997116288	0.0243179 3	0.243153172	1.508037177	0.759090909	AVLT_Immediate, AVLT_Recognition, AVLT_long_term_delay, AVLT_short_term_delay, BDS, BNT, CDT, FDS
Boruta	RidgeRegression	8	0.986103963	0.992546667	0.124627788	0.85401558	7.858471954	0.759090909	AVLT_Immediate, AVLT_Recognition, AVLT_long_term_delay, AVLT_short_term_delay, BDS, BNT, CDT, FDS
MutualInfo	LogisticRegression	8	0.978383942	0.98808365	0.056351381	0.405868456	1.779971649	0.777777778	AVLT_Immediate, AVLT_Recognition, AVLT_long_term_delay, AVLT_short_term_delay, BDS, FDS, changyanchi_in, jike_in
MutualInfo	NaiveBayes	8	0.983015955	0.990583303	0.032439809	0.019740958	0.449250968	0.777777778	AVLT_Immediate, AVLT_Recognition, AVLT_long_term_delay, AVLT_short_term_delay, BDS, FDS, changyanchi_in, jike_in
MutualInfo	NeuralNetwork	8	0.970149254	0.983736988	0.043078896	0.177491133	0.678954896	0.777777778	AVLT_Immediate, AVLT_Recognition, AVLT_long_term_delay, AVLT_short_term_delay, BDS, FDS, changyanchi_in, jike_in
MutualInfo	RandomForest	8	0.999485332	0.99956738	0.023326851	-1.676856505	9.527577671	0.777777778	AVLT_Immediate, AVLT_Recognition, AVLT_long_term_delay, AVLT_short_term_de

									lay, BDS, FDS, changyanchi_in, jike_in
MutualInfo	SVM	8	0.992537313	0.994270029	0.031594595	0.295904345	1.379488745	0.777777778	AVLT_Immediate, AVLT_Recognition, AVLT_long_term_delay, AVLT_short_term_delay, BDS, FDS, changyanchi_in, jike_in
MutualInfo	XGBoost	8	0.996654658	0.996951744	0.023117358	0.066283192	1.478759814	0.777777778	AVLT_Immediate, AVLT_Recognition, AVLT_long_term_delay, AVLT_short_term_delay, BDS, FDS, changyanchi_in, jike_in
MutualInfo	RidgeRegression	8	0.983787957	0.991015613	0.125143946	0.876553507	7.122718621	0.777777778	AVLT_Immediate, AVLT_Recognition, AVLT_long_term_delay, AVLT_short_term_delay, BDS, FDS, changyanchi_in, jike_in
Pearson	LogisticRegression	8	0.963973237	0.980782833	0.068117552	0.463437083	1.436215695	0.777777778	AVLT_Recognition, AVLT_long_term_delay, AVLT_Immediate, AVLT_short_term_delay, BDS, FDS, VFT_in1, changyanchi_in
Pearson	NaiveBayes	8	0.976582604	0.985792587	0.051893452	-0.000425292	0.385705349	0.777777778	AVLT_Recognition, AVLT_long_term_delay, AVLT_Immediate, AVLT_short_term_delay, BDS, FDS, VFT_in1, changyanchi_in
Pearson	NeuralNetwork	8	0.965517241	0.981166634	0.042811455	0.246805883	0.745844242	0.777777778	AVLT_Recognition, AVLT_long_term_delay,

									AVLT_Immediate, AVLT_short_term_delay, BDS, FDS, VFT_in1, changyanchi_in
Pearson	RandomForest	8	0.99871333	0.99886877	0.029488386	-0.909532028	5.891194587	0.777777778	AVLT_Recognition, AVLT_long_term_delay, AVLT_Immediate, AVLT_short_term_delay, BDS, FDS, VFT_in1, changyanchi_in
Pearson	SVM	8	0.986361297	0.991061833	0.034980607	0.403091162	1.509961661	0.777777778	AVLT_Recognition, AVLT_long_term_delay, AVLT_Immediate, AVLT_short_term_delay, BDS, FDS, VFT_in1, changyanchi_in
Pearson	XGBoost	8	0.997169326	0.99739249	0.021905846	-0.066173272	1.592352306	0.777777778	AVLT_Recognition, AVLT_long_term_delay, AVLT_Immediate, AVLT_short_term_delay, BDS, FDS, VFT_in1, changyanchi_in
Pearson	RidgeRegression	8	0.986103963	0.990844881	0.124603068	1.184004711	7.774931408	0.777777778	AVLT_Recognition, AVLT_long_term_delay, AVLT_Immediate, AVLT_short_term_delay, BDS, FDS, VFT_in1, changyanchi_in
Spearman	LogisticRegression	8	0.96989192	0.983817815	0.045077624	0.382309862	1.045019676	0.851851852	AVLT_Recognition, BDS, AVLT_long_term_delay, AVLT_Immediate, FDS, AVLT_short_term_delay, BNT, VFT_in1

Spearman	NaiveBayes	8	0.981214617	0.989812006	0.032933951	0.478220365	0.458434342	0.851851852	AVLT_Recognition, BDS, AVLT_long_term_delay, AVLT_Immediate, FDS, AVLT_short_term_delay, BNT, VFT_in1
Spearman	NeuralNetwork	8	0.961142563	0.98025679	0.041799497	0.277103521	0.650372802	0.851851852	AVLT_Recognition, BDS, AVLT_long_term_delay, AVLT_Immediate, FDS, AVLT_short_term_delay, BNT, VFT_in1
Spearman	RandomForest	8	0.999613999	0.99956738	0.024032373	-2.41537119	15.02649525	0.851851852	AVLT_Recognition, BDS, AVLT_long_term_delay, AVLT_Immediate, FDS, AVLT_short_term_delay, BNT, VFT_in1
Spearman	SVM	8	0.993309315	0.994954106	0.029636948	0.268722723	1.723705674	0.851851852	AVLT_Recognition, BDS, AVLT_long_term_delay, AVLT_Immediate, FDS, AVLT_short_term_delay, BNT, VFT_in1
Spearman	XGBoost	8	0.996654658	0.996981774	0.025113413	0.11328781	1.374827599	0.851851852	AVLT_Recognition, BDS, AVLT_long_term_delay, AVLT_Immediate, FDS, AVLT_short_term_delay, BNT, VFT_in1
Spearman	RidgeRegression	8	0.987133299	0.992140808	0.124409723	1.167328894	8.149325693	0.851851852	AVLT_Recognition, BDS, AVLT_long_term_delay, AVLT_Immediate, FDS,

									AVLT_short_term_delay, BNT, VFT_in1
Kendall	LogisticRegression	8	0.96989192	0.983817815	0.045077624	0.382309862	1.045019676	0.851851852	AVLT_Recognition, BDS, AVLT_long_term_delay, FDS, AVLT_Immediate, AVLT_short_term_delay, BNT, VFT_in1
Kendall	NaiveBayes	8	0.981214617	0.989812006	0.032933951	0.478220365	0.458434342	0.851851852	AVLT_Recognition, BDS, AVLT_long_term_delay, FDS, AVLT_Immediate, AVLT_short_term_delay, BNT, VFT_in1
Kendall	NeuralNetwork	8	0.961399897	0.980363166	0.041056206	0.234214523	0.64729816	0.851851852	AVLT_Recognition, BDS, AVLT_long_term_delay, FDS, AVLT_Immediate, AVLT_short_term_delay, BNT, VFT_in1
Kendall	RandomForest	8	0.999613999	0.99956738	0.023863685	-2.470420104	14.70293818	0.851851852	AVLT_Recognition, BDS, AVLT_long_term_delay, FDS, AVLT_Immediate, AVLT_short_term_delay, BNT, VFT_in1
Kendall	SVM	8	0.993309315	0.994954106	0.029636948	0.268722723	1.723705674	0.851851852	AVLT_Recognition, BDS, AVLT_long_term_delay, FDS, AVLT_Immediate, AVLT_short_term_delay, BNT, VFT_in1
Kendall	XGBoost	8	0.996654658	0.996981774	0.025234234	0.108665168	1.377280436	0.851851852	AVLT_Recognition, BDS, AVLT_long_term_delay, FDS, AVLT_Immediate, AVLT_short_term_delay, BNT, VFT_in1
Kendall	RidgeRegression	8	0.987133299	0.992140808	0.124409723	1.167328894	8.149325693	0.851851852	AVLT_Recognition, BDS,

									AVLT_long_term_delay, FDS, AVLT_Immediate, AVLT_short_term_delay, BNT, VFT_in1
ANOVA_F	LogisticRegression	8	0.963973237	0.980782833	0.068117552	0.463437083	1.436215695	0.777777778	AVLT_Immediate, AVLT_Recognition, AVLT_long_term_delay, AVLT_short_term_delay, BDS, FDS, VFT_in1, changyanchi_in
ANOVA_F	NaiveBayes	8	0.976582604	0.985792587	0.051893452	-0.000425292	0.385705349	0.777777778	AVLT_Immediate, AVLT_Recognition, AVLT_long_term_delay, AVLT_short_term_delay, BDS, FDS, VFT_in1, changyanchi_in
ANOVA_F	NeuralNetwork	8	0.960113227	0.979163022	0.044593852	0.291096385	0.673633418	0.777777778	AVLT_Immediate, AVLT_Recognition, AVLT_long_term_delay, AVLT_short_term_delay, BDS, FDS, VFT_in1, changyanchi_in
ANOVA_F	RandomForest	8	0.999485332	0.99956738	0.025590995	-0.85471024	5.625481718	0.777777778	AVLT_Immediate, AVLT_Recognition, AVLT_long_term_delay, AVLT_short_term_delay, BDS, FDS, VFT_in1, changyanchi_in
ANOVA_F	SVM	8	0.986361297	0.991061833	0.034980607	0.403091162	1.509961661	0.777777778	AVLT_Immediate, AVLT_Recognition, AVLT_long_term_delay, AVLT_short_term_delay, BDS, FDS, VFT_in1, changyanchi_in

ANOVA_F	XGBoost	8	0.996911992	0.99712802	0.022747359	0.027117065	1.558303225	0.777777778	AVLT_Immediate, AVLT_Recognition, AVLT_long_term_delay, AVLT_short_term_delay, BDS, FDS, VFT_in1, changyanchi_in
ANOVA_F	RidgeRegression	8	0.986103963	0.990844881	0.124603068	1.184004711	7.774931408	0.777777778	AVLT_Immediate, AVLT_Recognition, AVLT_long_term_delay, AVLT_short_term_delay, BDS, FDS, VFT_in1, changyanchi_in
VarianceThreshold	LogisticRegression	28	0.960627895	0.976162409	0.07558505	0.345678317	1.245604202	1	AVLT_Immediate, AVLT_Recognition, AVLT_long_term_delay, AVLT_short_term_delay, BDS, BNT, BNT_in, CDT, CDT30_in, FDS, Fisher, H_H, MMSE_in, MoCA_in, STTA_in1, STTB_in1, VFT_in1, WFNS1n, age, changyanchi_in, duanyanchi_in, gender, jike_in, location1, location2, mRSin, mod_educationyear, zairen_in
VarianceThreshold	NaiveBayes	28	0.959341225	0.977109622	0.061842106	0.050249037	0.28775576	1	AVLT_Immediate, AVLT_Recognition, AVLT_long_term_delay, AVLT_short_term_delay, BDS, BNT, BNT_in, CDT, CDT30_in, FDS, Fisher, H_H, MMSE_in, MoCA_in,

SUPPLEMENTARY DATA

									STTA_in1, STTB_in1, VFT_in1, WFNS1n, age, changyanchi_in, duanyanchi_in, gender, jike_in, location1, location2, mRSin, mod_educationyear, zairen_in
VarianceThreshold	NeuralNetwork	28	0.927431806	0.948369564	0.113066258	0.014726816	0.519413829	1	AVLT_Immediate, AVLT_Recognition, AVLT_long_term_delay, AVLT_short_term_delay, BDS, BNT, BNT_in, CDT, CDT30_in, FDS, Fisher, H_H, MMSE_in, MoCA_in, STTA_in1, STTB_in1, VFT_in1, WFNS1n, age, changyanchi_in, duanyanchi_in, gender, jike_in, location1, location2, mRSin, mod_educationyear, zairen_in
VarianceThreshold	RandomForest	28	0.998841997	0.998902257	0.036004834	-0.253354762	5.478251431	1	AVLT_Immediate, AVLT_Recognition, AVLT_long_term_delay, AVLT_short_term_delay, BDS, BNT, BNT_in, CDT, CDT30_in, FDS, Fisher, H_H, MMSE_in, MoCA_in, STTA_in1, STTB_in1, VFT_in1, WFNS1n, age, changyanchi_in, duanyanchi_in, gender, jike_in,

SUPPLEMENTARY DATA

									location1, location2, mRSin, mod_educationyear, zairen_in
VarianceThreshold	SVM	28	0.961399897	0.973438226	0.074660183	0.288436066	1.227002414	1	AVLT_Immediate, AVLT_Recognition, AVLT_long_term_delay, AVLT_short_term_delay, BDS, BNT, BNT_in, CDT, CDT30_in, FDS, Fisher, H_H, MMSE_in, MoCA_in, STTA_in1, STTB_in1, VFT_in1, WFNS1n, age, changyanchi_in, duanyanchi_in, gender, jike_in, location1, location2, mRSin, mod_educationyear, zairen_in
VarianceThreshold	XGBoost	28	0.996911992	0.997116288	0.024634389	0.311038253	1.530153722	1	AVLT_Immediate, AVLT_Recognition, AVLT_long_term_delay, AVLT_short_term_delay, BDS, BNT, BNT_in, CDT, CDT30_in, FDS, Fisher, H_H, MMSE_in, MoCA_in, STTA_in1, STTB_in1, VFT_in1, WFNS1n, age, changyanchi_in, duanyanchi_in, gender, jike_in, location1, location2, mRSin, mod_educationyear, zairen_in
VarianceThreshold	RidgeRegression	28	0.982758621	0.988187772	0.123461003	0.669906889	6.501403766	1	AVLT_Immediate, AVLT_Recognition,

									AVLT_long_term_delay, AVLT_short_term_delay, BDS, BNT, BNT_in, CDT, CDT30_in, FDS, Fisher, H_H, MMSE_in, MoCA_in, STTA_in1, STTB_in1, VFT_in1, WFNS1n, age, changyanchi_in, duanyanchi_in, gender, jike_in, location1, location2, mRSin, mod_educationyear, zairen_in
ForwardSelection	LogisticRegression	8	0.970149254	0.985460391	0.052355194	0.188643288	0.949785218	0.373737374	AVLT_Recognition, BDS, FDS, H_H, STTA_in1, VFT_in1, changyanchi_in, duanyanchi_in
ForwardSelection	NaiveBayes	8	0.954194545	0.974953585	0.04485664	-0.002920989	0.318454412	0.373737374	AVLT_Recognition, BDS, FDS, H_H, STTA_in1, VFT_in1, changyanchi_in, duanyanchi_in
ForwardSelection	NeuralNetwork	8	0.959598559	0.976970192	0.059907288	0.088100173	0.628433209	0.373737374	AVLT_Recognition, BDS, FDS, H_H, STTA_in1, VFT_in1, changyanchi_in, duanyanchi_in
ForwardSelection	RandomForest	8	0.998970664	0.999128399	0.03613517	0.082938699	4.770102374	0.373737374	AVLT_Recognition, BDS, FDS, H_H, STTA_in1, VFT_in1, changyanchi_in, duanyanchi_in
ForwardSelection	SVM	8	0.984817293	0.990126384	0.04300594	0.386815964	1.557757027	0.373737374	AVLT_Recognition, BDS, FDS, H_H, STTA_in1, VFT_in1, changyanchi_in, duanyanchi_in
ForwardSelection	XGBoost	8	0.993180648	0.9943818	0.032144878	-0.051808856	1.192645635	0.373737374	AVLT_Recognition, BDS, FDS, H_H, STTA_in1, VFT_in1,

									changyanchi_in, duanyanchi_in
ForwardSelection	RidgeRegression	8	0.969377252	0.982992204	0.129966334	0.426501227	4.945038796	0.373737374	AVLT_Recognition, BDS, FDS, H_H, STTA_in1, VFT_in1, changyanchi_in, duanyanchi_in
NoFeatureSelection	LogisticRegression	28	0.960627895	0.976162409	0.07558505	0.345678317	1.245604202	1	AVLT_Immediate, AVLT_Recognition, AVLT_long_term_delay, AVLT_short_term_delay, BDS, BNT, BNT_in, CDT, CDT30_in, FDS, Fisher, H_H, MMSE_in, MoCA_in, STTA_in1, STTB_in1, VFT_in1, WFNS1n, age, changyanchi_in, duanyanchi_in, gender, jike_in, location1, location2, mRSin, mod_educationyear, zairen_in
NoFeatureSelection	NaiveBayes	28	0.959341225	0.977109622	0.061842106	0.050249037	0.28775576	1	AVLT_Immediate, AVLT_Recognition, AVLT_long_term_delay, AVLT_short_term_delay, BDS, BNT, BNT_in, CDT, CDT30_in, FDS, Fisher, H_H, MMSE_in, MoCA_in, STTA_in1, STTB_in1, VFT_in1, WFNS1n, age, changyanchi_in, duanyanchi_in, gender, jike_in, location1, location2, mRSin,

SUPPLEMENTARY DATA

									mod_educationyear, zairen_in
NoFeatureSelection	NeuralNetwork	28	0.927431806	0.948369564	0.113066258	0.014726816	0.519413829	1	AVLT_Immediate, AVLT_Recognition, AVLT_long_term_delay, AVLT_short_term_delay, BDS, BNT, BNT_in, CDT, CDT30_in, FDS, Fisher, H_H, MMSE_in, MoCA_in, STTA_in1, STTB_in1, VFT_in1, WFNS1n, age, changyanchi_in, duanyanchi_in, gender, jike_in, location1, location2, mRSin, mod_educationyear, zairen_in
NoFeatureSelection	RandomForest	28	0.998841997	0.998902257	0.036004834	-0.253354762	5.478251431	1	AVLT_Immediate, AVLT_Recognition, AVLT_long_term_delay, AVLT_short_term_delay, BDS, BNT, BNT_in, CDT, CDT30_in, FDS, Fisher, H_H, MMSE_in, MoCA_in, STTA_in1, STTB_in1, VFT_in1, WFNS1n, age, changyanchi_in, duanyanchi_in, gender, jike_in, location1, location2, mRSin, mod_educationyear, zairen_in
NoFeatureSelection	SVM	28	0.961399897	0.973438226	0.074660183	0.288436066	1.227002414	1	AVLT_Immediate, AVLT_Recognition, AVLT_long_term_delay,

SUPPLEMENTARY DATA

									AVLT_short_term_delay, BDS, BNT, BNT_in, CDT, CDT30_in, FDS, Fisher, H_H, MMSE_in, MoCA_in, STTA_in1, STTB_in1, VFT_in1, WFNS1n, age, changyanchi_in, duanyanchi_in, gender, jike_in, location1, location2, mRSin, mod_educationyear, zairen_in
NoFeatureSelection	XGBoost	28	0.996911992	0.997116288	0.024634389	0.311038253	1.530153722	1	AVLT_Immediate, AVLT_Recognition, AVLT_long_term_delay, AVLT_short_term_delay, BDS, BNT, BNT_in, CDT, CDT30_in, FDS, Fisher, H_H, MMSE_in, MoCA_in, STTA_in1, STTB_in1, VFT_in1, WFNS1n, age, changyanchi_in, duanyanchi_in, gender, jike_in, location1, location2, mRSin, mod_educationyear, zairen_in
NoFeatureSelection	RidgeRegression	28	0.982758621	0.988187772	0.123461003	0.669906889	6.501403766	1	AVLT_Immediate, AVLT_Recognition, AVLT_long_term_delay, AVLT_short_term_delay, BDS, BNT, BNT_in, CDT, CDT30_in, FDS, Fisher, H_H, MMSE_in, MoCA_in,

SUPPLEMENTARY DATA

									STTA_in1, STTB_in1, VFT_in1, WFNS1n, age, changyanchi_in, duanyanchi_in, gender, jike_in, location1, location2, mRSin, mod_educationyear, zairen_in

Supplemental table 5. Core plus blood full selector–learner _all 91 candidates screening output.

selector	model	n_selected_features	oof_AUROC	oof_AUPRC	oof_Brier	oof_cal_intercept	oof_cal_slope	feature_stability	selected_features
LASSO	LogisticRegression	3	0.641483516	0.629348986	0.234025775	0.121328818	1.407514965	0.4	Plasma_ab42_ab40, Plasma_pTau, gender
LASSO	NaiveBayes	3	0.616758242	0.606138954	0.309679157	0.085039452	0.117895837	0.4	Plasma_ab42_ab40, Plasma_pTau, gender
LASSO	NeuralNetwork	3	0.644230769	0.601609242	0.262740493	0.071682405	0.164510896	0.4	Plasma_ab42_ab40, Plasma_pTau, gender
LASSO	RandomForest	3	0.583791209	0.582795908	0.26536294	0.103068076	0.316429618	0.4	Plasma_ab42_ab40, Plasma_pTau, gender
LASSO	SVM	3	0.548076923	0.528339818	0.271098628	0.069337324	0.188567746	0.4	Plasma_ab42_ab40, Plasma_pTau, gender
LASSO	XGBoost	3	0.510989011	0.529283633	0.318977871	0.087272271	0.111425067	0.4	Plasma_ab42_ab40, Plasma_pTau, gender
LASSO	RidgeRegression	3	0.64010989	0.628808533	0.234751343	0.079847435	1.049348165	0.4	Plasma_ab42_ab40, Plasma_pTau, gender
ElasticNet	LogisticRegression	6	0.651098901	0.644157672	0.238874977	0.160202407	0.641783412	0.402777778	H_H, Plasma_ab40, Plasma_ab42_ab40, Plasma_pTau, Plasma_ptau_tau, gender
ElasticNet	NaiveBayes	6	0.629120879	0.641866107	0.339425111	0.099635574	0.108020271	0.402777778	H_H, Plasma_ab40, Plasma_ab42_ab40, Plasma_pTau, Plasma_ptau_tau, gender
ElasticNet	NeuralNetwork	6	0.622252747	0.63034546	0.309852065	0.135783856	0.128705256	0.402777778	H_H, Plasma_ab40, Plasma_ab42_ab40, Plasma_pTau, Plasma_ptau_tau, gender
ElasticNet	RandomForest	6	0.644230769	0.683170298	0.234875027	0.120612514	0.621130551	0.402777778	H_H, Plasma_ab40, Plasma_ab42_ab4

									0, Plasma_pTau, Plasma_ptau_tau, gender
ElasticNet	SVM	6	0.557692308	0.574282081	0.255492047	0.063857287	0.344618179	0.402777778	H_H, Plasma_ab40, Plasma_ab42_ab40, Plasma_pTau, Plasma_ptau_tau, gender
ElasticNet	XGBoost	6	0.576923077	0.561989039	0.275500854	0.059326807	0.256441302	0.402777778	H_H, Plasma_ab40, Plasma_ab42_ab40, Plasma_pTau, Plasma_ptau_tau, gender
ElasticNet	RidgeRegression	6	0.637362637	0.634063916	0.233543601	0.124593964	1.069590244	0.402777778	H_H, Plasma_ab40, Plasma_ab42_ab40, Plasma_pTau, Plasma_ptau_tau, gender
RFE	LogisticRegression	8	0.726648352	0.664370764	0.220663966	0.140986426	1.832128765	0.551515152	Fisher, H_H, Plasma_ab42_ab40, Plasma_pTau, Plasma_tau_ab42, gender, location2, mRSin
RFE	NaiveBayes	8	0.67032967	0.600466268	0.259681679	0.090598465	0.142526531	0.551515152	Fisher, H_H, Plasma_ab42_ab40, Plasma_pTau, Plasma_tau_ab42, gender, location2, mRSin
RFE	NeuralNetwork	8	0.739010989	0.679155448	0.236986292	0.153904165	0.228861059	0.551515152	Fisher, H_H, Plasma_ab42_ab40, Plasma_pTau, Plasma_tau_ab42, gender, location2, mRSin
RFE	RandomForest	8	0.673076923	0.644473092	0.232200746	0.056783016	0.604026235	0.551515152	Fisher, H_H, Plasma_ab42_ab40, Plasma_pTau, Plasma_tau_ab42, gender, location2, mRSin

RFE	SVM	8	0.681318681	0.688620343	0.22644037	-0.082362784	0.979950616	0.551515152	Fisher, H_H, Plasma_ab42_ab40, Plasma_pTau, Plasma_tau_ab42, gender, location2, mRSin
RFE	XGBoost	8	0.637362637	0.611404687	0.249744386	0.052270666	0.407044284	0.551515152	Fisher, H_H, Plasma_ab42_ab40, Plasma_pTau, Plasma_tau_ab42, gender, location2, mRSin
RFE	RidgeRegression	8	0.706043956	0.653054318	0.224414967	0.111742837	0.965161612	0.551515152	Fisher, H_H, Plasma_ab42_ab40, Plasma_pTau, Plasma_tau_ab42, gender, location2, mRSin
PCA	LogisticRegression	11	0.708791209	0.668426076	0.224728426	0.17346686	1.44835891	1	PC1, PC2, PC3, PC4, PC5, PC6, PC7, PC8, PC9, PC10, PC11
PCA	NaiveBayes	11	0.472527473	0.530722875	0.34319214	0.075986055	-0.01188782	1	PC1, PC2, PC3, PC4, PC5, PC6, PC7, PC8, PC9, PC10, PC11
PCA	NeuralNetwork	11	0.638736264	0.634141737	0.306116324	0.099151426	0.134817524	1	PC1, PC2, PC3, PC4, PC5, PC6, PC7, PC8, PC9, PC10, PC11
PCA	RandomForest	11	0.647664835	0.635565889	0.233857932	0.041641931	0.822724835	1	PC1, PC2, PC3, PC4, PC5, PC6, PC7, PC8, PC9, PC10, PC11
PCA	SVM	11	0.441620879	0.538424359	0.259810217	0.073456111	0.257979923	1	PC1, PC2, PC3, PC4, PC5, PC6, PC7, PC8, PC9, PC10, PC11
PCA	XGBoost	11	0.635989011	0.696892788	0.263675082	0.107459243	0.31726982	1	PC1, PC2, PC3, PC4, PC5, PC6, PC7, PC8, PC9, PC10, PC11
PCA	RidgeRegression	11	0.679945055	0.652912767	0.229139824	0.131097771	1.153131418	1	PC1, PC2, PC3, PC4, PC5, PC6, PC7, PC8, PC9, PC10, PC11

Boruta	LogisticRegression	10	0.657967033	0.633139087	0.236419244	0.151066825	0.671474728	0.366666667	Plasma_ptau_ab42, Plasma_pTau, Plasma_ptau_tau, Plasma_ab40, gender, Plasma_tau_ab42, Plasma_ab42_ab40, Plasma_ab42, Plasma_Tau, age
Boruta	NaiveBayes	10	0.622252747	0.635871187	0.345310995	0.100041928	0.102760991	0.366666667	Plasma_ptau_ab42, Plasma_pTau, Plasma_ptau_tau, Plasma_ab40, gender, Plasma_tau_ab42, Plasma_ab42_ab40, Plasma_ab42, Plasma_Tau, age
Boruta	NeuralNetwork	10	0.693681319	0.696238346	0.252660671	0.104311233	0.223486713	0.366666667	Plasma_ptau_ab42, Plasma_pTau, Plasma_ptau_tau, Plasma_ab40, gender, Plasma_tau_ab42, Plasma_ab42_ab40, Plasma_ab42, Plasma_Tau, age
Boruta	RandomForest	10	0.628434066	0.657532693	0.237599964	0.151156533	0.619683013	0.366666667	Plasma_ptau_ab42, Plasma_pTau, Plasma_ptau_tau, Plasma_ab40, gender, Plasma_tau_ab42, Plasma_ab42_ab40, Plasma_ab42, Plasma_Tau, age
Boruta	SVM	10	0.532967033	0.577501976	0.26350066	0.049113988	0.272570509	0.366666667	Plasma_ptau_ab42, Plasma_pTau, Plasma_ptau_tau, Plasma_ab40, gender, Plasma_tau_ab42, Plasma_ab42_ab40, Plasma_ab42, Plasma_Tau, age

SUPPLEMENTARY DATA

Boruta	XGBoost	10	0.621565934	0.61958672	0.260685131	0.105393632	0.342694498	0.366666667	Plasma_ptau_ab42, Plasma_pTau, Plasma_ptau_tau, Plasma_ab40, gender, Plasma_tau_ab42, Plasma_ab42_ab40, Plasma_ab42, Plasma_Tau, age
Boruta	RidgeRegression	10	0.666208791	0.660159233	0.227376151	0.089260922	1.212046487	0.366666667	Plasma_ptau_ab42, Plasma_pTau, Plasma_ptau_tau, Plasma_ab40, gender, Plasma_tau_ab42, Plasma_ab42_ab40, Plasma_ab42, Plasma_Tau, age
MutualInfo	LogisticRegression	8	0.677197802	0.648350347	0.232742186	0.129439046	0.855833557	0.373737374	Plasma_Tau, Plasma_ab40, Plasma_ab42_ab40, Plasma_pTau, Plasma_ptau_ab42, Plasma_ptau_tau, WFNS1n, gender
MutualInfo	NaiveBayes	8	0.644230769	0.657491543	0.32700065	0.133775518	0.120792231	0.373737374	Plasma_Tau, Plasma_ab40, Plasma_ab42_ab40, Plasma_pTau, Plasma_ptau_ab42, Plasma_ptau_tau, WFNS1n, gender
MutualInfo	NeuralNetwork	8	0.629120879	0.625718324	0.315820035	0.050768927	0.111397627	0.373737374	Plasma_Tau, Plasma_ab40, Plasma_ab42_ab40, Plasma_pTau, Plasma_ptau_ab42, Plasma_ptau_tau, WFNS1n, gender
MutualInfo	RandomForest	8	0.585164835	0.584422297	0.245301615	0.099093833	0.556126643	0.373737374	Plasma_Tau, Plasma_ab40, Plasma_ab42_ab40, Plasma_pTau, Plasma_ptau_ab42, Plasma_ptau_tau, WFNS1n, gender

MutualInfo	SVM	8	0.46978022	0.509751858	0.273047636	0.073982686	0.024061854	0.373737374	Plasma_Tau, Plasma_ab40, Plasma_ab42_ab40, Plasma_pTau, Plasma_ptau_ab42, Plasma_ptau_tau, WFNS1n, gender
MutualInfo	XGBoost	8	0.56456044	0.521583	0.288821174	0.094331915	0.190743813	0.373737374	Plasma_Tau, Plasma_ab40, Plasma_ab42_ab40, Plasma_pTau, Plasma_ptau_ab42, Plasma_ptau_tau, WFNS1n, gender
MutualInfo	RidgeRegression	8	0.664835165	0.660125271	0.228679672	0.101348211	1.380644574	0.373737374	Plasma_Tau, Plasma_ab40, Plasma_ab42_ab40, Plasma_pTau, Plasma_ptau_ab42, Plasma_ptau_tau, WFNS1n, gender
Pearson	LogisticRegression	8	0.710164835	0.671115115	0.224303023	0.160858932	1.429585227	0.414141414	gender, Plasma_pTau, Plasma_ptau_tau, Plasma_ab42_ab40, Plasma_ptau_ab42, Plasma_ab40, H_H, WFNS1n
Pearson	NaiveBayes	8	0.667582418	0.66792329	0.3207112	0.122291086	0.121427771	0.414141414	gender, Plasma_pTau, Plasma_ptau_tau, Plasma_ab42_ab40, Plasma_ptau_ab42, Plasma_ab40, H_H, WFNS1n
Pearson	NeuralNetwork	8	0.711538462	0.717279113	0.265449756	0.128959828	0.184059323	0.414141414	gender, Plasma_pTau, Plasma_ptau_tau, Plasma_ab42_ab40, Plasma_ptau_ab42, Plasma_ab40, H_H, WFNS1n

SUPPLEMENTARY DATA

Pearson	RandomForest	8	0.625	0.619357494	0.235126976	0.055928687	0.690744632	0.414141414	gender, Plasma_pTau, Plasma_ptau_tau, Plasma_ab42_ab40, Plasma_ptau_ab42, Plasma_ab40, H_H, WFNS1n
Pearson	SVM	8	0.464285714	0.477498055	0.282000921	0.082003348	-0.157408923	0.414141414	gender, Plasma_pTau, Plasma_ptau_tau, Plasma_ab42_ab40, Plasma_ptau_ab42, Plasma_ab40, H_H, WFNS1n
Pearson	XGBoost	8	0.59271978	0.597189207	0.27072494	0.070387553	0.276664496	0.414141414	gender, Plasma_pTau, Plasma_ptau_tau, Plasma_ab42_ab40, Plasma_ptau_ab42, Plasma_ab40, H_H, WFNS1n
Pearson	RidgeRegression	8	0.712912088	0.685600248	0.219587401	0.12725598	1.492012204	0.414141414	gender, Plasma_pTau, Plasma_ptau_tau, Plasma_ab42_ab40, Plasma_ptau_ab42, Plasma_ab40, H_H, WFNS1n
Spearman	LogisticRegression	8	0.701923077	0.685190671	0.22371112	0.090034512	1.422997384	0.462626263	gender, Plasma_pTau, Plasma_ptau_ab42, Plasma_ptau_tau, Plasma_ab40, WFNS1n, Plasma_ab42_ab40, H_H
Spearman	NaiveBayes	8	0.645604396	0.665089386	0.32726299	0.082811016	0.119670889	0.462626263	gender, Plasma_pTau, Plasma_ptau_ab42, Plasma_ptau_tau, Plasma_ab40, WFNS1n,

									Plasma_ab42_ab40, H_H
Spearman	NeuralNetwork	8	0.627747253	0.670087461	0.342882369	0.043081863	0.141142155	0.462626263	gender, Plasma_pTau, Plasma_ptau_ab42, Plasma_ptau_tau, Plasma_ab40, WFNS1n, Plasma_ab42_ab40, H_H
Spearman	RandomForest	8	0.646978022	0.646993388	0.227627063	0.004268771	0.759906436	0.462626263	gender, Plasma_pTau, Plasma_ptau_ab42, Plasma_ptau_tau, Plasma_ab40, WFNS1n, Plasma_ab42_ab40, H_H
Spearman	SVM	8	0.546703297	0.561113166	0.256034	0.050647226	0.345042916	0.462626263	gender, Plasma_pTau, Plasma_ptau_ab42, Plasma_ptau_tau, Plasma_ab40, WFNS1n, Plasma_ab42_ab40, H_H
Spearman	XGBoost	8	0.603708791	0.600132473	0.26216841	0.023726528	0.338071258	0.462626263	gender, Plasma_pTau, Plasma_ptau_ab42, Plasma_ptau_tau, Plasma_ab40, WFNS1n, Plasma_ab42_ab40, H_H
Spearman	RidgeRegression	8	0.690934066	0.667389641	0.22385592	0.043533864	1.181583131	0.462626263	gender, Plasma_pTau, Plasma_ptau_ab42, Plasma_ptau_tau, Plasma_ab40, WFNS1n, Plasma_ab42_ab40, H_H
Kendall	LogisticRegression	8	0.701923077	0.685190671	0.22371112	0.090034512	1.422997384	0.462626263	gender, Plasma_pTau, Plasma_ptau_ab42, Plasma_ptau_tau,

SUPPLEMENTARY DATA

									Plasma_ab40, WFNS1n, Plasma_ab42_ab40, H_H
Kendall	NaiveBayes	8	0.645604396	0.665089386	0.32726299	0.082811016	0.119670889	0.462626263	gender, Plasma_pTau, Plasma_ptau_ab42, Plasma_ptau_tau, Plasma_ab40, WFNS1n, Plasma_ab42_ab40, H_H
Kendall	NeuralNetwork	8	0.673076923	0.669994009	0.293918394	0.055946485	0.168483498	0.462626263	gender, Plasma_pTau, Plasma_ptau_ab42, Plasma_ptau_tau, Plasma_ab40, WFNS1n, Plasma_ab42_ab40, H_H
Kendall	RandomForest	8	0.648351648	0.647161339	0.226691232	0.035345153	0.742357949	0.462626263	gender, Plasma_pTau, Plasma_ptau_ab42, Plasma_ptau_tau, Plasma_ab40, WFNS1n, Plasma_ab42_ab40, H_H
Kendall	SVM	8	0.546703297	0.561113166	0.256034	0.050647226	0.345042916	0.462626263	gender, Plasma_pTau, Plasma_ptau_ab42, Plasma_ptau_tau, Plasma_ab40, WFNS1n, Plasma_ab42_ab40, H_H
Kendall	XGBoost	8	0.613324176	0.614495651	0.265653714	0.04611007	0.320266878	0.462626263	gender, Plasma_pTau, Plasma_ptau_ab42, Plasma_ptau_tau, Plasma_ab40, WFNS1n, Plasma_ab42_ab40, H_H
Kendall	RidgeRegression	8	0.690934066	0.667389641	0.22385592	0.043533864	1.181583131	0.462626263	gender, Plasma_pTau,

									Plasma_ptau_ab42, Plasma_ptau_tau, Plasma_ab40, WFNS1n, Plasma_ab42_ab40, H_H
ANOVA_F	LogisticRegression	8	0.710164835	0.671115115	0.224303023	0.160858932	1.429585227	0.414141414	H_H, Plasma_ab40, Plasma_ab42_ab40, Plasma_pTau, Plasma_ptau_ab42, Plasma_ptau_tau, WFNS1n, gender
ANOVA_F	NaiveBayes	8	0.667582418	0.66792329	0.3207112	0.122291086	0.121427771	0.414141414	H_H, Plasma_ab40, Plasma_ab42_ab40, Plasma_pTau, Plasma_ptau_ab42, Plasma_ptau_tau, WFNS1n, gender
ANOVA_F	NeuralNetwork	8	0.637362637	0.621970823	0.335850002	0.108938975	0.115117433	0.414141414	H_H, Plasma_ab40, Plasma_ab42_ab40, Plasma_pTau, Plasma_ptau_ab42, Plasma_ptau_tau, WFNS1n, gender
ANOVA_F	RandomForest	8	0.638736264	0.624746775	0.234065054	0.07606434	0.693512319	0.414141414	H_H, Plasma_ab40, Plasma_ab42_ab40, Plasma_pTau, Plasma_ptau_ab42, Plasma_ptau_tau, WFNS1n, gender
ANOVA_F	SVM	8	0.464285714	0.477498055	0.282000921	0.082003348	-0.157408923	0.414141414	H_H, Plasma_ab40, Plasma_ab42_ab40, Plasma_pTau, Plasma_ptau_ab42, Plasma_ptau_tau, WFNS1n, gender
ANOVA_F	XGBoost	8	0.60782967	0.605474192	0.26793781	0.06706902	0.283788692	0.414141414	H_H, Plasma_ab40, Plasma_ab42_ab40, Plasma_pTau, Plasma_ptau_ab42

									, Plasma_ptau_tau, WFNS1n, gender
ANOVA_F	RidgeRegression	8	0.712912088	0.685600248	0.219587401	0.12725598	1.492012204	0.414141414	H_H, Plasma_ab40, Plasma_ab42_ab40, Plasma_pTau, Plasma_ptau_ab42, Plasma_ptau_tau, WFNS1n, gender
VarianceThreshold	LogisticRegression	17	0.743131868	0.716941438	0.212610091	0.089207074	0.908412029	1	Fisher, H_H, Plasma_Tau, Plasma_ab40, Plasma_ab42, Plasma_ab42_ab40, Plasma_pTau, Plasma_ptau_ab42, Plasma_ptau_tau, Plasma_tau_ab42, WFNS1n, age, gender, location1, location2, mRSin, mod_educationyear
VarianceThreshold	NaiveBayes	17	0.681318681	0.678040825	0.286492158	0.126750376	0.14149704	1	Fisher, H_H, Plasma_Tau, Plasma_ab40, Plasma_ab42, Plasma_ab42_ab40, Plasma_pTau, Plasma_ptau_ab42, Plasma_ptau_tau, Plasma_tau_ab42, WFNS1n, age, gender, location1, location2, mRSin, mod_educationyear
VarianceThreshold	NeuralNetwork	17	0.82967033	0.826156076	0.183041998	0.120655043	0.413846066	1	Fisher, H_H, Plasma_Tau, Plasma_ab40, Plasma_ab42, Plasma_ab42_ab40, Plasma_pTau, Plasma_ptau_ab42, Plasma_ptau_tau, Plasma_tau_ab42,

SUPPLEMENTARY DATA

									WFNS1n, age, gender, location1, location2, mRSin, mod_educationyear
VarianceThreshold	RandomForest	17	0.723901099	0.706727398	0.216956086	0.070717738	1.317156588	1	Fisher, H_H, Plasma_Tau, Plasma_ab40, Plasma_ab42, Plasma_ab42_ab40, Plasma_pTau, Plasma_ptau_ab42, Plasma_ptau_tau, Plasma_tau_ab42, WFNS1n, age, gender, location1, location2, mRSin, mod_educationyear
VarianceThreshold	SVM	17	0.770604396	0.729050978	0.241492938	-0.013320048	1.264916576	1	Fisher, H_H, Plasma_Tau, Plasma_ab40, Plasma_ab42, Plasma_ab42_ab40, Plasma_pTau, Plasma_ptau_ab42, Plasma_ptau_tau, Plasma_tau_ab42, WFNS1n, age, gender, location1, location2, mRSin, mod_educationyear
VarianceThreshold	XGBoost	17	0.615384615	0.630647541	0.263283604	0.001443753	0.33217689	1	Fisher, H_H, Plasma_Tau, Plasma_ab40, Plasma_ab42, Plasma_ab42_ab40, Plasma_pTau, Plasma_ptau_ab42, Plasma_ptau_tau, Plasma_tau_ab42, WFNS1n, age, gender, location1, location2, mRSin,

									mod_educationyear
VarianceThreshold	RidgeRegression	17	0.671703297	0.6355497	0.2266927 7	0.008636941	0.926602884	1	Fisher, H_H, Plasma_Tau, Plasma_ab40, Plasma_ab42, Plasma_ab42_ab40, Plasma_pTau, Plasma_ptau_ab42, Plasma_ptau_tau, Plasma_tau_ab42, WFNS1n, age, gender, location1, location2, mRSin, mod_educationyear
ForwardSelection	LogisticRegression	8	0.679945055	0.644517792	0.229874361	0.18159211	0.865849418	0.414141414	Plasma_ab40, Plasma_pTau, Plasma_ptau_ab42, Plasma_ptau_tau, Plasma_tau_ab42, age, gender, location2
ForwardSelection	NaiveBayes	8	0.615384615	0.61812395	0.329867755	0.103585179	0.085870638	0.414141414	Plasma_ab40, Plasma_pTau, Plasma_ptau_ab42, Plasma_ptau_tau, Plasma_tau_ab42, age, gender, location2
ForwardSelection	NeuralNetwork	8	0.675824176	0.63580133	0.280449316	0.002284888	0.147285222	0.414141414	Plasma_ab40, Plasma_pTau, Plasma_ptau_ab42, Plasma_ptau_tau, Plasma_tau_ab42, age, gender, location2
ForwardSelection	RandomForest	8	0.652472527	0.640375024	0.234914409	0.045584922	0.756417827	0.414141414	Plasma_ab40, Plasma_pTau, Plasma_ptau_ab42, Plasma_ptau_tau, Plasma_tau_ab42, age, gender, location2

ForwardSelection	SVM	8	0.401098901	0.491931434	0.302205037	0.111494066	-0.457147816	0.414141414	Plasma_ab40, Plasma_pTau, Plasma_ptau_ab42, Plasma_ptau_tau, Plasma_tau_ab42, age, gender, location2
ForwardSelection	XGBoost	8	0.600274725	0.58928446	0.263448364	0.038583619	0.30253147	0.414141414	Plasma_ab40, Plasma_pTau, Plasma_ptau_ab42, Plasma_ptau_tau, Plasma_tau_ab42, age, gender, location2
ForwardSelection	RidgeRegression	8	0.682692308	0.624832607	0.232778323	0.063112488	0.914439316	0.414141414	Plasma_ab40, Plasma_pTau, Plasma_ptau_ab42, Plasma_ptau_tau, Plasma_tau_ab42, age, gender, location2
NoFeatureSelection	LogisticRegression	17	0.743131868	0.716941438	0.212610091	0.089207074	0.908412029	1	Fisher, H_H, Plasma_Tau, Plasma_ab40, Plasma_ab42, Plasma_ab42_ab40, Plasma_pTau, Plasma_ptau_ab42, Plasma_ptau_tau, Plasma_tau_ab42, WFNS1n, age, gender, location1, location2, mRSin, mod_educationyear
NoFeatureSelection	NaiveBayes	17	0.681318681	0.678040825	0.286492158	0.126750376	0.14149704	1	Fisher, H_H, Plasma_Tau, Plasma_ab40, Plasma_ab42, Plasma_ab42_ab40, Plasma_pTau, Plasma_ptau_ab42, Plasma_ptau_tau, Plasma_tau_ab42, WFNS1n, age, gender, location1,

									location2, mRSin, mod_educationyear
NoFeatureSelection	NeuralNetwork	17	0.82967033	0.826156076	0.183041998	0.120655043	0.413846066	1	Fisher, H_H, Plasma_Tau, Plasma_ab40, Plasma_ab42, Plasma_ab42_ab40, Plasma_pTau, Plasma_ptau_ab42, Plasma_ptau_tau, Plasma_tau_ab42, WFNS1n, age, gender, location1, location2, mRSin, mod_educationyear
NoFeatureSelection	RandomForest	17	0.723901099	0.706727398	0.216956086	0.070717738	1.317156588	1	Fisher, H_H, Plasma_Tau, Plasma_ab40, Plasma_ab42, Plasma_ab42_ab40, Plasma_pTau, Plasma_ptau_ab42, Plasma_ptau_tau, Plasma_tau_ab42, WFNS1n, age, gender, location1, location2, mRSin, mod_educationyear
NoFeatureSelection	SVM	17	0.770604396	0.729050978	0.241492938	-0.013320048	1.264916576	1	Fisher, H_H, Plasma_Tau, Plasma_ab40, Plasma_ab42, Plasma_ab42_ab40, Plasma_pTau, Plasma_ptau_ab42, Plasma_ptau_tau, Plasma_tau_ab42, WFNS1n, age, gender, location1, location2, mRSin, mod_educationyear

NoFeatureSelection	XGBoost	17	0.615384615	0.630647541	0.263283604	0.001443753	0.33217689	1	Fisher, H_H, Plasma_Tau, Plasma_ab40, Plasma_ab42, Plasma_ab42_ab40, Plasma_pTau, Plasma_ptau_ab42, Plasma_ptau_tau, Plasma_tau_ab42, WFNS1n, age, gender, location1, location2, mRSin, mod_educationyear
NoFeatureSelection	RidgeRegression	17	0.671703297	0.6355497	0.22669277	0.008636941	0.926602884	1	Fisher, H_H, Plasma_Tau, Plasma_ab40, Plasma_ab42, Plasma_ab42_ab40, Plasma_pTau, Plasma_ptau_ab42, Plasma_ptau_tau, Plasma_tau_ab42, WFNS1n, age, gender, location1, location2, mRSin, mod_educationyear

Supplemental table 6. Core plus ERP full selector–learner _all 91 candidates screening output.

selector	model	n_selected_features	oof_AUROC	oof_AUPRC	oof_Brier	oof_cal_intercept	oof_cal_slope	feature_stability	selected_features
LASSO	LogisticRegression	11	0.9368	0.939492733	0.104180103	-0.001273785	1.553314463	0.226717752	CP1_ITPC, CP1_Latency, CP2_ITPC, CZ_ITPC, F4_Amplitude, F4_ITPC, O1_Latency, OZ_Latency, P4_Latency, P7_Latency, T4_ITPC
LASSO	NaiveBayes	11	0.9528	0.959529003	0.087130468	0.19379097	0.257405153	0.226717752	CP1_ITPC, CP1_Latency, CP2_ITPC, CZ_ITPC, F4_Amplitude, F4_ITPC, O1_Latency, OZ_Latency, P4_Latency, P7_Latency, T4_ITPC
LASSO	NeuralNetwork	11	0.926	0.927160333	0.106237259	0.060025966	0.588461412	0.226717752	CP1_ITPC, CP1_Latency, CP2_ITPC, CZ_ITPC, F4_Amplitude, F4_ITPC, O1_Latency, OZ_Latency, P4_Latency, P7_Latency, T4_ITPC
LASSO	RandomForest	11	0.9662	0.967311747	0.078781938	-0.051553549	1.870335999	0.226717752	CP1_ITPC, CP1_Latency, CP2_ITPC, CZ_ITPC, F4_Amplitude, F4_ITPC, O1_Latency, OZ_Latency, P4_Latency, P7_Latency, T4_ITPC
LASSO	SVM	11	0.95	0.960394294	0.086606002	0.15703387	1.049243436	0.226717752	CP1_ITPC, CP1_Latency, CP2_ITPC, CZ_ITPC, F4_Amplitude, F4_ITPC, O1_Latency, OZ_Latency, P4_Latency, P7_Latency, T4_ITPC
LASSO	XGBoost	11	0.9396	0.926090096	0.075700636	-0.10942358	0.943361993	0.226717752	CP1_ITPC, CP1_Latency, CP2_ITPC, CZ_ITPC,

									F4_Amplitude, F4_ITPC, O1_Latency, OZ_Latency, P4_Latency, P7_Latency, T4_ITPC
LASSO	RidgeRegression	11	0.9332	0.933391474	0.157151481	0.267221729	4.574448201	0.226717752	CP1_ITPC, CP1_Latency, CP2_ITPC, CZ_ITPC, F4_Amplitude, F4_ITPC, O1_Latency, OZ_Latency, P4_Latency, P7_Latency, T4_ITPC
ElasticNet	LogisticRegression	20	0.908	0.907476488	0.114700864	-0.095934085	0.981099038	0.216548158	C3_Amplitude, CP1_ITPC, CP1_Latency, CP2_Amplitude, CP2_ITPC, CP2_Latency, CZ_ITPC, CZ_Latency, F3_ITPC, F4_Amplitude, F4_ITPC, FZ_ITPC, O1_Latency, OZ_Latency, P4_Latency, P7_Latency, PO4_Latency, T3_ITPC, T4_ITPC, age
ElasticNet	NaiveBayes	20	0.9228	0.927064677	0.094778923	0.067707391	0.215908087	0.216548158	C3_Amplitude, CP1_ITPC, CP1_Latency, CP2_Amplitude, CP2_ITPC, CP2_Latency, CZ_ITPC, CZ_Latency, F3_ITPC, F4_Amplitude, F4_ITPC, FZ_ITPC, O1_Latency, OZ_Latency, P4_Latency, P7_Latency,

SUPPLEMENTARY DATA

									PO4_Latency, T3_ITPC, T4_ITPC, age
ElasticNet	NeuralNetwork	20	0.9024	0.899647752	0.119699055	-0.24864184	0.546204702	0.216548158	C3_Amplitude, CP1_ITPC, CP1_Latency, CP2_Amplitude, CP2_ITPC, CP2_Latency, CZ_ITPC, CZ_Latency, F3_ITPC, F4_Amplitude, F4_ITPC, FZ_ITPC, O1_Latency, OZ_Latency, P4_Latency, P7_Latency, PO4_Latency, T3_ITPC, T4_ITPC, age
ElasticNet	RandomForest	20	0.9426	0.925788861	0.092656641	-0.204173965	1.510961484	0.216548158	C3_Amplitude, CP1_ITPC, CP1_Latency, CP2_Amplitude, CP2_ITPC, CP2_Latency, CZ_ITPC, CZ_Latency, F3_ITPC, F4_Amplitude, F4_ITPC, FZ_ITPC, O1_Latency, OZ_Latency, P4_Latency, P7_Latency, PO4_Latency, T3_ITPC, T4_ITPC, age
ElasticNet	SVM	20	0.9124	0.926682466	0.113828123	-0.275121149	0.857876328	0.216548158	C3_Amplitude, CP1_ITPC, CP1_Latency, CP2_Amplitude, CP2_ITPC, CP2_Latency, CZ_ITPC,

									CZ_Latency, F3_ITPC, F4_Amplitude, F4_ITPC, FZ_ITPC, O1_Latency, OZ_Latency, P4_Latency, P7_Latency, PO4_Latency, T3_ITPC, T4_ITPC, age
ElasticNet	XGBoost	20	0.9328	0.916987768	0.080990764	-0.103726613	0.841438428	0.216548158	C3_Amplitude, CP1_ITPC, CP1_Latency, CP2_Amplitude, CP2_ITPC, CP2_Latency, CZ_ITPC, CZ_Latency, F3_ITPC, F4_Amplitude, F4_ITPC, FZ_ITPC, O1_Latency, OZ_Latency, P4_Latency, P7_Latency, PO4_Latency, T3_ITPC, T4_ITPC, age
ElasticNet	RidgeRegression	20	0.8872	0.899697476	0.16772732	-0.054611177	3.273260526	0.216548158	C3_Amplitude, CP1_ITPC, CP1_Latency, CP2_Amplitude, CP2_ITPC, CP2_Latency, CZ_ITPC, CZ_Latency, F3_ITPC, F4_Amplitude, F4_ITPC, FZ_ITPC, O1_Latency, OZ_Latency, P4_Latency, P7_Latency, PO4_Latency,

SUPPLEMENTARY DATA

									T3_ITPC, T4_ITPC, age
RFE	LogisticRegression	8	0.9224	0.926159492	0.119004138	-0.105097081	1.666490702	0.146764347	C4_Amplitude, CP1_ITPC, F3_ITPC, F4_Amplitude, O2_ITPC, OZ_ITPC, P4_Amplitude, T4_ITPC
RFE	NaiveBayes	8	0.9248	0.922283186	0.139886006	-0.221425521	0.260955166	0.146764347	C4_Amplitude, CP1_ITPC, F3_ITPC, F4_Amplitude, O2_ITPC, OZ_ITPC, P4_Amplitude, T4_ITPC
RFE	NeuralNetwork	8	0.9384	0.920225475	0.097773433	0.032545613	0.591657713	0.146764347	C4_Amplitude, CP1_ITPC, F3_ITPC, F4_Amplitude, O2_ITPC, OZ_ITPC, P4_Amplitude, T4_ITPC
RFE	RandomForest	8	0.9248	0.913730068	0.110901119	-0.216133537	1.319578249	0.146764347	C4_Amplitude, CP1_ITPC, F3_ITPC, F4_Amplitude, O2_ITPC, OZ_ITPC, P4_Amplitude, T4_ITPC
RFE	SVM	8	0.9356	0.886827073	0.094650806	0.051513457	0.620897167	0.146764347	C4_Amplitude, CP1_ITPC, F3_ITPC, F4_Amplitude, O2_ITPC, OZ_ITPC, P4_Amplitude, T4_ITPC
RFE	XGBoost	8	0.9264	0.894287484	0.113018335	-0.173484179	0.843835206	0.146764347	C4_Amplitude, CP1_ITPC, F3_ITPC, F4_Amplitude, O2_ITPC, OZ_ITPC, P4_Amplitude, T4_ITPC
RFE	RidgeRegression	8	0.8968	0.886987723	0.177393489	-0.094571568	4.58793924	0.146764347	C4_Amplitude, CP1_ITPC, F3_ITPC, F4_Amplitude, O2_ITPC, OZ_ITPC, P4_Amplitude, T4_ITPC
PCA	LogisticRegression	36	0.9436	0.946020529	0.10155889	-0.333047902	1.47448563	0.962698413	PC1, PC2, PC3, PC4, PC5, PC6, PC7, PC8,

SUPPLEMENTARY DATA

									PC9, PC10, PC11, PC12, PC13, PC14, PC15, PC16, PC17, PC18, PC19, PC20, PC21, PC22, PC23, PC24, PC25, PC26, PC27, PC28, PC29, PC30, PC31, PC32, PC33, PC34, PC35, PC36
PCA	NaiveBayes	36	0.8176	0.827689016	0.179138489	0.094156549	0.487275425	0.962698413	PC1, PC2, PC3, PC4, PC5, PC6, PC7, PC8, PC9, PC10, PC11, PC12, PC13, PC14, PC15, PC16, PC17, PC18, PC19, PC20, PC21, PC22, PC23, PC24, PC25, PC26, PC27, PC28, PC29, PC30, PC31, PC32, PC33, PC34, PC35, PC36
PCA	NeuralNetwork	36	0.9148	0.915486103	0.119568635	-0.115623084	0.9007109	0.962698413	PC1, PC2, PC3, PC4, PC5, PC6, PC7, PC8, PC9, PC10, PC11, PC12, PC13, PC14, PC15, PC16, PC17, PC18, PC19, PC20, PC21, PC22, PC23, PC24, PC25, PC26, PC27, PC28, PC29, PC30, PC31, PC32, PC33, PC34, PC35, PC36
PCA	RandomForest	36	0.889	0.889065221	0.172856888	0.094711781	3.230855206	0.962698413	PC1, PC2, PC3, PC4, PC5, PC6, PC7, PC8, PC9, PC10, PC11, PC12, PC13, PC14, PC15, PC16, PC17, PC18, PC19, PC20, PC21, PC22, PC23, PC24, PC25, PC26, PC27, PC28, PC29, PC30, PC31, PC32, PC33, PC34, PC35, PC36

PCA	SVM	36	0.8014	0.816614034	0.169678882	-0.018110746	1.096360346	0.962698413	PC1, PC2, PC3, PC4, PC5, PC6, PC7, PC8, PC9, PC10, PC11, PC12, PC13, PC14, PC15, PC16, PC17, PC18, PC19, PC20, PC21, PC22, PC23, PC24, PC25, PC26, PC27, PC28, PC29, PC30, PC31, PC32, PC33, PC34, PC35, PC36
PCA	XGBoost	36	0.8708	0.854113464	0.144860843	0.098250235	0.815274778	0.962698413	PC1, PC2, PC3, PC4, PC5, PC6, PC7, PC8, PC9, PC10, PC11, PC12, PC13, PC14, PC15, PC16, PC17, PC18, PC19, PC20, PC21, PC22, PC23, PC24, PC25, PC26, PC27, PC28, PC29, PC30, PC31, PC32, PC33, PC34, PC35, PC36
PCA	RidgeRegression	36	0.936	0.94344746	0.148872206	-0.226295946	4.391870247	0.962698413	PC1, PC2, PC3, PC4, PC5, PC6, PC7, PC8, PC9, PC10, PC11, PC12, PC13, PC14, PC15, PC16, PC17, PC18, PC19, PC20, PC21, PC22, PC23, PC24, PC25, PC26, PC27, PC28, PC29, PC30, PC31, PC32, PC33, PC34, PC35, PC36
Boruta	LogisticRegression	10	0.9316	0.916904118	0.103963447	-0.074748037	1.278272845	0.385780886	A2_ITPC, C4_ITPC, CP2_Amplitude, CP2_ITPC, CZ_ITPC, F3_ITPC, F4_Amplitude, F4_ITPC, FZ_ITPC, T4_ITPC
Boruta	NaiveBayes	10	0.914	0.897944376	0.100210604	-0.064528097	0.217180994	0.385780886	A2_ITPC, C4_ITPC, CP2_Amplitude, CP2_ITPC, CZ_ITPC,

SUPPLEMENTARY DATA

									F3_ITPC, F4_Amplitude, F4_ITPC, FZ_ITPC, T4_ITPC
Boruta	NeuralNetwork	10	0.944	0.905469886	0.063961581	-0.101791551	0.72730709	0.385780886	A2_ITPC, C4_ITPC, CP2_Amplitude, CP2_ITPC, CZ_ITPC, F3_ITPC, F4_Amplitude, F4_ITPC, FZ_ITPC, T4_ITPC
Boruta	RandomForest	10	0.936	0.910825739	0.093711907	-0.189244472	1.113563576	0.385780886	A2_ITPC, C4_ITPC, CP2_Amplitude, CP2_ITPC, CZ_ITPC, F3_ITPC, F4_Amplitude, F4_ITPC, FZ_ITPC, T4_ITPC
Boruta	SVM	10	0.954	0.923900137	0.066894627	-0.102592592	1.086768927	0.385780886	A2_ITPC, C4_ITPC, CP2_Amplitude, CP2_ITPC, CZ_ITPC, F3_ITPC, F4_Amplitude, F4_ITPC, FZ_ITPC, T4_ITPC
Boruta	XGBoost	10	0.9376	0.912357116	0.083760411	-0.195509282	0.771734387	0.385780886	A2_ITPC, C4_ITPC, CP2_Amplitude, CP2_ITPC, CZ_ITPC, F3_ITPC, F4_Amplitude, F4_ITPC, FZ_ITPC, T4_ITPC
Boruta	RidgeRegression	10	0.9548	0.950773591	0.149227071	-0.312145692	6.295084199	0.385780886	A2_ITPC, C4_ITPC, CP2_Amplitude, CP2_ITPC, CZ_ITPC, F3_ITPC, F4_Amplitude, F4_ITPC, FZ_ITPC, T4_ITPC
MutualInfo	LogisticRegression	8	0.9248	0.869109279	0.097221816	0.032260125	1.025589368	0.299145299	CP2_ITPC, CZ_ITPC, F3_ITPC, F4_Amplitude, F4_ITPC, FZ_ITPC, T4_ITPC, gender
MutualInfo	NaiveBayes	8	0.89	0.844325358	0.114159902	-0.01673585	0.194339126	0.299145299	CP2_ITPC, CZ_ITPC, F3_ITPC,

									F4_Amplitude, F4_ITPC, FZ_ITPC, T4_ITPC, gender
MutualInfo	NeuralNetwork	8	0.9352	0.858081734	0.073344638	0.000982994	0.552897677	0.299145299	CP2_ITPC, CZ_ITPC, F3_ITPC, F4_Amplitude, F4_ITPC, FZ_ITPC, T4_ITPC, gender
MutualInfo	RandomForest	8	0.94	0.924340942	0.093366842	-0.14489243	1.22995371	0.299145299	CP2_ITPC, CZ_ITPC, F3_ITPC, F4_Amplitude, F4_ITPC, FZ_ITPC, T4_ITPC, gender
MutualInfo	SVM	8	0.9388	0.907254055	0.089581443	-0.227983018	0.963683428	0.299145299	CP2_ITPC, CZ_ITPC, F3_ITPC, F4_Amplitude, F4_ITPC, FZ_ITPC, T4_ITPC, gender
MutualInfo	XGBoost	8	0.9336	0.916077651	0.087973451	-0.164110785	0.776847337	0.299145299	CP2_ITPC, CZ_ITPC, F3_ITPC, F4_Amplitude, F4_ITPC, FZ_ITPC, T4_ITPC, gender
MutualInfo	RidgeRegression	8	0.9216	0.873891533	0.165665844	-0.062893017	3.912067558	0.299145299	CP2_ITPC, CZ_ITPC, F3_ITPC, F4_Amplitude, F4_ITPC, FZ_ITPC, T4_ITPC, gender
Pearson	LogisticRegression	8	0.9532	0.950317064	0.079671472	0.054623864	1.242219464	0.481481481	F4_ITPC, CP2_ITPC, F4_Amplitude, FZ_ITPC, CZ_ITPC, F3_ITPC, A2_ITPC, T4_ITPC
Pearson	NaiveBayes	8	0.9248	0.905341487	0.099366638	-0.136598994	0.22093493	0.481481481	F4_ITPC, CP2_ITPC, F4_Amplitude, FZ_ITPC, CZ_ITPC, F3_ITPC, A2_ITPC, T4_ITPC
Pearson	NeuralNetwork	8	0.9648	0.959822939	0.077832094	0.492515021	0.858912129	0.481481481	F4_ITPC, CP2_ITPC, F4_Amplitude, FZ_ITPC, CZ_ITPC, F3_ITPC, A2_ITPC, T4_ITPC
Pearson	RandomForest	8	0.9444	0.925056499	0.090192154	-0.237383605	1.366641836	0.481481481	F4_ITPC, CP2_ITPC, F4_Amplitude, FZ_ITPC, CZ_ITPC,

									F3_ITPC, A2_ITPC, T4_ITPC
Pearson	SVM	8	0.9476	0.9337192 1	0.0695874 24	-0.054864087	1.18620077 3	0.481481481	F4_ITPC, CP2_ITPC, F4_Amplitude, FZ_ITPC, CZ_ITPC, F3_ITPC, A2_ITPC, T4_ITPC
Pearson	XGBoost	8	0.9432	0.9096907 84	0.0722583 85	-0.190646038	1.02033684 2	0.481481481	F4_ITPC, CP2_ITPC, F4_Amplitude, FZ_ITPC, CZ_ITPC, F3_ITPC, A2_ITPC, T4_ITPC
Pearson	RidgeRegressio n	8	0.9492	0.9454375 8	0.1578405 47	-0.209232373	6.62742921 8	0.481481481	F4_ITPC, CP2_ITPC, F4_Amplitude, FZ_ITPC, CZ_ITPC, F3_ITPC, A2_ITPC, T4_ITPC
Spearman	LogisticRegress ion	8	0.9408	0.9265699 25	0.0880564 06	-0.19390602	1.14253536 1	0.562289562	F4_ITPC, F4_Amplitude, CP2_ITPC, CZ_ITPC, A2_ITPC, FZ_ITPC, CP1_ITPC, CP2_Amplitude
Spearman	NaiveBayes	8	0.9156	0.8974120 97	0.116402	-0.246894029	0.21121584 3	0.562289562	F4_ITPC, F4_Amplitude, CP2_ITPC, CZ_ITPC, A2_ITPC, FZ_ITPC, CP1_ITPC, CP2_Amplitude
Spearman	NeuralNetwork	8	0.964	0.9593842 77	0.0736024 82	0.533452368	1.12041632 6	0.562289562	F4_ITPC, F4_Amplitude, CP2_ITPC, CZ_ITPC, A2_ITPC, FZ_ITPC, CP1_ITPC, CP2_Amplitude
Spearman	RandomForest	8	0.9336	0.9105548 65	0.0940866 1	-0.229115882	1.1380195	0.562289562	F4_ITPC, F4_Amplitude, CP2_ITPC, CZ_ITPC, A2_ITPC, FZ_ITPC, CP1_ITPC, CP2_Amplitude
Spearman	SVM	8	0.9416	0.9179672 87	0.0783565 42	-0.196340329	1.05098319 8	0.562289562	F4_ITPC, F4_Amplitude, CP2_ITPC, CZ_ITPC, A2_ITPC, FZ_ITPC,

SUPPLEMENTARY DATA

									CP1_ITPC, CP2_Amplitude
Spearman	XGBoost	8	0.9392	0.932856968	0.085165093	-0.223167228	0.736998579	0.562289562	F4_ITPC, F4_Amplitude, CP2_ITPC, CZ_ITPC, A2_ITPC, FZ_ITPC, CP1_ITPC, CP2_Amplitude
Spearman	RidgeRegression	8	0.9576	0.954099527	0.155569579	-0.49536212	7.429159621	0.562289562	F4_ITPC, F4_Amplitude, CP2_ITPC, CZ_ITPC, A2_ITPC, FZ_ITPC, CP1_ITPC, CP2_Amplitude
Kendall	LogisticRegression	8	0.9408	0.926569925	0.088056406	-0.19390602	1.142535361	0.562289562	F4_ITPC, F4_Amplitude, CP2_ITPC, CZ_ITPC, A2_ITPC, FZ_ITPC, CP1_ITPC, CP2_Amplitude
Kendall	NaiveBayes	8	0.9156	0.897412097	0.116402	-0.246894029	0.211215843	0.562289562	F4_ITPC, F4_Amplitude, CP2_ITPC, CZ_ITPC, A2_ITPC, FZ_ITPC, CP1_ITPC, CP2_Amplitude
Kendall	NeuralNetwork	8	0.964	0.959384277	0.073602482	0.533452368	1.120416326	0.562289562	F4_ITPC, F4_Amplitude, CP2_ITPC, CZ_ITPC, A2_ITPC, FZ_ITPC, CP1_ITPC, CP2_Amplitude
Kendall	RandomForest	8	0.9336	0.910554865	0.0940866 1	-0.229115882	1.1380195	0.562289562	F4_ITPC, F4_Amplitude, CP2_ITPC, CZ_ITPC, A2_ITPC, FZ_ITPC, CP1_ITPC, CP2_Amplitude
Kendall	SVM	8	0.9416	0.917967287	0.078356542	-0.196340329	1.050983198	0.562289562	F4_ITPC, F4_Amplitude, CP2_ITPC, CZ_ITPC, A2_ITPC, FZ_ITPC, CP1_ITPC, CP2_Amplitude
Kendall	XGBoost	8	0.9392	0.932856968	0.085165093	-0.223167228	0.736998579	0.562289562	F4_ITPC, F4_Amplitude,

									CP2_ITPC, CZ_ITPC, A2_ITPC, FZ_ITPC, CP1_ITPC, CP2_Amplitude
Kendall	RidgeRegression	8	0.9576	0.954099527	0.155569579	-0.49536212	7.429159621	0.562289562	F4_ITPC, F4_Amplitude, CP2_ITPC, CZ_ITPC, A2_ITPC, FZ_ITPC, CP1_ITPC, CP2_Amplitude
ANOVA_F	LogisticRegression	8	0.9532	0.950317064	0.079671472	0.054623864	1.242219464	0.481481481	A2_ITPC, CP2_ITPC, CZ_ITPC, F3_ITPC, F4_Amplitude, F4_ITPC, FZ_ITPC, T4_ITPC
ANOVA_F	NaiveBayes	8	0.9248	0.905341487	0.099366638	-0.136598994	0.22093493	0.481481481	A2_ITPC, CP2_ITPC, CZ_ITPC, F3_ITPC, F4_Amplitude, F4_ITPC, FZ_ITPC, T4_ITPC
ANOVA_F	NeuralNetwork	8	0.9648	0.955379136	0.06983739	1.062094462	1.075724992	0.481481481	A2_ITPC, CP2_ITPC, CZ_ITPC, F3_ITPC, F4_Amplitude, F4_ITPC, FZ_ITPC, T4_ITPC
ANOVA_F	RandomForest	8	0.9526	0.94421912	0.08391693	-0.189036393	1.460864796	0.481481481	A2_ITPC, CP2_ITPC, CZ_ITPC, F3_ITPC, F4_Amplitude, F4_ITPC, FZ_ITPC, T4_ITPC
ANOVA_F	SVM	8	0.9476	0.93371921	0.069587424	-0.054864087	1.186200773	0.481481481	A2_ITPC, CP2_ITPC, CZ_ITPC, F3_ITPC, F4_Amplitude, F4_ITPC, FZ_ITPC, T4_ITPC
ANOVA_F	XGBoost	8	0.942	0.930690065	0.071989958	-0.277818486	0.915730697	0.481481481	A2_ITPC, CP2_ITPC, CZ_ITPC, F3_ITPC, F4_Amplitude, F4_ITPC, FZ_ITPC, T4_ITPC
ANOVA_F	RidgeRegression	8	0.9492	0.94543758	0.157840547	-0.209232373	6.627429218	0.481481481	A2_ITPC, CP2_ITPC, CZ_ITPC, F3_ITPC, F4_Amplitude, F4_ITPC, FZ_ITPC, T4_ITPC

SUPPLEMENTARY DATA

VarianceThreshold	LogisticRegression	105	0.942	0.947705327	0.09564151	-0.093091494	1.282376251	1	A1_Amplitude, A1_ITPC, A1_Latency, A2_Amplitude, A2_ITPC, A2_Latency, C3_Amplitude, C3_ITPC, C3_Latency, C4_Amplitude, C4_ITPC, C4_Latency, CP1_Amplitude, CP1_ITPC, CP1_Latency, CP2_Amplitude, CP2_ITPC, CP2_Latency, CP5_Amplitude, CP5_ITPC, CP5_Latency, CP6_Amplitude, CP6_ITPC, CP6_Latency, CZ_Amplitude, CZ_ITPC, CZ_Latency, F3_Amplitude, F3_ITPC, F3_Latency, F4_Amplitude, F4_ITPC, F4_Latency, F7_Amplitude, F7_ITPC, F7_Latency, F8_Amplitude, F8_ITPC, F8_Latency, FC1_Amplitude, FC1_ITPC, FC1_Latency, FC2_Amplitude, FC2_ITPC, FC2_Latency, FC5_Amplitude, FC5_ITPC, FC5_Latency, FC6_Amplitude, FC6_ITPC,

									FC6_Latency, FP1_Amplitude, FP1_ITPC, FP1_Latency, FP2_Amplitude, FP2_ITPC, FP2_Latency, FZ_Amplitude, FZ_ITPC, FZ_Latency, Fisher, H_H, O1_Amplitude, O1_ITPC, O1_Latency, O2_Amplitude, O2_ITPC, O2_Latency, OZ_Amplitude, OZ_ITPC, OZ_Latency, P3_Amplitude, P3_ITPC, P3_Latency, P4_Amplitude, P4_ITPC, P4_Latency, P7_Amplitude, P7_ITPC, P7_Latency, P8_Amplitude, P8_ITPC, P8_Latency, PO3_Amplitude, PO3_ITPC, PO3_Latency, PO4_Amplitude, PO4_ITPC, PO4_Latency, PZ_Amplitude, PZ_ITPC, PZ_Latency, T3_Amplitude, T3_ITPC, T3_Latency, T4_Amplitude, T4_ITPC, T4_Latency, WFNS1n, age, gender, location1, location2, mRSin, mod_educationyear
VarianceThreshold	NaiveBayes	105	0.8992	0.903464174	0.145701618	-0.27676392	0.15046589	1	A1_Amplitude, A1_ITPC,

SUPPLEMENTARY DATA

									A1_Latency, A2_Amplitude, A2_ITPC, A2_Latency, C3_Amplitude, C3_ITPC, C3_Latency, C4_Amplitude, C4_ITPC, C4_Latency, CP1_Amplitude, CP1_ITPC, CP1_Latency, CP2_Amplitude, CP2_ITPC, CP2_Latency, CP5_Amplitude, CP5_ITPC, CP5_Latency, CP6_Amplitude, CP6_ITPC, CP6_Latency, CZ_Amplitude, CZ_ITPC, CZ_Latency, F3_Amplitude, F3_ITPC, F3_Latency, F4_Amplitude, F4_ITPC, F4_Latency, F7_Amplitude, F7_ITPC, F7_Latency, F8_Amplitude, F8_ITPC, F8_Latency, FC1_Amplitude, FC1_ITPC, FC1_Latency, FC2_Amplitude, FC2_ITPC, FC2_Latency, FC5_Amplitude, FC5_ITPC, FC5_Latency, FC6_Amplitude, FC6_ITPC, FC6_Latency, FP1_Amplitude,

									FP1_ITPC, FP1_Latency, FP2_Amplitude, FP2_ITPC, FP2_Latency, FZ_Amplitude, FZ_ITPC, FZ_Latency, Fisher, H_H, O1_Amplitude, O1_ITPC, O1_Latency, O2_Amplitude, O2_ITPC, O2_Latency, OZ_Amplitude, OZ_ITPC, OZ_Latency, P3_Amplitude, P3_ITPC, P3_Latency, P4_Amplitude, P4_ITPC, P4_Latency, P7_Amplitude, P7_ITPC, P7_Latency, P8_Amplitude, P8_ITPC, P8_Latency, PO3_Amplitude, PO3_ITPC, PO3_Latency, PO4_Amplitude, PO4_ITPC, PO4_Latency, PZ_Amplitude, PZ_ITPC, PZ_Latency, T3_Amplitude, T3_ITPC, T3_Latency, T4_Amplitude, T4_ITPC, T4_Latency, WFNS1n, age, gender, location1, location2, mRSin, mod_educationyear
VarianceThreshold	NeuralNetwork	105	0.87	0.887899387	0.157190343	-0.008335225	0.483266249	1	A1_Amplitude, A1_ITPC, A1_Latency, A2_Amplitude,

SUPPLEMENTARY DATA

									A2_ITPC, A2_Latency, C3_Amplitude, C3_ITPC, C3_Latency, C4_Amplitude, C4_ITPC, C4_Latency, CP1_Amplitude, CP1_ITPC, CP1_Latency, CP2_Amplitude, CP2_ITPC, CP2_Latency, CP5_Amplitude, CP5_ITPC, CP5_Latency, CP6_Amplitude, CP6_ITPC, CP6_Latency, CZ_Amplitude, CZ_ITPC, CZ_Latency, F3_Amplitude, F3_ITPC, F3_Latency, F4_Amplitude, F4_ITPC, F4_Latency, F7_Amplitude, F7_ITPC, F7_Latency, F8_Amplitude, F8_ITPC, F8_Latency, FC1_Amplitude, FC1_ITPC, FC1_Latency, FC2_Amplitude, FC2_ITPC, FC2_Latency, FC5_Amplitude, FC5_ITPC, FC5_Latency, FC6_Amplitude, FC6_ITPC, FC6_Latency, FP1_Amplitude, FP1_ITPC, FP1_Latency,

									FP2_Amplitude, FP2_ITPC, FP2_Latency, FZ_Amplitude, FZ_ITPC, FZ_Latency, Fisher, H_H, O1_Amplitude, O1_ITPC, O1_Latency, O2_Amplitude, O2_ITPC, O2_Latency, OZ_Amplitude, OZ_ITPC, OZ_Latency, P3_Amplitude, P3_ITPC, P3_Latency, P4_Amplitude, P4_ITPC, P4_Latency, P7_Amplitude, P7_ITPC, P7_Latency, P8_Amplitude, P8_ITPC, P8_Latency, PO3_Amplitude, PO3_ITPC, PO3_Latency, PO4_Amplitude, PO4_ITPC, PO4_Latency, PZ_Amplitude, PZ_ITPC, PZ_Latency, T3_Amplitude, T3_ITPC, T3_Latency, T4_Amplitude, T4_ITPC, T4_Latency, WFNS1n, age, gender, location1, location2, mRSin, mod_educationyear
VarianceThreshold	RandomForest	105	0.941	0.940083078	0.110153481	-0.096275439	2.139846474	1	A1_Amplitude, A1_ITPC, A1_Latency, A2_Amplitude, A2_ITPC, A2_Latency,

									C3_Amplitude, C3_ITPC, C3_Latency, C4_Amplitude, C4_ITPC, C4_Latency, CP1_Amplitude, CP1_ITPC, CP1_Latency, CP2_Amplitude, CP2_ITPC, CP2_Latency, CP5_Amplitude, CP5_ITPC, CP5_Latency, CP6_Amplitude, CP6_ITPC, CP6_Latency, CZ_Amplitude, CZ_ITPC, CZ_Latency, F3_Amplitude, F3_ITPC, F3_Latency, F4_Amplitude, F4_ITPC, F4_Latency, F7_Amplitude, F7_ITPC, F7_Latency, F8_Amplitude, F8_ITPC, F8_Latency, FC1_Amplitude, FC1_ITPC, FC1_Latency, FC2_Amplitude, FC2_ITPC, FC2_Latency, FC5_Amplitude, FC5_ITPC, FC5_Latency, FC6_Amplitude, FC6_ITPC, FC6_Latency, FP1_Amplitude, FP1_ITPC, FP1_Latency, FP2_Amplitude, FP2_ITPC,

									FP2_Latency, FZ_Amplitude, FZ_ITPC, FZ_Latency, Fisher, H_H, O1_Amplitude, O1_ITPC, O1_Latency, O2_Amplitude, O2_ITPC, O2_Latency, OZ_Amplitude, OZ_ITPC, OZ_Latency, P3_Amplitude, P3_ITPC, P3_Latency, P4_Amplitude, P4_ITPC, P4_Latency, P7_Amplitude, P7_ITPC, P7_Latency, P8_Amplitude, P8_ITPC, P8_Latency, PO3_Amplitude, PO3_ITPC, PO3_Latency, PO4_Amplitude, PO4_ITPC, PO4_Latency, PZ_Amplitude, PZ_ITPC, PZ_Latency, T3_Amplitude, T3_ITPC, T3_Latency, T4_Amplitude, T4_ITPC, T4_Latency, WFNS1n, age, gender, location1, location2, mRSin, mod_educationyear
VarianceThreshold	SVM	105	0.8944	0.89827245	0.142429077	-0.032012144	1.454343799	1	A1_Amplitude, A1_ITPC, A1_Latency, A2_Amplitude, A2_ITPC, A2_Latency, C3_Amplitude, C3_ITPC,

									C3_Latency, C4_Amplitude, C4_ITPC, C4_Latency, CP1_Amplitude, CP1_ITPC, CP1_Latency, CP2_Amplitude, CP2_ITPC, CP2_Latency, CP5_Amplitude, CP5_ITPC, CP5_Latency, CP6_Amplitude, CP6_ITPC, CP6_Latency, CZ_Amplitude, CZ_ITPC, CZ_Latency, F3_Amplitude, F3_ITPC, F3_Latency, F4_Amplitude, F4_ITPC, F4_Latency, F7_Amplitude, F7_ITPC, F7_Latency, F8_Amplitude, F8_ITPC, F8_Latency, FC1_Amplitude, FC1_ITPC, FC1_Latency, FC2_Amplitude, FC2_ITPC, FC2_Latency, FC5_Amplitude, FC5_ITPC, FC5_Latency, FC6_Amplitude, FC6_ITPC, FC6_Latency, FP1_Amplitude, FP1_ITPC, FP1_Latency, FP2_Amplitude, FP2_ITPC, FP2_Latency, FZ_Amplitude,

									FZ_ITPC, FZ_Latency, Fisher, H_H, O1_Amplitude, O1_ITPC, O1_Latency, O2_Amplitude, O2_ITPC, O2_Latency, OZ_Amplitude, OZ_ITPC, OZ_Latency, P3_Amplitude, P3_ITPC, P3_Latency, P4_Amplitude, P4_ITPC, P4_Latency, P7_Amplitude, P7_ITPC, P7_Latency, P8_Amplitude, P8_ITPC, P8_Latency, PO3_Amplitude, PO3_ITPC, PO3_Latency, PO4_Amplitude, PO4_ITPC, PO4_Latency, PZ_Amplitude, PZ_ITPC, PZ_Latency, T3_Amplitude, T3_ITPC, T3_Latency, T4_Amplitude, T4_ITPC, T4_Latency, WFNS1n, age, gender, location1, location2, mRSin, mod_educationyear
VarianceThreshold	XGBoost	105	0.9596	0.956505405	0.068419996	-0.266066474	1.11375789	1	A1_Amplitude, A1_ITPC, A1_Latency, A2_Amplitude, A2_ITPC, A2_Latency, C3_Amplitude, C3_ITPC, C3_Latency, C4_Amplitude,

									C4_ITPC, C4_Latency, CP1_Amplitude, CP1_ITPC, CP1_Latency, CP2_Amplitude, CP2_ITPC, CP2_Latency, CP5_Amplitude, CP5_ITPC, CP5_Latency, CP6_Amplitude, CP6_ITPC, CP6_Latency, CZ_Amplitude, CZ_ITPC, CZ_Latency, F3_Amplitude, F3_ITPC, F3_Latency, F4_Amplitude, F4_ITPC, F4_Latency, F7_Amplitude, F7_ITPC, F7_Latency, F8_Amplitude, F8_ITPC, F8_Latency, FC1_Amplitude, FC1_ITPC, FC1_Latency, FC2_Amplitude, FC2_ITPC, FC2_Latency, FC5_Amplitude, FC5_ITPC, FC5_Latency, FC6_Amplitude, FC6_ITPC, FC6_Latency, FP1_Amplitude, FP1_ITPC, FP1_Latency, FP2_Amplitude, FP2_ITPC, FP2_Latency, FZ_Amplitude, FZ_ITPC, FZ_Latency, Fisher,

									H_H, O1_Amplitude, O1_ITPC, O1_Latency, O2_Amplitude, O2_ITPC, O2_Latency, OZ_Amplitude, OZ_ITPC, OZ_Latency, P3_Amplitude, P3_ITPC, P3_Latency, P4_Amplitude, P4_ITPC, P4_Latency, P7_Amplitude, P7_ITPC, P7_Latency, P8_Amplitude, P8_ITPC, P8_Latency, PO3_Amplitude, PO3_ITPC, PO3_Latency, PO4_Amplitude, PO4_ITPC, PO4_Latency, PZ_Amplitude, PZ_ITPC, PZ_Latency, T3_Amplitude, T3_ITPC, T3_Latency, T4_Amplitude, T4_ITPC, T4_Latency, WFNS1n, age, gender, location1, location2, mRSin, mod_educationyear
VarianceThreshold	RidgeRegression	105	0.9428	0.938968901	0.143596997	-0.209742162	4.034766824	1	A1_Amplitude, A1_ITPC, A1_Latency, A2_Amplitude, A2_ITPC, A2_Latency, C3_Amplitude, C3_ITPC, C3_Latency, C4_Amplitude, C4_ITPC, C4_Latency,

									CP1_Amplitude, CP1_ITPC, CP1_Latency, CP2_Amplitude, CP2_ITPC, CP2_Latency, CP5_Amplitude, CP5_ITPC, CP5_Latency, CP6_Amplitude, CP6_ITPC, CP6_Latency, CZ_Amplitude, CZ_ITPC, CZ_Latency, F3_Amplitude, F3_ITPC, F3_Latency, F4_Amplitude, F4_ITPC, F4_Latency, F7_Amplitude, F7_ITPC, F7_Latency, F8_Amplitude, F8_ITPC, F8_Latency, FC1_Amplitude, FC1_ITPC, FC1_Latency, FC2_Amplitude, FC2_ITPC, FC2_Latency, FC5_Amplitude, FC5_ITPC, FC5_Latency, FC6_Amplitude, FC6_ITPC, FC6_Latency, FP1_Amplitude, FP1_ITPC, FP1_Latency, FP2_Amplitude, FP2_ITPC, FP2_Latency, FZ_Amplitude, FZ_ITPC, FZ_Latency, Fisher, H_H, O1_Amplitude, O1_ITPC,

									O1_Latency, O2_Amplitude, O2_ITPC, O2_Latency, OZ_Amplitude, OZ_ITPC, OZ_Latency, P3_Amplitude, P3_ITPC, P3_Latency, P4_Amplitude, P4_ITPC, P4_Latency, P7_Amplitude, P7_ITPC, P7_Latency, P8_Amplitude, P8_ITPC, P8_Latency, PO3_Amplitude, PO3_ITPC, PO3_Latency, PO4_Amplitude, PO4_ITPC, PO4_Latency, PZ_Amplitude, PZ_ITPC, PZ_Latency, T3_Amplitude, T3_ITPC, T3_Latency, T4_Amplitude, T4_ITPC, T4_Latency, WFNS1n, age, gender, location1, location2, mRSin, mod_educationyear
ForwardSelection	LogisticRegression	8	0.9472	0.929966446	0.083671437	0.16156043	1.236000793	0.373737374	CP2_Amplitude, CP2_ITPC, CZ_ITPC, F4_Amplitude, F4_ITPC, F7_ITPC, T3_ITPC, T4_ITPC
ForwardSelection	NaiveBayes	8	0.942	0.94402731	0.08766846	0.353868112	0.253897337	0.373737374	CP2_Amplitude, CP2_ITPC, CZ_ITPC, F4_Amplitude, F4_ITPC, F7_ITPC, T3_ITPC, T4_ITPC
ForwardSelection	NeuralNetwork	8	0.9484	0.933870454	0.080288727	0.105326817	0.635141744	0.373737374	CP2_Amplitude, CP2_ITPC, CZ_ITPC, F4_Amplitude,

									F4_ITPC, F7_ITPC, T3_ITPC, T4_ITPC
ForwardSelection	RandomForest	8	0.9518	0.943938615	0.087031006	0.045902071	1.576368645	0.373737374	CP2_Amplitude, CP2_ITPC, CZ_ITPC, F4_Amplitude, F4_ITPC, F7_ITPC, T3_ITPC, T4_ITPC
ForwardSelection	SVM	8	0.9504	0.918908509	0.080322892	0.127656983	1.159600761	0.373737374	CP2_Amplitude, CP2_ITPC, CZ_ITPC, F4_Amplitude, F4_ITPC, F7_ITPC, T3_ITPC, T4_ITPC
ForwardSelection	XGBoost	8	0.928	0.897679526	0.095144413	-0.008390816	0.790132874	0.373737374	CP2_Amplitude, CP2_ITPC, CZ_ITPC, F4_Amplitude, F4_ITPC, F7_ITPC, T3_ITPC, T4_ITPC
ForwardSelection	RidgeRegression	8	0.9176	0.901471521	0.16468137	0.026415048	4.461582617	0.373737374	CP2_Amplitude, CP2_ITPC, CZ_ITPC, F4_Amplitude, F4_ITPC, F7_ITPC, T3_ITPC, T4_ITPC
NoFeatureSelection	LogisticRegression	105	0.942	0.947705327	0.09564151	-0.093091494	1.282376251	1	A1_Amplitude, A1_ITPC, A1_Latency, A2_Amplitude, A2_ITPC, A2_Latency, C3_Amplitude, C3_ITPC, C3_Latency, C4_Amplitude, C4_ITPC, C4_Latency, CP1_Amplitude, CP1_ITPC, CP1_Latency, CP2_Amplitude, CP2_ITPC, CP2_Latency, CP5_Amplitude, CP5_ITPC, CP5_Latency, CP6_Amplitude, CP6_ITPC, CP6_Latency,

SUPPLEMENTARY DATA

									CZ_Amplitude, CZ_ITPC, CZ_Latency, F3_Amplitude, F3_ITPC, F3_Latency, F4_Amplitude, F4_ITPC, F4_Latency, F7_Amplitude, F7_ITPC, F7_Latency, F8_Amplitude, F8_ITPC, F8_Latency, FC1_Amplitude, FC1_ITPC, FC1_Latency, FC2_Amplitude, FC2_ITPC, FC2_Latency, FC5_Amplitude, FC5_ITPC, FC5_Latency, FC6_Amplitude, FC6_ITPC, FC6_Latency, FP1_Amplitude, FP1_ITPC, FP1_Latency, FP2_Amplitude, FP2_ITPC, FP2_Latency, FZ_Amplitude, FZ_ITPC, FZ_Latency, Fisher, H_H, O1_Amplitude, O1_ITPC, O1_Latency, O2_Amplitude, O2_ITPC, O2_Latency, OZ_Amplitude, OZ_ITPC, OZ_Latency, P3_Amplitude, P3_ITPC, P3_Latency, P4_Amplitude, P4_ITPC, P4_Latency, P7_Amplitude,

SUPPLEMENTARY DATA

									P7_ITPC, P7_Latency, P8_Amplitude, P8_ITPC, P8_Latency, PO3_Amplitude, PO3_ITPC, PO3_Latency, PO4_Amplitude, PO4_ITPC, PO4_Latency, PZ_Amplitude, PZ_ITPC, PZ_Latency, T3_Amplitude, T3_ITPC, T3_Latency, T4_Amplitude, T4_ITPC, T4_Latency, WFNS1n, age, gender, location1, location2, mRSin, mod_educationyear
NoFeatureSelection	NaiveBayes	105	0.8992	0.903464174	0.145701618	-0.27676392	0.15046589	1	A1_Amplitude, A1_ITPC, A1_Latency, A2_Amplitude, A2_ITPC, A2_Latency, C3_Amplitude, C3_ITPC, C3_Latency, C4_Amplitude, C4_ITPC, C4_Latency, CP1_Amplitude, CP1_ITPC, CP1_Latency, CP2_Amplitude, CP2_ITPC, CP2_Latency, CP5_Amplitude, CP5_ITPC, CP5_Latency, CP6_Amplitude, CP6_ITPC, CP6_Latency, CZ_Amplitude, CZ_ITPC,

									CZ_Latency, F3_Amplitude, F3_ITPC, F3_Latency, F4_Amplitude, F4_ITPC, F4_Latency, F7_Amplitude, F7_ITPC, F7_Latency, F8_Amplitude, F8_ITPC, F8_Latency, FC1_Amplitude, FC1_ITPC, FC1_Latency, FC2_Amplitude, FC2_ITPC, FC2_Latency, FC5_Amplitude, FC5_ITPC, FC5_Latency, FC6_Amplitude, FC6_ITPC, FC6_Latency, FP1_Amplitude, FP1_ITPC, FP1_Latency, FP2_Amplitude, FP2_ITPC, FP2_Latency, FZ_Amplitude, FZ_ITPC, FZ_Latency, Fisher, H_H, O1_Amplitude, O1_ITPC, O1_Latency, O2_Amplitude, O2_ITPC, O2_Latency, OZ_Amplitude, OZ_ITPC, OZ_Latency, P3_Amplitude, P3_ITPC, P3_Latency, P4_Amplitude, P4_ITPC, P4_Latency, P7_Amplitude, P7_ITPC, P7_Latency, P8_Amplitude,

									P8_ITPC, P8_Latency, PO3_Amplitude, PO3_ITPC, PO3_Latency, PO4_Amplitude, PO4_ITPC, PO4_Latency, PZ_Amplitude, PZ_ITPC, PZ_Latency, T3_Amplitude, T3_ITPC, T3_Latency, T4_Amplitude, T4_ITPC, T4_Latency, WFNS1n, age, gender, location1, location2, mRSin, mod_educationyear
NoFeatureSelection	NeuralNetwork	105	0.87	0.887899387	0.157190343	-0.008335225	0.483266249	1	A1_Amplitude, A1_ITPC, A1_Latency, A2_Amplitude, A2_ITPC, A2_Latency, C3_Amplitude, C3_ITPC, C3_Latency, C4_Amplitude, C4_ITPC, C4_Latency, CP1_Amplitude, CP1_ITPC, CP1_Latency, CP2_Amplitude, CP2_ITPC, CP2_Latency, CP5_Amplitude, CP5_ITPC, CP5_Latency, CP6_Amplitude, CP6_ITPC, CP6_Latency, CZ_Amplitude, CZ_ITPC, CZ_Latency, F3_Amplitude,

									F3_ITPC, F3_Latency, F4_Amplitude, F4_ITPC, F4_Latency, F7_Amplitude, F7_ITPC, F7_Latency, F8_Amplitude, F8_ITPC, F8_Latency, FC1_Amplitude, FC1_ITPC, FC1_Latency, FC2_Amplitude, FC2_ITPC, FC2_Latency, FC5_Amplitude, FC5_ITPC, FC5_Latency, FC6_Amplitude, FC6_ITPC, FC6_Latency, FP1_Amplitude, FP1_ITPC, FP1_Latency, FP2_Amplitude, FP2_ITPC, FP2_Latency, FZ_Amplitude, FZ_ITPC, FZ_Latency, Fisher, H_H, O1_Amplitude, O1_ITPC, O1_Latency, O2_Amplitude, O2_ITPC, O2_Latency, OZ_Amplitude, OZ_ITPC, OZ_Latency, P3_Amplitude, P3_ITPC, P3_Latency, P4_Amplitude, P4_ITPC, P4_Latency, P7_Amplitude, P7_ITPC, P7_Latency, P8_Amplitude, P8_ITPC, P8_Latency, PO3_Amplitude,

SUPPLEMENTARY DATA

									PO3_ITPC, PO3_Latency, PO4_Amplitude, PO4_ITPC, PO4_Latency, PZ_Amplitude, PZ_ITPC, PZ_Latency, T3_Amplitude, T3_ITPC, T3_Latency, T4_Amplitude, T4_ITPC, T4_Latency, WFNS1n, age, gender, location1, location2, mRSin, mod_educationyear
NoFeatureSelection	RandomForest	105	0.941	0.940083078	0.110153481	-0.096275439	2.139846474	1	A1_Amplitude, A1_ITPC, A1_Latency, A2_Amplitude, A2_ITPC, A2_Latency, C3_Amplitude, C3_ITPC, C3_Latency, C4_Amplitude, C4_ITPC, C4_Latency, CP1_Amplitude, CP1_ITPC, CP1_Latency, CP2_Amplitude, CP2_ITPC, CP2_Latency, CP5_Amplitude, CP5_ITPC, CP5_Latency, CP6_Amplitude, CP6_ITPC, CP6_Latency, CZ_Amplitude, CZ_ITPC, CZ_Latency, F3_Amplitude, F3_ITPC, F3_Latency, F4_Amplitude,

									F4_ITPC, F4_Latency, F7_Amplitude, F7_ITPC, F7_Latency, F8_Amplitude, F8_ITPC, F8_Latency, FC1_Amplitude, FC1_ITPC, FC1_Latency, FC2_Amplitude, FC2_ITPC, FC2_Latency, FC5_Amplitude, FC5_ITPC, FC5_Latency, FC6_Amplitude, FC6_ITPC, FC6_Latency, FP1_Amplitude, FP1_ITPC, FP1_Latency, FP2_Amplitude, FP2_ITPC, FP2_Latency, FZ_Amplitude, FZ_ITPC, FZ_Latency, Fisher, H_H, O1_Amplitude, O1_ITPC, O1_Latency, O2_Amplitude, O2_ITPC, O2_Latency, OZ_Amplitude, OZ_ITPC, OZ_Latency, P3_Amplitude, P3_ITPC, P3_Latency, P4_Amplitude, P4_ITPC, P4_Latency, P7_Amplitude, P7_ITPC, P7_Latency, P8_Amplitude, P8_ITPC, P8_Latency, PO3_Amplitude, PO3_ITPC, PO3_Latency,

									PO4_Amplitude, PO4_ITPC, PO4_Latency, PZ_Amplitude, PZ_ITPC, PZ_Latency, T3_Amplitude, T3_ITPC, T3_Latency, T4_Amplitude, T4_ITPC, T4_Latency, WFNS1n, age, gender, location1, location2, mRSin, mod_educationyear
NoFeatureSelection	SVM	105	0.8944	0.89827245	0.142429077	-0.032012144	1.454343799	1	A1_Amplitude, A1_ITPC, A1_Latency, A2_Amplitude, A2_ITPC, A2_Latency, C3_Amplitude, C3_ITPC, C3_Latency, C4_Amplitude, C4_ITPC, C4_Latency, CP1_Amplitude, CP1_ITPC, CP1_Latency, CP2_Amplitude, CP2_ITPC, CP2_Latency, CP5_Amplitude, CP5_ITPC, CP5_Latency, CP6_Amplitude, CP6_ITPC, CP6_Latency, CZ_Amplitude, CZ_ITPC, CZ_Latency, F3_Amplitude, F3_ITPC, F3_Latency, F4_Amplitude, F4_ITPC, F4_Latency, F7_Amplitude,

SUPPLEMENTARY DATA

									F7_ITPC, F7_Latency, F8_Amplitude, F8_ITPC, F8_Latency, FC1_Amplitude, FC1_ITPC, FC1_Latency, FC2_Amplitude, FC2_ITPC, FC2_Latency, FC5_Amplitude, FC5_ITPC, FC5_Latency, FC6_Amplitude, FC6_ITPC, FC6_Latency, FP1_Amplitude, FP1_ITPC, FP1_Latency, FP2_Amplitude, FP2_ITPC, FP2_Latency, FZ_Amplitude, FZ_ITPC, FZ_Latency, Fisher, H_H, O1_Amplitude, O1_ITPC, O1_Latency, O2_Amplitude, O2_ITPC, O2_Latency, OZ_Amplitude, OZ_ITPC, OZ_Latency, P3_Amplitude, P3_ITPC, P3_Latency, P4_Amplitude, P4_ITPC, P4_Latency, P7_Amplitude, P7_ITPC, P7_Latency, P8_Amplitude, P8_ITPC, P8_Latency, PO3_Amplitude, PO3_ITPC, PO3_Latency, PO4_Amplitude, PO4_ITPC,

									PO4_Latency, PZ_Amplitude, PZ_ITPC, PZ_Latency, T3_Amplitude, T3_ITPC, T3_Latency, T4_Amplitude, T4_ITPC, T4_Latency, WFNS1n, age, gender, location1, location2, mRSin, mod_educationyear
NoFeatureSelection	XGBoost	105	0.9596	0.956505405	0.068419996	-0.266066474	1.11375789	1	A1_Amplitude, A1_ITPC, A1_Latency, A2_Amplitude, A2_ITPC, A2_Latency, C3_Amplitude, C3_ITPC, C3_Latency, C4_Amplitude, C4_ITPC, C4_Latency, CP1_Amplitude, CP1_ITPC, CP1_Latency, CP2_Amplitude, CP2_ITPC, CP2_Latency, CP5_Amplitude, CP5_ITPC, CP5_Latency, CP6_Amplitude, CP6_ITPC, CP6_Latency, CZ_Amplitude, CZ_ITPC, CZ_Latency, F3_Amplitude, F3_ITPC, F3_Latency, F4_Amplitude, F4_ITPC, F4_Latency, F7_Amplitude, F7_ITPC, F7_Latency, F8_Amplitude,

									F8_ITPC, F8_Latency, FC1_Amplitude, FC1_ITPC, FC1_Latency, FC2_Amplitude, FC2_ITPC, FC2_Latency, FC5_Amplitude, FC5_ITPC, FC5_Latency, FC6_Amplitude, FC6_ITPC, FC6_Latency, FP1_Amplitude, FP1_ITPC, FP1_Latency, FP2_Amplitude, FP2_ITPC, FP2_Latency, FZ_Amplitude, FZ_ITPC, FZ_Latency, Fisher, H_H, O1_Amplitude, O1_ITPC, O1_Latency, O2_Amplitude, O2_ITPC, O2_Latency, OZ_Amplitude, OZ_ITPC, OZ_Latency, P3_Amplitude, P3_ITPC, P3_Latency, P4_Amplitude, P4_ITPC, P4_Latency, P7_Amplitude, P7_ITPC, P7_Latency, P8_Amplitude, P8_ITPC, P8_Latency, PO3_Amplitude, PO3_ITPC, PO3_Latency, PO4_Amplitude, PO4_ITPC, PO4_Latency, PZ_Amplitude,

									PZ_ITPC, PZ_Latency, T3_Amplitude, T3_ITPC, T3_Latency, T4_Amplitude, T4_ITPC, T4_Latency, WFNS1n, age, gender, location1, location2, mRSin, mod_educationyear
NoFeatureSelection	RidgeRegression	105	0.9428	0.938968901	0.143596997	-0.209742162	4.034766824	1	A1_Amplitude, A1_ITPC, A1_Latency, A2_Amplitude, A2_ITPC, A2_Latency, C3_Amplitude, C3_ITPC, C3_Latency, C4_Amplitude, C4_ITPC, C4_Latency, CP1_Amplitude, CP1_ITPC, CP1_Latency, CP2_Amplitude, CP2_ITPC, CP2_Latency, CP5_Amplitude, CP5_ITPC, CP5_Latency, CP6_Amplitude, CP6_ITPC, CP6_Latency, CZ_Amplitude, CZ_ITPC, CZ_Latency, F3_Amplitude, F3_ITPC, F3_Latency, F4_Amplitude, F4_ITPC, F4_Latency, F7_Amplitude, F7_ITPC, F7_Latency, F8_Amplitude, F8_ITPC, F8_Latency, FC1_Amplitude,

SUPPLEMENTARY DATA

									FC1_ITPC, FC1_Latency, FC2_Amplitude, FC2_ITPC, FC2_Latency, FC5_Amplitude, FC5_ITPC, FC5_Latency, FC6_Amplitude, FC6_ITPC, FC6_Latency, FP1_Amplitude, FP1_ITPC, FP1_Latency, FP2_Amplitude, FP2_ITPC, FP2_Latency, FZ_Amplitude, FZ_ITPC, FZ_Latency, Fisher, H_H, O1_Amplitude, O1_ITPC, O1_Latency, O2_Amplitude, O2_ITPC, O2_Latency, OZ_Amplitude, OZ_ITPC, OZ_Latency, P3_Amplitude, P3_ITPC, P3_Latency, P4_Amplitude, P4_ITPC, P4_Latency, P7_Amplitude, P7_ITPC, P7_Latency, P8_Amplitude, P8_ITPC, P8_Latency, PO3_Amplitude, PO3_ITPC, PO3_Latency, PO4_Amplitude, PO4_ITPC, PO4_Latency, PZ_Amplitude, PZ_ITPC, PZ_Latency,

SUPPLEMENTARY DATA

									T3_Amplitude, T3_ITPC, T3_Latency, T4_Amplitude, T4_ITPC, T4_Latency, WFNS1n, age, gender, location1, location2, mRSin, mod_educationyear

SUPPLEMENTARY DATA

Supplemental table 7. Core plus MRI full selector–learner _all 91 candidates screening output.

selector	model	n_selected_features	oof_AUROC	oof_AUPRC	oof_Brier	oof_cal_intercept	oof_cal_slope	feature_stability	selected_features
LASSO	LogisticRegression	7	0.881818182	0.864286828	0.169530032	-0.188026775	2.726718376	0.393939394	CAUR, HPCL, IFGR, IPLR, PrCGL, gender, mod_educationyear
LASSO	NaiveBayes	7	0.822727273	0.810759944	0.219258697	-0.15007829	0.26123534	0.393939394	CAUR, HPCL, IFGR, IPLR, PrCGL, gender, mod_educationyear
LASSO	NeuralNetwork	7	0.881818182	0.864804668	0.16185429	-0.025827013	0.407434376	0.393939394	CAUR, HPCL, IFGR, IPLR, PrCGL, gender, mod_educationyear
LASSO	RandomForest	7	0.876136364	0.854030203	0.143723958	-0.284539347	1.415547931	0.393939394	CAUR, HPCL, IFGR, IPLR, PrCGL, gender, mod_educationyear
LASSO	SVM	7	0.868181818	0.830565852	0.150756337	-0.290726058	0.94504099	0.393939394	CAUR, HPCL, IFGR, IPLR, PrCGL, gender, mod_educationyear
LASSO	XGBoost	7	0.875	0.884511708	0.145231762	0.169950853	0.920891635	0.393939394	CAUR, HPCL, IFGR, IPLR, PrCGL, gender, mod_educationyear
LASSO	RidgeRegression	7	0.881818182	0.865950364	0.152680218	-0.056264492	2.095597241	0.393939394	CAUR, HPCL, IFGR, IPLR, PrCGL, gender, mod_educationyear
ElasticNet	LogisticRegression	5	0.9	0.883796515	0.160333884	-0.100386344	3.347495418	0.405597327	CAUR, HPCL, IFGR, IPLR, mOFCR
ElasticNet	NaiveBayes	5	0.852272727	0.850057006	0.214591883	-0.03320181	0.25209214	0.405597327	CAUR, HPCL, IFGR, IPLR, mOFCR

SUPPLEMENTARY DATA

ElasticNet	NeuralNetwork	5	0.920454545	0.898163329	0.112455841	0.129807898	0.595506279	0.405597327	CAUR, HPCL, IFGR, IPLR, mOFCR
ElasticNet	RandomForest	5	0.897727273	0.893696568	0.144610227	-0.076444739	2.637431663	0.405597327	CAUR, HPCL, IFGR, IPLR, mOFCR
ElasticNet	SVM	5	0.897727273	0.88616436	0.136075937	-0.190227587	1.621374582	0.405597327	CAUR, HPCL, IFGR, IPLR, mOFCR
ElasticNet	XGBoost	5	0.931818182	0.929496735	0.112703624	0.64640949	1.654916397	0.405597327	CAUR, HPCL, IFGR, IPLR, mOFCR
ElasticNet	RidgeRegression	5	0.884090909	0.83575339	0.16063174	0.089965065	2.130388013	0.405597327	CAUR, HPCL, IFGR, IPLR, mOFCR
RFE	LogisticRegression	6	0.825	0.834606068	0.190134776	-0.357427019	2.448248659	0.344444444	HPCL, IFGR, IPLR, PrCGL, WFNS1n, gender
RFE	NaiveBayes	6	0.797727273	0.773011312	0.234231433	-0.327852921	0.191903984	0.344444444	HPCL, IFGR, IPLR, PrCGL, WFNS1n, gender
RFE	NeuralNetwork	6	0.836363636	0.816100898	0.187353234	-0.349486793	0.330899445	0.344444444	HPCL, IFGR, IPLR, PrCGL, WFNS1n, gender
RFE	RandomForest	6	0.836363636	0.836870319	0.171836434	-0.490528335	1.442797638	0.344444444	HPCL, IFGR, IPLR, PrCGL, WFNS1n, gender
RFE	SVM	6	0.802272727	0.776907977	0.189131433	-0.450266461	0.78738432	0.344444444	HPCL, IFGR, IPLR, PrCGL, WFNS1n, gender
RFE	XGBoost	6	0.856818182	0.898369784	0.166259517	-0.288172656	0.935801905	0.344444444	HPCL, IFGR, IPLR, PrCGL, WFNS1n, gender
RFE	RidgeRegression	6	0.836363636	0.834476487	0.188195514	-0.244838314	2.455215894	0.344444444	HPCL, IFGR, IPLR, PrCGL, WFNS1n, gender
PCA	LogisticRegression	14	0.875	0.871178915	0.146475614	-0.097493669	1.422043204	1	PC1, PC2, PC3, PC4, PC5, PC6, PC7, PC8, PC9, PC10, PC11, PC12, PC13, PC14
PCA	NaiveBayes	14	0.825	0.750747284	0.174969861	-0.135220272	0.347349898	1	PC1, PC2, PC3, PC4, PC5, PC6, PC7, PC8, PC9, PC10, PC11,

SUPPLEMENTARY DATA

									PC12, PC13, PC14
PCA	NeuralNetwork	14	0.834090909	0.823048447	0.188801668	-0.218049886	0.495439686	1	PC1, PC2, PC3, PC4, PC5, PC6, PC7, PC8, PC9, PC10, PC11, PC12, PC13, PC14
PCA	RandomForest	14	0.779545455	0.818154254	0.193384024	-0.132787758	2.211407113	1	PC1, PC2, PC3, PC4, PC5, PC6, PC7, PC8, PC9, PC10, PC11, PC12, PC13, PC14
PCA	SVM	14	0.795454545	0.772477212	0.210432697	-0.283840929	0.654960751	1	PC1, PC2, PC3, PC4, PC5, PC6, PC7, PC8, PC9, PC10, PC11, PC12, PC13, PC14
PCA	XGBoost	14	0.768181818	0.7875013	0.207856721	0.103612555	0.553480137	1	PC1, PC2, PC3, PC4, PC5, PC6, PC7, PC8, PC9, PC10, PC11, PC12, PC13, PC14
PCA	RidgeRegression	14	0.888636364	0.878931281	0.157232469	-0.061927313	2.760813221	1	PC1, PC2, PC3, PC4, PC5, PC6, PC7, PC8, PC9, PC10, PC11, PC12, PC13, PC14
Boruta	LogisticRegression	5	0.927272727	0.928399933	0.13693137	-0.384927133	3.473068619	0.461904762	HPCL, IFGR, IPLR, PrCGL, mOFCR
Boruta	NaiveBayes	5	0.845454545	0.838949562	0.180077992	-0.163412716	0.298743412	0.461904762	HPCL, IFGR, IPLR, PrCGL, mOFCR
Boruta	NeuralNetwork	5	0.895454545	0.877273738	0.144095163	-0.219283085	0.41327112	0.461904762	HPCL, IFGR, IPLR, PrCGL, mOFCR
Boruta	RandomForest	5	0.888636364	0.907031961	0.142361813	-0.130128826	1.257476573	0.461904762	HPCL, IFGR, IPLR, PrCGL, mOFCR

Boruta	SVM	5	0.859090909	0.852973643	0.149924788	-0.278153569	0.902415557	0.461904762	HPCL, IFGR, IPLR, PrCGL, mOFCR
Boruta	XGBoost	5	0.879545455	0.892194617	0.144434672	-0.077145111	1.096736013	0.461904762	HPCL, IFGR, IPLR, PrCGL, mOFCR
Boruta	RidgeRegression	5	0.861363636	0.822064454	0.170152757	-0.174890479	2.130684695	0.461904762	HPCL, IFGR, IPLR, PrCGL, mOFCR
MutualInfo	LogisticRegression	6	0.911363636	0.879820316	0.159578158	-0.32087774	1.562824791	0.5	CAUL, IFGR, IPLR, RD_Cluster_1, location2, mod_educationyear
MutualInfo	NaiveBayes	6	0.829545455	0.829617127	0.193959484	-0.095255374	0.279703193	0.5	CAUL, IFGR, IPLR, RD_Cluster_1, location2, mod_educationyear
MutualInfo	NeuralNetwork	6	0.918181818	0.916556485	0.134097585	-0.003306028	0.429273477	0.5	CAUL, IFGR, IPLR, RD_Cluster_1, location2, mod_educationyear
MutualInfo	RandomForest	6	0.902272727	0.915283043	0.133533211	-0.148179558	1.78448876	0.5	CAUL, IFGR, IPLR, RD_Cluster_1, location2, mod_educationyear
MutualInfo	SVM	6	0.879545455	0.866859247	0.143316498	-0.228237115	1.193076162	0.5	CAUL, IFGR, IPLR, RD_Cluster_1, location2, mod_educationyear
MutualInfo	XGBoost	6	0.925	0.926918857	0.11787768	0.336259536	1.426701265	0.5	CAUL, IFGR, IPLR, RD_Cluster_1, location2, mod_educationyear

SUPPLEMENTARY DATA

MutualInfo	RidgeRegression	6	0.890909091	0.89059786	0.154444598	-0.05114721	2.945918073	0.5	CAUL, IFGR, IPLR, RD_Cluster_1, location2, mod_educationyear
Pearson	LogisticRegression	6	0.904545455	0.905827729	0.14758353	-0.213695754	2.273034538	0.642857143	IFGR, IPLR, mOFCR, HPCL, CAUL, CAUR
Pearson	NaiveBayes	6	0.863636364	0.850516513	0.170786234	-0.233473814	0.31145478	0.642857143	IFGR, IPLR, mOFCR, HPCL, CAUL, CAUR
Pearson	NeuralNetwork	6	0.913636364	0.900459979	0.12321613	-0.170679273	0.537710382	0.642857143	IFGR, IPLR, mOFCR, HPCL, CAUL, CAUR
Pearson	RandomForest	6	0.939772727	0.949077572	0.118583482	-0.411954464	2.486309383	0.642857143	IFGR, IPLR, mOFCR, HPCL, CAUL, CAUR
Pearson	SVM	6	0.9	0.887853135	0.131008516	-0.510196876	1.222810624	0.642857143	IFGR, IPLR, mOFCR, HPCL, CAUL, CAUR
Pearson	XGBoost	6	0.929545455	0.932036763	0.110946578	0.588406039	1.580953977	0.642857143	IFGR, IPLR, mOFCR, HPCL, CAUL, CAUR
Pearson	RidgeRegression	6	0.865909091	0.824213787	0.168025048	-0.015063785	2.130582739	0.642857143	IFGR, IPLR, mOFCR, HPCL, CAUL, CAUR
Spearman	LogisticRegression	6	0.906818182	0.89593354	0.166396638	-0.356759194	4.45105312	0.5	IFGR, IPLR, mOFCR, HPCL, CAUL, WFNS1n
Spearman	NaiveBayes	6	0.811363636	0.784117885	0.200826011	-0.192868451	0.202829874	0.5	IFGR, IPLR, mOFCR, HPCL, CAUL, WFNS1n
Spearman	NeuralNetwork	6	0.931818182	0.934734364	0.136309261	-0.530258157	0.553640808	0.5	IFGR, IPLR, mOFCR, HPCL, CAUL, WFNS1n
Spearman	RandomForest	6	0.947727273	0.952207633	0.11971875	-0.359112642	2.796045823	0.5	IFGR, IPLR, mOFCR, HPCL, CAUL, WFNS1n
Spearman	SVM	6	0.886363636	0.862619133	0.134019756	-0.251853972	1.216832728	0.5	IFGR, IPLR, mOFCR, HPCL, CAUL, WFNS1n
Spearman	XGBoost	6	0.922727273	0.927879809	0.117160657	0.760329455	1.852590128	0.5	IFGR, IPLR, mOFCR, HPCL, CAUL, WFNS1n

SUPPLEMENTARY DATA

Spearman	RidgeRegression	6	0.865909091	0.836883115	0.169660732	-0.029924016	2.240969404	0.5	IFGR, IPLR, mOFCR, HPCL, CAUL, WFNS1n
Kendall	LogisticRegression	6	0.893181818	0.882778165	0.173206481	-0.377550959	3.867391406	0.388888889	IFGR, IPLR, mOFCR, HPCL, WFNS1n, CAUL
Kendall	NaiveBayes	6	0.802272727	0.768640994	0.212306269	-0.190067866	0.204550164	0.388888889	IFGR, IPLR, mOFCR, HPCL, WFNS1n, CAUL
Kendall	NeuralNetwork	6	0.856818182	0.81112711	0.184371638	-0.271290992	0.389755746	0.388888889	IFGR, IPLR, mOFCR, HPCL, WFNS1n, CAUL
Kendall	RandomForest	6	0.925	0.929221948	0.129020036	-0.33043588	2.667609564	0.388888889	IFGR, IPLR, mOFCR, HPCL, WFNS1n, CAUL
Kendall	SVM	6	0.859090909	0.847097393	0.152158003	-0.236978975	1.028727825	0.388888889	IFGR, IPLR, mOFCR, HPCL, WFNS1n, CAUL
Kendall	XGBoost	6	0.936363636	0.938453864	0.113990198	0.679877049	1.90882075	0.388888889	IFGR, IPLR, mOFCR, HPCL, WFNS1n, CAUL
Kendall	RidgeRegression	6	0.843181818	0.804406623	0.17532194	-0.073552138	2.176538029	0.388888889	IFGR, IPLR, mOFCR, HPCL, WFNS1n, CAUL
ANOVA_F	LogisticRegression	6	0.904545455	0.905827729	0.14758353	-0.213695754	2.273034538	0.642857143	CAUL, CAUR, HPCL, IFGR, IPLR, mOFCR
ANOVA_F	NaiveBayes	6	0.863636364	0.850516513	0.170786234	-0.233473814	0.31145478	0.642857143	CAUL, CAUR, HPCL, IFGR, IPLR, mOFCR
ANOVA_F	NeuralNetwork	6	0.931818182	0.919994374	0.120814216	-0.312265994	0.48961103	0.642857143	CAUL, CAUR, HPCL, IFGR, IPLR, mOFCR
ANOVA_F	RandomForest	6	0.9375	0.947909656	0.124204911	-0.641181574	2.449961817	0.642857143	CAUL, CAUR, HPCL, IFGR, IPLR, mOFCR
ANOVA_F	SVM	6	0.9	0.887853135	0.131008516	-0.510196876	1.222810624	0.642857143	CAUL, CAUR, HPCL, IFGR, IPLR, mOFCR
ANOVA_F	XGBoost	6	0.925	0.92959041	0.115693012	0.39034518	1.341072095	0.642857143	CAUL, CAUR, HPCL, IFGR, IPLR, mOFCR
ANOVA_F	RidgeRegression	6	0.865909091	0.824213787	0.168025048	-0.015063785	2.130582739	0.642857143	CAUL, CAUR, HPCL, IFGR, IPLR, mOFCR

SUPPLEMENTARY DATA

VarianceThreshold	LogisticRegression	27	0.9	0.88214529	0.140274006	-0.32931772	1.396453907	1	ACCR, AD_Cluster_1, AD_Cluster_2, AD_Cluster_3, CAUL, CAUR, Fisher, HPCL, HPCR, H_H, IFGR, IPLR, MD_Cluster_1, MD_Cluster_2, MD_Cluster_3, MD_Cluster_4, PrCGL, RD_Cluster_1, TPL, WFNS1n, age, gender, location1, location2, mOFCR, mRSin, mod_educationyear
VarianceThreshold	NaiveBayes	27	0.861363636	0.854611909	0.192057688	-0.122015369	0.204410705	1	ACCR, AD_Cluster_1, AD_Cluster_2, AD_Cluster_3, CAUL, CAUR, Fisher, HPCL, HPCR, H_H, IFGR, IPLR, MD_Cluster_1, MD_Cluster_2, MD_Cluster_3, MD_Cluster_4, PrCGL, RD_Cluster_1, TPL, WFNS1n, age, gender, location1, location2, mOFCR, mRSin, mod_educationyear
VarianceThreshold	NeuralNetwork	27	0.861363636	0.869498541	0.194338886	-0.084628567	0.503852839	1	ACCR, AD_Cluster_1, AD_Cluster_2, AD_Cluster_3,

SUPPLEMENTARY DATA

									CAUL, CAUR, Fisher, HPCL, HPCR, H_H, IFGR, IPLR, MD_Cluster_1, MD_Cluster_2, MD_Cluster_3, MD_Cluster_4, PrCGL, RD_Cluster_1, TPL, WFNS1n, age, gender, location1, location2, mOFCR, mRSin, mod_educationyear
VarianceThreshold	RandomForest	27	0.890909091	0.889589458	0.16298712	-0.061213464	2.916234822	1	ACCR, AD_Cluster_1, AD_Cluster_2, AD_Cluster_3, CAUL, CAUR, Fisher, HPCL, HPCR, H_H, IFGR, IPLR, MD_Cluster_1, MD_Cluster_2, MD_Cluster_3, MD_Cluster_4, PrCGL, RD_Cluster_1, TPL, WFNS1n, age, gender, location1, location2, mOFCR, mRSin, mod_educationyear
VarianceThreshold	SVM	27	0.613636364	0.652132183	0.244611124	-0.304083685	0.572006611	1	ACCR, AD_Cluster_1, AD_Cluster_2, AD_Cluster_3, CAUL, CAUR, Fisher, HPCL, HPCR, H_H, IFGR, IPLR,

SUPPLEMENTARY DATA

									MD_Cluster_1, MD_Cluster_2, MD_Cluster_3, MD_Cluster_4, PrCGL, RD_Cluster_1, TPL, WFNS1n, age, gender, location1, location2, mOFCR, mRSin, mod_educationyear
VarianceThreshold	XGBoost	27	0.925	0.923500046	0.117463879	0.43091591	1.866263153	1	ACCR, AD_Cluster_1, AD_Cluster_2, AD_Cluster_3, CAUL, CAUR, Fisher, HPCL, HPCR, H_H, IFGR, IPLR, MD_Cluster_1, MD_Cluster_2, MD_Cluster_3, MD_Cluster_4, PrCGL, RD_Cluster_1, TPL, WFNS1n, age, gender, location1, location2, mOFCR, mRSin, mod_educationyear
VarianceThreshold	RidgeRegression	27	0.877272727	0.850595394	0.151877341	-0.181768947	2.038927263	1	ACCR, AD_Cluster_1, AD_Cluster_2, AD_Cluster_3, CAUL, CAUR, Fisher, HPCL, HPCR, H_H, IFGR, IPLR, MD_Cluster_1, MD_Cluster_2, MD_Cluster_3, MD_Cluster_4,

									PrCGL, RD_Cluster_1, TPL, WFNS1n, age, gender, location1, location2, mOFCR, mRSin, mod_educationyear
ForwardSelection	LogisticRegression	6	0.875	0.825461883	0.168620294	-0.033545365	2.902553557	0.46031746	AD_Cluster_2, AD_Cluster_3, CAUL, CAUR, IFGR, IPLR
ForwardSelection	NaiveBayes	6	0.829545455	0.802053225	0.218408686	-0.029059978	0.256085403	0.46031746	AD_Cluster_2, AD_Cluster_3, CAUL, CAUR, IFGR, IPLR
ForwardSelection	NeuralNetwork	6	0.881818182	0.845100442	0.163142051	0.147866122	0.336048962	0.46031746	AD_Cluster_2, AD_Cluster_3, CAUL, CAUR, IFGR, IPLR
ForwardSelection	RandomForest	6	0.918181818	0.917902039	0.125126028	-0.102026741	2.295147864	0.46031746	AD_Cluster_2, AD_Cluster_3, CAUL, CAUR, IFGR, IPLR
ForwardSelection	SVM	6	0.859090909	0.844253358	0.152721444	-0.054786892	0.992490599	0.46031746	AD_Cluster_2, AD_Cluster_3, CAUL, CAUR, IFGR, IPLR
ForwardSelection	XGBoost	6	0.936363636	0.930913313	0.117219012	0.641295442	1.576893404	0.46031746	AD_Cluster_2, AD_Cluster_3, CAUL, CAUR, IFGR, IPLR
ForwardSelection	RidgeRegression	6	0.893181818	0.840615755	0.15774627	0.21988467	2.307907669	0.46031746	AD_Cluster_2, AD_Cluster_3, CAUL, CAUR, IFGR, IPLR
NoFeatureSelection	LogisticRegression	27	0.9	0.88214529	0.140274006	-0.32931772	1.396453907	1	ACCR, AD_Cluster_1, AD_Cluster_2, AD_Cluster_3, CAUL, CAUR, Fisher, HPCL, HPCR, H_H, IFGR, IPLR, MD_Cluster_1,

SUPPLEMENTARY DATA

									MD_Cluster_2, MD_Cluster_3, MD_Cluster_4, PrCGL, RD_Cluster_1, TPL, WFNS1n, age, gender, location1, location2, mOFCR, mRSin, mod_educationyear
NoFeatureSelection	NaiveBayes	27	0.861363636	0.854611909	0.192057688	-0.122015369	0.204410705	1	ACCR, AD_Cluster_1, AD_Cluster_2, AD_Cluster_3, CAUL, CAUR, Fisher, HPCL, HPCR, H_H, IFGR, IPLR, MD_Cluster_1, MD_Cluster_2, MD_Cluster_3, MD_Cluster_4, PrCGL, RD_Cluster_1, TPL, WFNS1n, age, gender, location1, location2, mOFCR, mRSin, mod_educationyear
NoFeatureSelection	NeuralNetwork	27	0.861363636	0.869498541	0.194338886	-0.084628567	0.503852839	1	ACCR, AD_Cluster_1, AD_Cluster_2, AD_Cluster_3, CAUL, CAUR, Fisher, HPCL, HPCR, H_H, IFGR, IPLR, MD_Cluster_1, MD_Cluster_2, MD_Cluster_3, MD_Cluster_4, PrCGL,

									RD_Cluster_1, TPL, WFNS1n, age, gender, location1, location2, mOFCR, mRSin, mod_educationyear
NoFeatureSelection	RandomForest	27	0.890909091	0.889589458	0.16298712	-0.061213464	2.916234822	1	ACCR, AD_Cluster_1, AD_Cluster_2, AD_Cluster_3, CAUL, CAUR, Fisher, HPCL, HPCR, H_H, IFGR, IPLR, MD_Cluster_1, MD_Cluster_2, MD_Cluster_3, MD_Cluster_4, PrCGL, RD_Cluster_1, TPL, WFNS1n, age, gender, location1, location2, mOFCR, mRSin, mod_educationyear
NoFeatureSelection	SVM	27	0.613636364	0.652132183	0.244611124	-0.304083685	0.572006611	1	ACCR, AD_Cluster_1, AD_Cluster_2, AD_Cluster_3, CAUL, CAUR, Fisher, HPCL, HPCR, H_H, IFGR, IPLR, MD_Cluster_1, MD_Cluster_2, MD_Cluster_3, MD_Cluster_4, PrCGL, RD_Cluster_1, TPL, WFNS1n, age, gender, location1,

SUPPLEMENTARY DATA

									location2, mOFCR, mRSin, mod_educationyear
NoFeatureSelection	XGBoost	27	0.925	0.923500046	0.117463879	0.43091591	1.866263153	1	ACCR, AD_Cluster_1, AD_Cluster_2, AD_Cluster_3, CAUL, CAUR, Fisher, HPCL, HPCR, H_H, IFGR, IPLR, MD_Cluster_1, MD_Cluster_2, MD_Cluster_3, MD_Cluster_4, PrCGL, RD_Cluster_1, TPL, WFNS1n, age, gender, location1, location2, mOFCR, mRSin, mod_educationyear
NoFeatureSelection	RidgeRegression	27	0.877272727	0.850595394	0.151877341	-0.181768947	2.038927263	1	ACCR, AD_Cluster_1, AD_Cluster_2, AD_Cluster_3, CAUL, CAUR, Fisher, HPCL, HPCR, H_H, IFGR, IPLR, MD_Cluster_1, MD_Cluster_2, MD_Cluster_3, MD_Cluster_4, PrCGL, RD_Cluster_1, TPL, WFNS1n, age, gender, location1, location2, mOFCR, mRSin, mod_educationyear

SUPPLEMENTARY DATA

SUPPLEMENTARY DATA

Supplemental table 8. Core plus CSF full selector–learner _all 91 candidates screening output.

selector	model	n_selected_features	oof_AUROC	oof_AUPRC	oof_Brier	oof_cal_intercept	oof_cal_slope	feature_stability	selected_features
LASSO	LogisticRegression	2	0.706521739	0.652172511	0.234415252	-0.137495178	0.283934186	0.193181818	CSF_ab42, CSF_ptau_tau
LASSO	NaiveBayes	2	0.675724638	0.655720347	0.282557192	-0.058587389	0.060506245	0.193181818	CSF_ab42, CSF_ptau_tau
LASSO	NeuralNetwork	2	0.652173913	0.613918525	0.2877226	-0.115942825	0.064974367	0.193181818	CSF_ab42, CSF_ptau_tau
LASSO	RandomForest	2	0.663949275	0.591595962	0.249304154	-0.023620289	0.192705894	0.193181818	CSF_ab42, CSF_ptau_tau
LASSO	SVM	2	0.509057971	0.537279326	0.255149516	0.106901639	0.446602502	0.193181818	CSF_ab42, CSF_ptau_tau
LASSO	XGBoost	2	0.704710145	0.671943359	0.237676693	-0.005967236	0.471260087	0.193181818	CSF_ab42, CSF_ptau_tau
LASSO	RidgeRegression	2	0.673913043	0.625654675	0.245456917	-0.065909094	0.054096413	0.193181818	CSF_ab42, CSF_ptau_tau
ElasticNet	LogisticRegression	6	0.679347826	0.626069327	0.244600594	-0.072436858	0.108544865	0.293831169	CSF_Tau, CSF_ab42, CSF_ab42_ab40, CSF_ptau_tau, WFNS1n, mRSin
ElasticNet	NaiveBayes	6	0.69384058	0.67928551	0.302388817	-0.106276349	0.079089931	0.293831169	CSF_Tau, CSF_ab42, CSF_ab42_ab40, CSF_ptau_tau, WFNS1n, mRSin
ElasticNet	NeuralNetwork	6	0.677536232	0.641524679	0.287780837	-0.229963635	0.090743808	0.293831169	CSF_Tau, CSF_ab42, CSF_ab42_ab40, CSF_ptau_tau, WFNS1n, mRSin
ElasticNet	RandomForest	6	0.702898551	0.619172497	0.221996427	-0.05045505	0.509693959	0.293831169	CSF_Tau, CSF_ab42, CSF_ab42_ab40, CSF_ptau_tau, WFNS1n, mRSin
ElasticNet	SVM	6	0.608695652	0.656927853	0.245594179	0.185368744	0.684249343	0.293831169	CSF_Tau, CSF_ab42, CSF_ab42_ab40, CSF_ptau_tau, WFNS1n, mRSin
ElasticNet	XGBoost	6	0.727355072	0.695508071	0.230877673	-0.043543833	0.404454889	0.293831169	CSF_Tau, CSF_ab42, CSF_ab42_ab40,

									CSF_ptau_tau, WFNS1n, mRSin
ElasticNet	RidgeRegression	6	0.679347826	0.639012374	0.241229444	-0.098041932	0.26328094	0.293831169	CSF_Tau, CSF_ab42, CSF_ab42_ab40, CSF_ptau_tau, WFNS1n, mRSin
RFE	LogisticRegression	5	0.596014493	0.715104713	0.248724596	-0.01533999	0.388140128	0.369047619	CSF_ab42_ab40, CSF_ptau_tau, Fisher, location1, mRSin
RFE	NaiveBayes	5	0.695652174	0.753161896	0.253001809	0.013241654	0.124879885	0.369047619	CSF_ab42_ab40, CSF_ptau_tau, Fisher, location1, mRSin
RFE	NeuralNetwork	5	0.570652174	0.647070497	0.360311042	-0.090646615	0.103621125	0.369047619	CSF_ab42_ab40, CSF_ptau_tau, Fisher, location1, mRSin
RFE	RandomForest	5	0.708333333	0.710927723	0.223218224	0.019741487	0.506098034	0.369047619	CSF_ab42_ab40, CSF_ptau_tau, Fisher, location1, mRSin
RFE	SVM	5	0.586956522	0.627827674	0.259390381	0.027663805	0.292054394	0.369047619	CSF_ab42_ab40, CSF_ptau_tau, Fisher, location1, mRSin
RFE	XGBoost	5	0.691123188	0.706941744	0.247071545	-0.10946676	0.364611227	0.369047619	CSF_ab42_ab40, CSF_ptau_tau, Fisher, location1, mRSin
RFE	RidgeRegression	5	0.579710145	0.679629026	0.250952173	-0.010744999	0.407529878	0.369047619	CSF_ab42_ab40, CSF_ptau_tau, Fisher, location1, mRSin
PCA	LogisticRegression	11	0.614130435	0.601566607	0.275032545	-0.056806295	0.081333415	0.939393939	PC1, PC2, PC3, PC4, PC5, PC6, PC7, PC8, PC9, PC10, PC11
PCA	NaiveBayes	11	0.645833333	0.605721891	0.276117111	-0.071416841	0.03076368	0.939393939	PC1, PC2, PC3, PC4, PC5, PC6, PC7, PC8, PC9, PC10, PC11
PCA	NeuralNetwork	11	0.690217391	0.721806058	0.264179814	-0.064000045	0.158230399	0.939393939	PC1, PC2, PC3, PC4, PC5, PC6,

									PC7, PC8, PC9, PC10, PC11
PCA	RandomForest	11	0.701086957	0.704466058	0.222456649	0.000553729	0.842256536	0.939393939	PC1, PC2, PC3, PC4, PC5, PC6, PC7, PC8, PC9, PC10, PC11
PCA	SVM	11	0.240942029	0.361680695	0.316672086	-0.727872777	-2.209188378	0.939393939	PC1, PC2, PC3, PC4, PC5, PC6, PC7, PC8, PC9, PC10, PC11
PCA	XGBoost	11	0.661231884	0.645648158	0.256854455	0.086057677	0.338633192	0.939393939	PC1, PC2, PC3, PC4, PC5, PC6, PC7, PC8, PC9, PC10, PC11
PCA	RidgeRegression	11	0.653985507	0.634764194	0.240487205	-0.091686727	0.53210958	0.939393939	PC1, PC2, PC3, PC4, PC5, PC6, PC7, PC8, PC9, PC10, PC11
Boruta	LogisticRegression	5	0.541666667	0.541146568	0.274057581	-0.081409278	0.099856053	0.352380952	CSF_Tau, CSF_ab42, CSF_ab42_ab40, CSF_ptau_ab42, CSF_ptau_tau
Boruta	NaiveBayes	5	0.652173913	0.62615513	0.286515045	-0.080043088	0.072277249	0.352380952	CSF_Tau, CSF_ab42, CSF_ab42_ab40, CSF_ptau_ab42, CSF_ptau_tau
Boruta	NeuralNetwork	5	0.708333333	0.728699967	0.254672693	-0.182958628	0.160216681	0.352380952	CSF_Tau, CSF_ab42, CSF_ab42_ab40, CSF_ptau_ab42, CSF_ptau_tau
Boruta	RandomForest	5	0.698369565	0.6848283	0.23603375	-0.002712882	0.142788787	0.352380952	CSF_Tau, CSF_ab42, CSF_ab42_ab40, CSF_ptau_ab42, CSF_ptau_tau
Boruta	SVM	5	0.527173913	0.595612435	0.26733333	0.023358575	0.218421503	0.352380952	CSF_Tau, CSF_ab42, CSF_ab42_ab40, CSF_ptau_ab42, CSF_ptau_tau
Boruta	XGBoost	5	0.735507246	0.724691663	0.224744772	-0.016149968	0.491140144	0.352380952	CSF_Tau, CSF_ab42, CSF_ab42_ab40,

									CSF_ptau_ab42, CSF_ptau_tau
Boruta	RidgeRegression	5	0.53442029	0.534971663	0.26204163	-0.050113237	0.028224394	0.352380952	CSF_Tau, CSF_ab42, CSF_ab42_ab40, CSF_ptau_ab42, CSF_ptau_tau
MutualInfo	LogisticRegression	5	0.670289855	0.643809066	0.255532434	-0.04506924	0.004533017	0.222222222	CSF_Tau, CSF_ab42, CSF_ptau_ab42, CSF_ptau_tau, Fisher
MutualInfo	NaiveBayes	5	0.621376812	0.608961464	0.339978453	-0.024524662	0.043288056	0.222222222	CSF_Tau, CSF_ab42, CSF_ptau_ab42, CSF_ptau_tau, Fisher
MutualInfo	NeuralNetwork	5	0.615942029	0.587959234	0.321223992	-0.013699906	0.07807581	0.222222222	CSF_Tau, CSF_ab42, CSF_ptau_ab42, CSF_ptau_tau, Fisher
MutualInfo	RandomForest	5	0.634057971	0.593063388	0.280227876	-0.075937957	0.192244703	0.222222222	CSF_Tau, CSF_ab42, CSF_ptau_ab42, CSF_ptau_tau, Fisher
MutualInfo	SVM	5	0.572463768	0.622308425	0.247623887	0.016422631	0.526169514	0.222222222	CSF_Tau, CSF_ab42, CSF_ptau_ab42, CSF_ptau_tau, Fisher
MutualInfo	XGBoost	5	0.692028986	0.697787825	0.264477467	-0.052167951	0.344543751	0.222222222	CSF_Tau, CSF_ab42, CSF_ptau_ab42, CSF_ptau_tau, Fisher
MutualInfo	RidgeRegression	5	0.626811594	0.607257121	0.257852008	-0.057999401	0.060186226	0.222222222	CSF_Tau, CSF_ab42, CSF_ptau_ab42, CSF_ptau_tau, Fisher
Pearson	LogisticRegression	5	0.664855072	0.633649517	0.241297805	-0.099811856	0.215555602	0.30952381	CSF_ab42, CSF_Tau, CSF_ptau_tau,

									CSF_ab42_ab40, mRSin
Pearson	NaiveBayes	5	0.695652174	0.685323714	0.26630289	-0.063398214	0.081542545	0.30952381	CSF_ab42, CSF_Tau, CSF_ptau_tau, CSF_ab42_ab40, mRSin
Pearson	NeuralNetwork	5	0.624094203	0.626957424	0.320428158	-0.111709041	0.063617752	0.30952381	CSF_ab42, CSF_Tau, CSF_ptau_tau, CSF_ab42_ab40, mRSin
Pearson	RandomForest	5	0.705615942	0.671898342	0.232914687	-0.02017277	0.420214536	0.30952381	CSF_ab42, CSF_Tau, CSF_ptau_tau, CSF_ab42_ab40, mRSin
Pearson	SVM	5	0.512681159	0.548281511	0.262977379	-0.048237357	0.198077123	0.30952381	CSF_ab42, CSF_Tau, CSF_ptau_tau, CSF_ab42_ab40, mRSin
Pearson	XGBoost	5	0.710144928	0.700746352	0.236670243	-0.008882338	0.432507684	0.30952381	CSF_ab42, CSF_Tau, CSF_ptau_tau, CSF_ab42_ab40, mRSin
Pearson	RidgeRegression	5	0.641304348	0.624062626	0.245807247	-0.080955507	0.248145963	0.30952381	CSF_ab42, CSF_Tau, CSF_ptau_tau, CSF_ab42_ab40, mRSin
Spearman	LogisticRegression	5	0.684782609	0.6377694	0.234582814	-0.123515887	0.251911039	1	CSF_ab42, CSF_ptau_tau, CSF_ptau_ab42, CSF_Tau, CSF_ab42_ab40
Spearman	NaiveBayes	5	0.737318841	0.703263838	0.225416148	-0.060133895	0.100863831	1	CSF_ab42, CSF_ptau_tau, CSF_ptau_ab42, CSF_Tau, CSF_ab42_ab40
Spearman	NeuralNetwork	5	0.75	0.720723514	0.214755086	-0.156894942	0.143632198	1	CSF_ab42, CSF_ptau_tau, CSF_ptau_ab42,

									CSF_Tau, CSF_ab42_ab40
Spearman	RandomForest	5	0.726449275	0.707851118	0.221716446	-0.102351319	0.367497861	1	CSF_ab42, CSF_ptau_tau, CSF_ptau_ab42, CSF_Tau, CSF_ab42_ab40
Spearman	SVM	5	0.577898551	0.665095875	0.250599319	-0.115771867	0.51062275	1	CSF_ab42, CSF_ptau_tau, CSF_ptau_ab42, CSF_Tau, CSF_ab42_ab40
Spearman	XGBoost	5	0.738224638	0.723126808	0.229883692	-0.081650475	0.430293649	1	CSF_ab42, CSF_ptau_tau, CSF_ptau_ab42, CSF_Tau, CSF_ab42_ab40
Spearman	RidgeRegression	5	0.686594203	0.637004083	0.24109026	-0.078920006	0.154632061	1	CSF_ab42, CSF_ptau_tau, CSF_ptau_ab42, CSF_Tau, CSF_ab42_ab40
Kendall	LogisticRegression	5	0.684782609	0.6377694	0.234582814	-0.123515887	0.251911039	1	CSF_ab42, CSF_ptau_tau, CSF_ptau_ab42, CSF_Tau, CSF_ab42_ab40
Kendall	NaiveBayes	5	0.737318841	0.703263838	0.225416148	-0.060133895	0.100863831	1	CSF_ab42, CSF_ptau_tau, CSF_ptau_ab42, CSF_Tau, CSF_ab42_ab40
Kendall	NeuralNetwork	5	0.75	0.720723514	0.214755086	-0.156894942	0.143632198	1	CSF_ab42, CSF_ptau_tau, CSF_ptau_ab42, CSF_Tau, CSF_ab42_ab40
Kendall	RandomForest	5	0.726449275	0.707851118	0.221716446	-0.102351319	0.367497861	1	CSF_ab42, CSF_ptau_tau, CSF_ptau_ab42, CSF_Tau, CSF_ab42_ab40
Kendall	SVM	5	0.577898551	0.665095875	0.250599319	-0.115771867	0.51062275	1	CSF_ab42, CSF_ptau_tau, CSF_ptau_ab42,

									CSF_Tau, CSF_ab42_ab40
Kendall	XGBoost	5	0.738224638	0.723126808	0.229883692	-0.081650475	0.430293649	1	CSF_ab42, CSF_ptau_tau, CSF_ptau_ab42, CSF_Tau, CSF_ab42_ab40
Kendall	RidgeRegression	5	0.686594203	0.637004083	0.24109026	-0.078920006	0.154632061	1	CSF_ab42, CSF_ptau_tau, CSF_ptau_ab42, CSF_Tau, CSF_ab42_ab40
ANOVA_F	LogisticRegression	5	0.664855072	0.633649517	0.241297805	-0.099811856	0.215555602	0.30952381	CSF_Tau, CSF_ab42, CSF_ab42_ab40, CSF_ptau_tau, mRSin
ANOVA_F	NaiveBayes	5	0.695652174	0.685323714	0.26630289	-0.063398214	0.081542545	0.30952381	CSF_Tau, CSF_ab42, CSF_ab42_ab40, CSF_ptau_tau, mRSin
ANOVA_F	NeuralNetwork	5	0.675724638	0.708175928	0.286018093	-0.128375195	0.118151451	0.30952381	CSF_Tau, CSF_ab42, CSF_ab42_ab40, CSF_ptau_tau, mRSin
ANOVA_F	RandomForest	5	0.697463768	0.641185377	0.228703184	-0.011991287	0.447778747	0.30952381	CSF_Tau, CSF_ab42, CSF_ab42_ab40, CSF_ptau_tau, mRSin
ANOVA_F	SVM	5	0.512681159	0.548281511	0.262977379	-0.048237357	0.198077123	0.30952381	CSF_Tau, CSF_ab42, CSF_ab42_ab40, CSF_ptau_tau, mRSin
ANOVA_F	XGBoost	5	0.719202899	0.700499058	0.236959334	0.026988031	0.404335203	0.30952381	CSF_Tau, CSF_ab42, CSF_ab42_ab40, CSF_ptau_tau, mRSin
ANOVA_F	RidgeRegression	5	0.641304348	0.624062626	0.245807247	-0.080955507	0.248145963	0.30952381	CSF_Tau, CSF_ab42, CSF_ab42_ab40,

									CSF_ptau_tau, mRSin
VarianceThreshold	LogisticRegression	17	0.637681159	0.640092961	0.25654038	-0.075222391	0.087775937	1	CSF_Tau, CSF_ab40, CSF_ab42, CSF_ab42_ab40, CSF_pTau, CSF_ptau_ab42, CSF_ptau_tau, CSF_tau_ab42, Fisher, H_H, WFNS1n, age, gender, location1, location2, mRSin, mod_educationyear
VarianceThreshold	NaiveBayes	17	0.701086957	0.689696237	0.302319761	-0.080514038	0.078958318	1	CSF_Tau, CSF_ab40, CSF_ab42, CSF_ab42_ab40, CSF_pTau, CSF_ptau_ab42, CSF_ptau_tau, CSF_tau_ab42, Fisher, H_H, WFNS1n, age, gender, location1, location2, mRSin, mod_educationyear
VarianceThreshold	NeuralNetwork	17	0.56884058	0.594020001	0.397373066	-0.110767559	0.043062452	1	CSF_Tau, CSF_ab40, CSF_ab42, CSF_ab42_ab40, CSF_pTau, CSF_ptau_ab42, CSF_ptau_tau, CSF_tau_ab42, Fisher, H_H, WFNS1n, age, gender, location1,

SUPPLEMENTARY DATA

									location2, mRSin, mod_educationyear
VarianceThreshold	RandomForest	17	0.721014493	0.63762412	0.216325244	-0.103041147	0.596414538	1	CSF_Tau, CSF_ab40, CSF_ab42, CSF_ab42_ab40, CSF_pTau, CSF_ptau_ab42, CSF_ptau_tau, CSF_tau_ab42, Fisher, H_H, WFNS1n, age, gender, location1, location2, mRSin, mod_educationyear
VarianceThreshold	SVM	17	0.351449275	0.449597926	0.312276034	-0.21346694	-0.400945682	1	CSF_Tau, CSF_ab40, CSF_ab42, CSF_ab42_ab40, CSF_pTau, CSF_ptau_ab42, CSF_ptau_tau, CSF_tau_ab42, Fisher, H_H, WFNS1n, age, gender, location1, location2, mRSin, mod_educationyear
VarianceThreshold	XGBoost	17	0.744565217	0.756356262	0.236186611	-0.060954009	0.408418926	1	CSF_Tau, CSF_ab40, CSF_ab42, CSF_ab42_ab40, CSF_pTau, CSF_ptau_ab42, CSF_ptau_tau, CSF_tau_ab42, Fisher, H_H, WFNS1n, age,

									gender, location1, location2, mRSin, mod_educationyear
VarianceThreshold	RidgeRegression	17	0.610507246	0.595686077	0.262329887	-0.058141189	0.041354736	1	CSF_Tau, CSF_ab40, CSF_ab42, CSF_ab42_ab40, CSF_pTau, CSF_ptau_ab42, CSF_ptau_tau, CSF_tau_ab42, Fisher, H_H, WFNS1n, age, gender, location1, location2, mRSin, mod_educationyear
ForwardSelection	LogisticRegression	5	0.71557971	0.755683169	0.211447543	-0.052615471	0.68857133	0.30952381	CSF_ab42_ab40, CSF_ptau_ab42, CSF_ptau_tau, Fisher, mRSin
ForwardSelection	NaiveBayes	5	0.77173913	0.80321007	0.211726129	0.024790359	0.157508166	0.30952381	CSF_ab42_ab40, CSF_ptau_ab42, CSF_ptau_tau, Fisher, mRSin
ForwardSelection	NeuralNetwork	5	0.664855072	0.726643159	0.275737063	-0.015352984	0.167469648	0.30952381	CSF_ab42_ab40, CSF_ptau_ab42, CSF_ptau_tau, Fisher, mRSin
ForwardSelection	RandomForest	5	0.762681159	0.700218565	0.205865172	0.044863383	0.417828967	0.30952381	CSF_ab42_ab40, CSF_ptau_ab42, CSF_ptau_tau, Fisher, mRSin
ForwardSelection	SVM	5	0.400362319	0.43553977	0.301042058	-0.074132891	-0.490501709	0.30952381	CSF_ab42_ab40, CSF_ptau_ab42, CSF_ptau_tau, Fisher, mRSin
ForwardSelection	XGBoost	5	0.758152174	0.703044442	0.206599768	0.009116358	0.558863892	0.30952381	CSF_ab42_ab40, CSF_ptau_ab42, CSF_ptau_tau, Fisher, mRSin

SUPPLEMENTARY DATA

ForwardSelection	RidgeRegression	5	0.702898551	0.750082699	0.21584051	0.052494723	1.390204226	0.30952381	CSF_ab42_ab40, CSF_ptau_ab42, CSF_ptau_tau, Fisher, mRSin
NoFeatureSelection	LogisticRegression	17	0.637681159	0.640092961	0.25654038	-0.075222391	0.087775937	1	CSF_Tau, CSF_ab40, CSF_ab42, CSF_ab42_ab40, CSF_pTau, CSF_ptau_ab42, CSF_ptau_tau, CSF_tau_ab42, Fisher, H_H, WFNS1n, age, gender, location1, location2, mRSin, mod_educationyear
NoFeatureSelection	NaiveBayes	17	0.701086957	0.689696237	0.302319761	-0.080514038	0.078958318	1	CSF_Tau, CSF_ab40, CSF_ab42, CSF_ab42_ab40, CSF_pTau, CSF_ptau_ab42, CSF_ptau_tau, CSF_tau_ab42, Fisher, H_H, WFNS1n, age, gender, location1, location2, mRSin, mod_educationyear
NoFeatureSelection	NeuralNetwork	17	0.56884058	0.594020001	0.397373066	-0.110767559	0.043062452	1	CSF_Tau, CSF_ab40, CSF_ab42, CSF_ab42_ab40, CSF_pTau, CSF_ptau_ab42, CSF_ptau_tau, CSF_tau_ab42, Fisher, H_H, WFNS1n, age,

									gender, location1, location2, mRSin, mod_educationyear
NoFeatureSelection	RandomForest	17	0.721014493	0.63762412	0.216325244	-0.103041147	0.596414538	1	CSF_Tau, CSF_ab40, CSF_ab42, CSF_ab42_ab40, CSF_pTau, CSF_ptau_ab42, CSF_ptau_tau, CSF_tau_ab42, Fisher, H_H, WFNS1n, age, gender, location1, location2, mRSin, mod_educationyear
NoFeatureSelection	SVM	17	0.351449275	0.449597926	0.312276034	-0.21346694	-0.400945682	1	CSF_Tau, CSF_ab40, CSF_ab42, CSF_ab42_ab40, CSF_pTau, CSF_ptau_ab42, CSF_ptau_tau, CSF_tau_ab42, Fisher, H_H, WFNS1n, age, gender, location1, location2, mRSin, mod_educationyear
NoFeatureSelection	XGBoost	17	0.744565217	0.756356262	0.236186611	-0.060954009	0.408418926	1	CSF_Tau, CSF_ab40, CSF_ab42, CSF_ab42_ab40, CSF_pTau, CSF_ptau_ab42, CSF_ptau_tau, CSF_tau_ab42,

SUPPLEMENTARY DATA

									Fisher, H_H, WFNS1n, age, gender, location1, location2, mRSin, mod_educationyear
NoFeatureSelection	RidgeRegression	17	0.610507246	0.595686077	0.262329887	-0.058141189	0.041354736	1	CSF_Tau, CSF_ab40, CSF_ab42, CSF_ab42_ab40, CSF_pTau, CSF_ptau_ab42, CSF_ptau_tau, CSF_tau_ab42, Fisher, H_H, WFNS1n, age, gender, location1, location2, mRSin, mod_educationyear

SUPPLEMENTARY DATA

Supplemental table 9. Retained scheme-level strategies after full 13 × 7 selector–learner screening.

scheme	event_rate	n_features_before_scan	strategy	top1_selector	top1_model	top1_oof_AUROC	top1_oof_AUPRC	top1_oof_Brier	top1_oof_cal_slope	selected_keys	selected_features
A_core_clinical	0.536	9	single_best	VarianceThreshold	LogisticRegression	0.607051	0.674646	0.239603	1.084395	VarianceThreshold__LogisticRegression	gender, H_H, Fisher, WFNS1n
B_core_plus_cognitive	0.536	28	single_best	VarianceThreshold	XGBoost	0.996912	0.997116	0.024634	1.530154	VarianceThreshold__XGBoost	AVLT_Recognition, AVLT_long_term_delay, AVLT_short_term_delay, BDS
C_core_plus_blood	0.518519	17	ensemble_top3	VarianceThreshold	LogisticRegression	0.743132	0.716941	0.21261	0.908412	VarianceThreshold__LogisticRegression | NoFeatureSelection__LogisticRegression | VarianceThreshold__NeuralNetwork	Plasma_Tau, Plasma_ab40, WFNS1n, mRSin
D_core_plus_erp	0.5	105	single_best	VarianceThreshold	XGBoost	0.9596	0.956505	0.06842	1.113758	VarianceThreshold__XGBoost	F4_ITPC, CP2_ITPC, F4_Amplitude, CP2_Amplitude, CZ_ITPC
E_core_plus_mri	0.47619	27	single_best	ANOVA_F	XGBoost	0.925	0.92959	0.115693	1.341072	ANOVA_F__XGBoost	CAUL, IFGR, IPLR, mOFCR, mod_educationyear
F_core_plus_csf	0.489362	17	ensemble_top3	Spearman	XGBoost	0.738225	0.723127	0.229884	0.430294	Spearman__XGBoost | Kendall__XGBoost | VarianceThreshold__XGBoost	CSF_Tau, CSF_ab42, CSF_ptau_ab42, CSF_ptau_tau

This table summarizes the retained scheme-level selector–learner strategies after implementation of the full 13 × 7 screening grid within each prespecified modeling scheme. Temporal internal validation was conducted as a secondary same-center drift assessment. Retained strategies represent internally supported signals; no external validation was performed. The grid was used for structured feature discovery and algorithm screening. Downstream bootstrap optimism correction, gate-based assessment, and temporal internal validation were performed using the frozen retained strategy within each scheme, without selector–learner reselection in validation data. Complete grid-level outputs are provided in Supplementary Data S3-8.

Supplemental Table 10. Effective modeling denominator, event count, and validation split by prediction scheme.

scheme	A_core_clinical	B_core_plus_cognitive	C_core_plus_blood	D_core_plus_erp	E_core_plus_mri	F_core_plus_csf
n_total	125	125	54	100	42	47
n_events	67	67	28	50	20	23
n_nonevents	58	58	26	50	22	24
event_rate	0.536	0.536	0.518518519	0.5	0.476190476	0.489361702
n_candidate_predictors_after_column_check	9	28	17	105	27	17
temporal_available	TRUE	TRUE	TRUE	TRUE	TRUE	TRUE
n_early_total	75	75	39	65	27	37
n_early_events	36	36	20	31	12	19
n_temporal_total	50	50	15	35	15	10
n_temporal_events	31	31	8	19	8	4
n_development	57	57	28	49	18	27
n_development_events	28	28	14	23	8	14
n_internal_validation	18	18	11	16	9	10
n_internal_validation_events	8	8	6	8	4	5
tier	main	main	main	main	exploratory	exploratory
n_features_before_scan	9	28	17	105	27	17
strategy	single_best	single_best	ensemble_top3	single_best	single_best	ensemble_top3
top1_selector	VarianceThreshold	VarianceThreshold	VarianceThreshold	VarianceThreshold	ANOVA_F	Spearman
top1_model	LogisticRegression	XGBoost	LogisticRegression	XGBoost	XGBoost	XGBoost
selected_features	gender, H_H, Fisher, WFNS1n	AVLT_Recognition, AVLT_long_term_delay, AVLT_short_term_delay, BDS	Plasma_Tau, Plasma_ab40, WFNS1n, mRSin	F4_ITPC, CP2_ITPC, F4_Amplitude, CP2_Amplitude, CZ_ITPC	CAUL, IFGR, IPLR, mOFCR, mod_educationyear	CSF_Tau, CSF_ab42, CSF_ptau_ab42, CSF_ptau_tau
top1_oof_AUROC	0.607050952	0.996911992	0.743131868	0.9596	0.925	0.738224638
top1_oof_AUPRC	0.67464642	0.997116288	0.716941438	0.956505405	0.92959041	0.723126808
top1_oof_Brier	0.239602976	0.024634389	0.212610091	0.068419996	0.115693012	0.229883692
top1_oof_cal_slope	1.084394905	1.530153722	0.908412029	1.11375789	1.341072095	0.430293649

The temporal subset represents same-center temporal internal validation rather than an independent external validation cohort. Effective denominators differ across schemes because structural modality non-availability was not imputed across MRI, ERP, plasma, and CSF schemes. Temporal validation refers to same-center temporal internal validation. CI = cognitive impairment; ERP = event-related potential; MRI = magnetic resonance imaging; CSF = cerebrospinal fluid.

SUPPLEMENTARY DATA

Supplemental table 11 Calibration and probabilistic prediction error of candidate models in internal and temporal internal validation cohort.

endpoint	Primary endpoint: adjusted MoCA <26	Primary endpoint: adjusted MoCA <26	Primary endpoint: adjusted MoCA <26	Primary endpoint: adjusted MoCA <26	Primary endpoint: adjusted MoCA <26	Primary endpoint: adjusted MoCA <26
model	Model_7_1cognitive	Model_7_1cognitive	Model_8_ERP_F4	Model_8_ERP_F4	Model_9_ERP_CP2	Model_9_ERP_CP2
model_short	Model G	Model G	Model H	Model H	Model I	Model I
model_label	Single cognitive marker	Single cognitive marker	ERP F4 pair	ERP F4 pair	ERP CP2 pair	ERP CP2 pair
cohort	internal	temporal	internal	temporal	internal	temporal
n	18	50	16	35	16	35
events	8	31	8	19	8	19
event_rate	0.444444444	0.62	0.5	0.542857143	0.5	0.542857143
AUROC	0.9875	1	0.9375	0.973684211	1	0.927631579
AUPRC	0.975	1	0.941517857	0.973972159	1	0.90697337
Brier	0.215568567	0.205311305	0.093578947	0.084938243	0.064948968	0.10259313
calibration_intercept	43.43279426	65.39704871	0.216675362	1.348039806	-53.5406898	0.855052613
calibration_slope	432.8786392	680.8520736	1.20112784	1.896073154	98.64088034	1.450831405
HL_p_descriptive	0.000890193	6.42E-07	0.214424795	0.093719486	0.161123838	0.406671048
HL_stat	11.04307078	41.52596815	1.541297385	9.411926875	1.963646783	5.076038646
HL_df	1	7	1	5	1	5
threshold	0.512274832	0.517360888	0.487355403	0.363353653	0.421572654	0.559172682
TP	7	27	7	18	8	15
FP	0	0	1	1	2	1
TN	10	19	7	15	6	15
FN	1	4	1	1	0	4
Sensitivity	0.875	0.870967742	0.875	0.947368421	1	0.789473684
Specificity	1	1	0.875	0.9375	0.75	0.9375
Accuracy	0.944444444	0.92	0.875	0.942857143	0.875	0.857142857
PPV	1	1	0.875	0.947368421	0.8	0.9375
NPV	0.909090909	0.826086957	0.875	0.9375	1	0.789473684
F1	0.933333333	0.931034483	0.875	0.947368421	0.888888889	0.857142857

Calibration metrics were estimated in internal and temporal internal validation cohorts. Temporal internal validation reflects same-center temporal drift assessment and does not establish transportability. Hosmer–Lemeshow P values are reported descriptively only. Calibration interpretation was based primarily on graphical calibration, calibration intercept/slope, and Brier score because Hosmer–Lemeshow testing has limited reliability in small temporal internal validation cohort.

SUPPLEMENTARY DATA

SUPPLEMENTARY DATA

Supplemental table 12. Interval-censored proportional hazards models for ERP risk scores

Cohort	Score	Model	HR (95% CI)	P value
ERP common cohort	ERP F4 pair score	S1 (unadjusted)	35.356 (9.885-126.458)	<0.001
ERP common cohort	ERP F4 pair score	S2 (adjusted)	not reliably estimable because of quasi-complete separation	<0.001
ERP common cohort	ERP CP2 pair score	S1 (unadjusted)	17.660 (6.645-46.938)	<0.001
ERP common cohort	ERP CP2 pair score	S2 (adjusted)	18.453 (6.775-50.259)	<0.001

S1 denotes the unadjusted model. S2 denotes the adjusted model including age, sex, education years, and baseline mRS. HRs are expressed per 1-SD increase in ERP risk score. ERP = event-related potential; CI = confidence interval; mRS = modified Rankin Scale.

Supplemental table 13 Sensitivity analysis using the conservative endpoint of education-adjusted MoCA <23.

Analysis	UIA	aSAH	Contrast / model
Primary endpoint CI, education-adjusted MoCA <26	9/89 (10.1%)	67/125 (53.6%)	—
Conservative endpoint CI, education-adjusted MoCA <23	3/89 (3.4%)	23/125 (18.4%)	—
Reclassified from CI to non-CI	6/89 (6.7%)	44/125 (35.2%)	—
24-month first-detected CI-free survival	90.90%	79.20%	—
RMST24	23.73 months	20.95 months	Difference 2.78 months (95% CI 1.44–3.90)
Prespecified ERP CP2 temporal AUROC	—	—	0.88
Prespecified ERP CP2 temporal AUPRC	—	—	0.682
Prespecified ERP CP2 temporal Brier	—	—	0.172
Prespecified ERP CP2 temporal calibration slope	—	—	2.37

The conservative endpoint was defined as education-adjusted MoCA <23. First-detected CI-free survival was estimated using Turnbull interval-censored methods. RMST was restricted mean first-detected CI-free time up to 24 months, with 95% confidence intervals obtained from 1,000 nonparametric bootstrap resamples. The ERP CP2 model was re-evaluated under the conservative endpoint without repeating feature selection. A calibration slope >1 indicates insufficient spread of predicted risks; therefore, the ERP CP2 calibration slope of 2.37 under the conservative endpoint suggests underfitting or overly conservative predictions and should not be interpreted as deployment-ready calibration. This endpoint-specific analysis was exploratory and should be interpreted as sensitivity evidence rather than confirmatory validation.

SUPPLEMENTARY DATA

Supplemental figure 1. Forest plot of interval-censored proportional hazards models for first-detected cognitive impairment.

Variable	N+	N−	HR (95% CI)	*P*
Patients				
UIA	9	80	1[Ref]	
aSAH	67	58	7.21(3.59-14.49)	**<0.001**
Gender				
Female	53	108	1[Ref]	
Male	23	30	1.42(0.86-2.36)	0.170
Age group				
<=52	19	38	1[Ref]	
53-60	16	39	0.85(0.42-1.72)	0.649
61-67	21	36	1.13(0.58-2.19)	0.712
>67	20	25	1.45(0.74-2.83)	0.277
Education year			0.95(0.91-1.00)	**0.037**
Aneurysm location				
PcomA	34	83	1[Ref]	
AcomA	21	24	1.83(1.01-3.34)	**0.048**
BA	10	18	1.29(0.61-2.70)	0.507
MCA	11	13	1.78(0.89-3.57)	0.102
Left or Right				
Left	29	49	1[Ref]	
Right	25	62	0.73(0.43-1.25)	0.251
Middle	22	27	1.28(0.73-2.25)	0.382
Fisher score				
1	6	10	1[Ref]	
2	52	34	1.98(0.77-5.05)	0.155
3	6	7	1.32(0.39-4.43)	0.657
4	3	7	0.76(0.18-3.13)	0.703

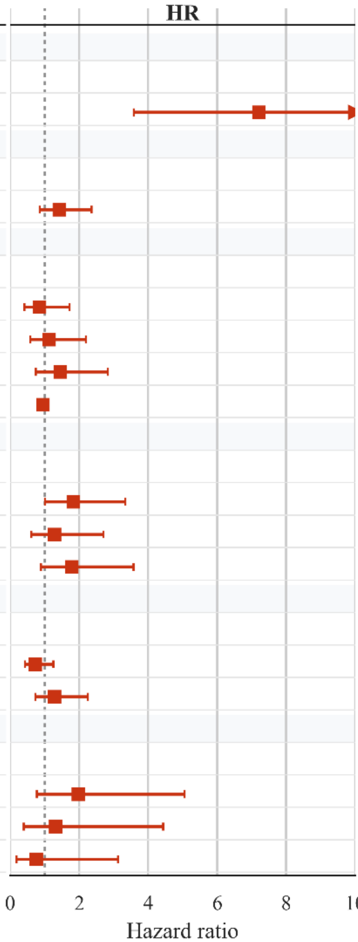

Squares indicate hazard ratios, and horizontal lines indicate 95% confidence intervals. Abbreviations: CI, cognitive impairment; UIA, unruptured intracranial aneurysm; aSAH, aneurysmal subarachnoid hemorrhage; RMST, restricted mean survival time; HR, hazard ratio.

SUPPLEMENTARY DATA

Supplemental figure 2. Kaplan–Meier sensitivity analysis based on time to first-detected CI in the overall cohort of aSAH and UIA patients.

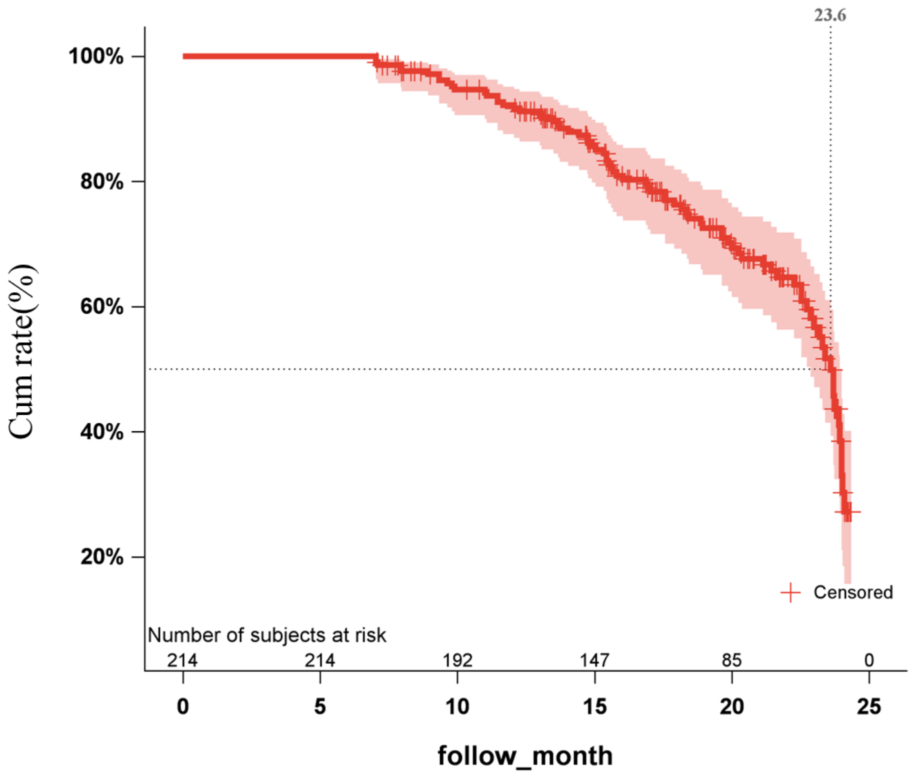

SUPPLEMENTARY DATA

Supplemental figure 3. Exploratory SHAP summaries for prespecified multimodal prediction schemes.

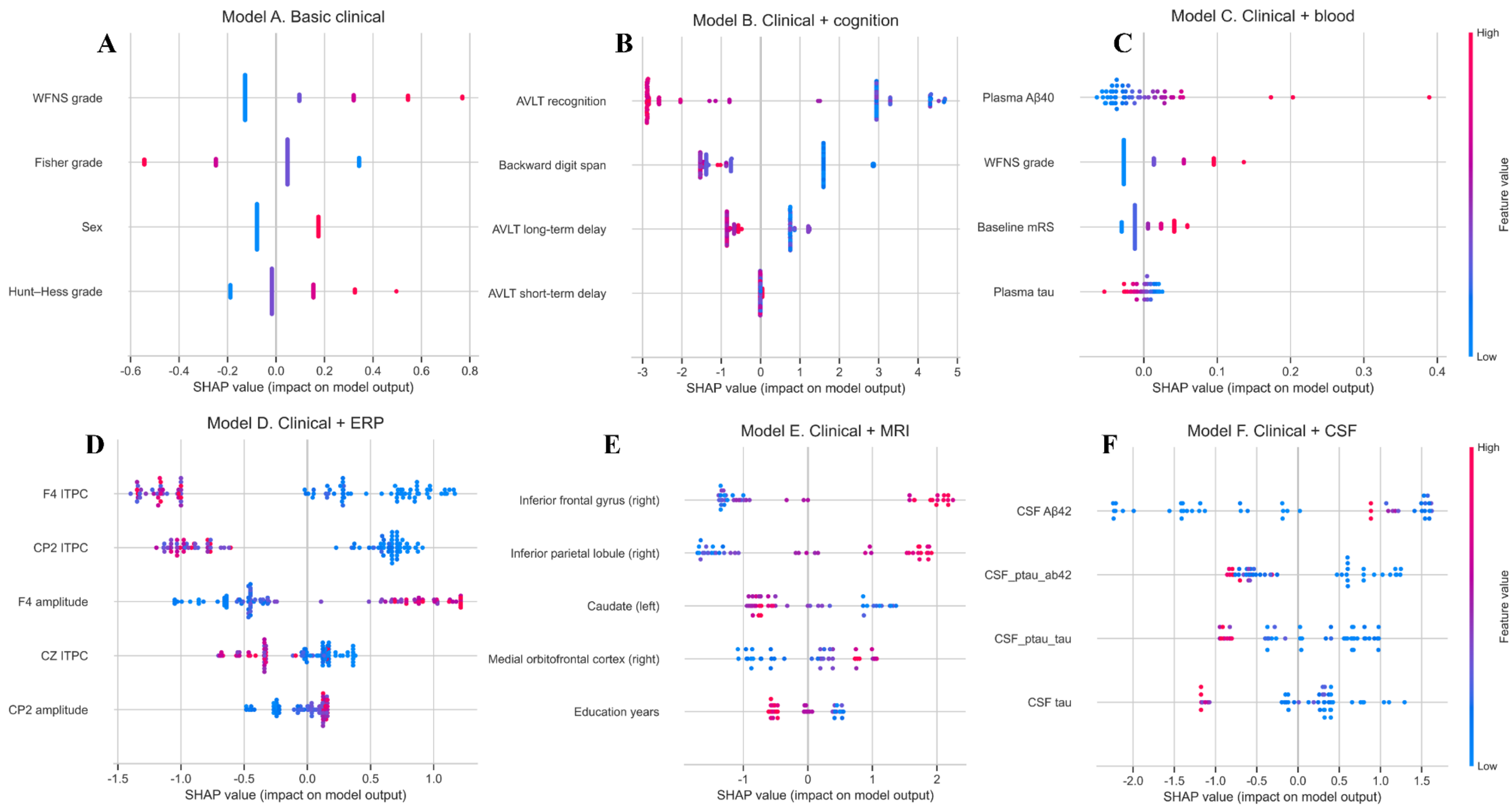

SHAP summary plots are shown for six prespecified resource-stratified schemes: Scheme A, core clinical variables; Scheme B, core clinical plus baseline cognition; Scheme C, core clinical plus plasma biomarkers; Scheme D, core clinical plus ERP-derived features; Scheme E, core clinical plus MRI-derived features; and Scheme F, core clinical plus CSF biomarkers. Each dot represents one participant in the scheme-specific modeling cohort. The x-axis shows the SHAP value, representing the direction and magnitude of each feature's contribution to the model output. Feature color denotes the original feature value, with blue indicating lower values and red indicating higher values. These plots were used for exploratory interpretation and should be considered in the context of scheme-specific sample size and modality availability. SHAP = SHapley Additive exPlanations; ERP = event-related potential; MRI = magnetic resonance imaging; CSF = cerebrospinal fluid.

SUPPLEMENTARY DATA

Supplemental figure 4. Interval-censored first-detected CI-free survival curves comparing low- and high-risk groups for ERP F4 and CP2 pair scores.

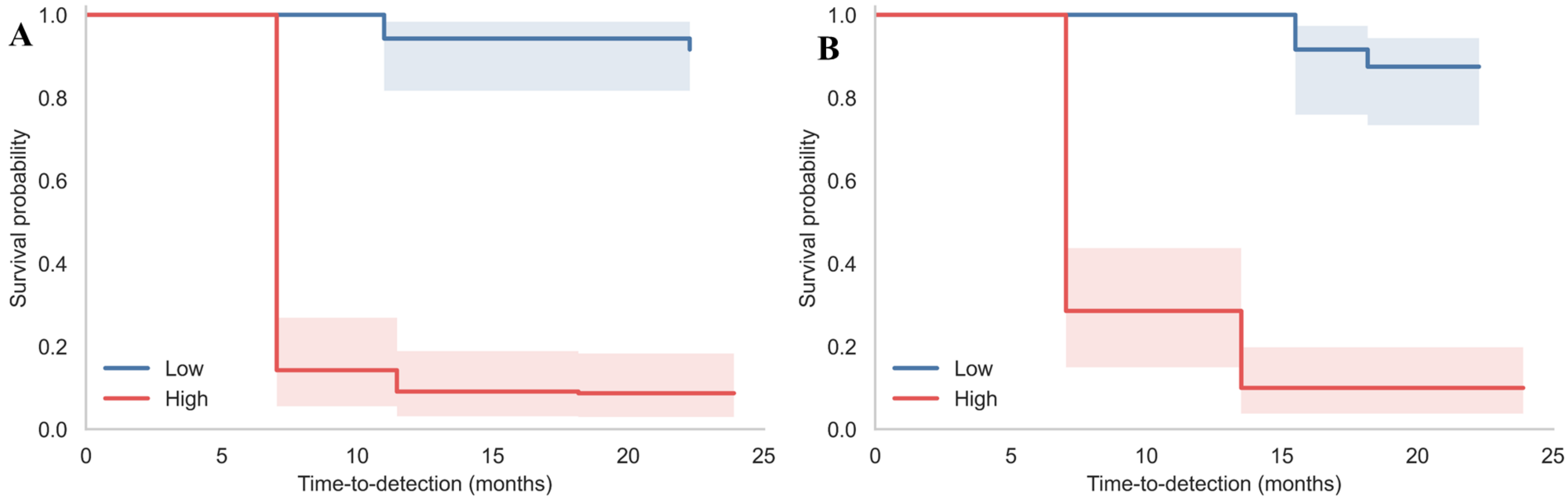

(A) Interval-censored survival curves for the ERP F4 pair score after dichotomization into low- and high-risk groups using the frozen median cutpoint derived from the early cohort. (B) Interval-censored survival curves for the ERP CP2 pair score using the same median-split strategy. Abbreviations: ERP, event-related potential.

SUPPLEMENTARY DATA

Supplemental figure 5. First-detected cognitive impairment–free survival and multivariable risk estimates using the Cox model as a sensitivity analysis.

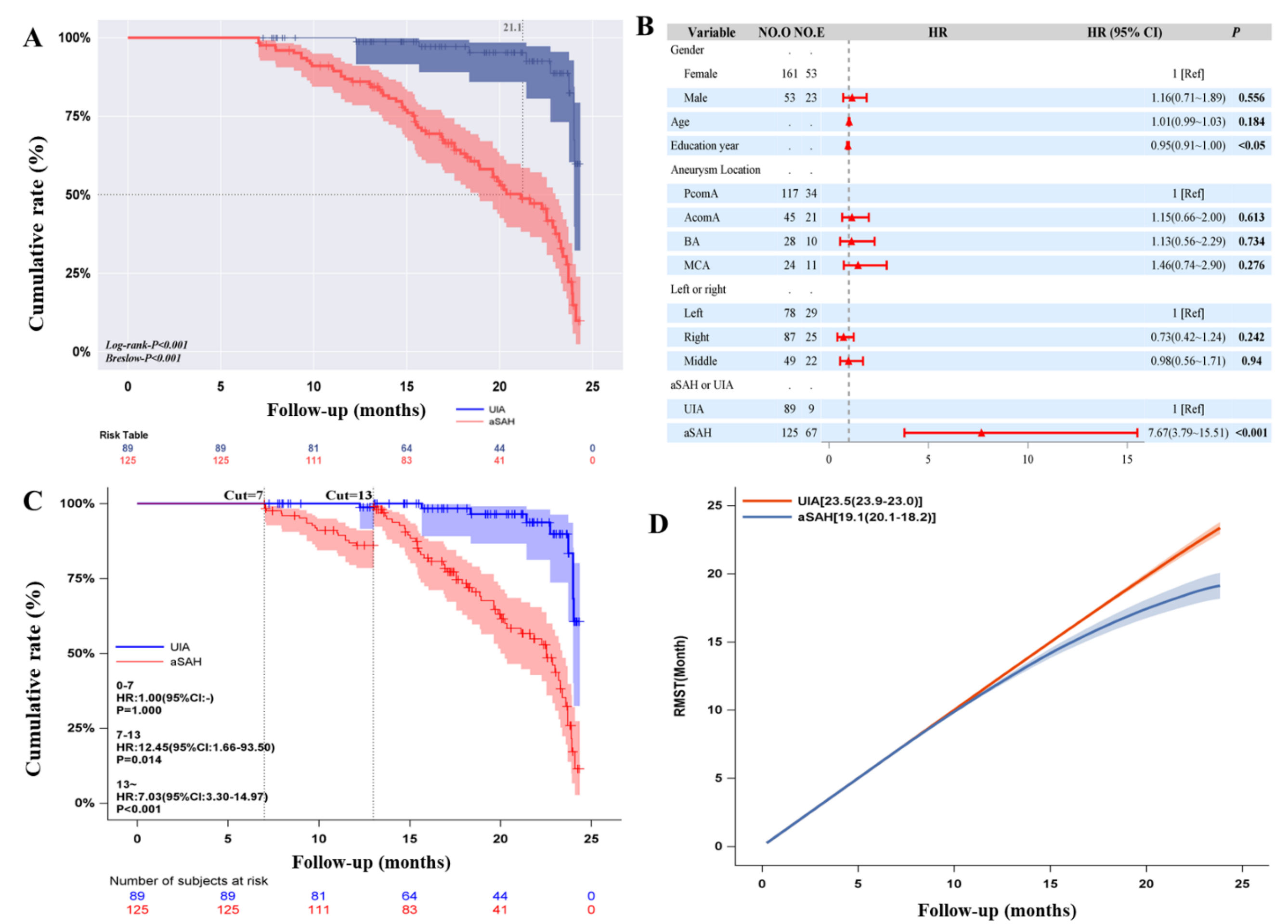

(A) K-M survival curves in patients with UIA and aSAH. Nonparametric estimates were used to depict cognitive impairment (CI)-free survival according to aneurysm group, with shaded areas indicating 95% confidence intervals. Vertical and horizontal dashed lines mark the estimated CI-free survival probabilities at 12, 18, and 24 months. The P value was derived from the Cox group comparison. (B) Cox regression analyses for first-detected cognitive impairment. Forest plot showing hazard ratios (HRs) and 95% confidence intervals from cox regression models for aneurysm group and selected baseline variables. Squares indicate point estimates and horizontal lines indicate 95% confidence intervals. Reference categories are shown as 1. (C) Restricted mean CI-free survival time derived from cox survival estimates in patients with UIA and aSAH. Restricted mean CI-free survival time was calculated by numerically integrating the Turnbull nonparametric cox survival estimates from 0 to 24 months. Shaded bands indicate 95% bootstrap confidence intervals. Abbreviations. CI = cognitive impairment (MoCA <26 at follow-up; +1 point for ≤12 years education); UIA = unruptured intracranial aneurysm; aSAH = aneurysmal subarachnoid hemorrhage.

SUPPLEMENTARY DATA

Supplemental figure 6. Performance of pattern-specific survival models and relative prognostic contributions of different modalities.

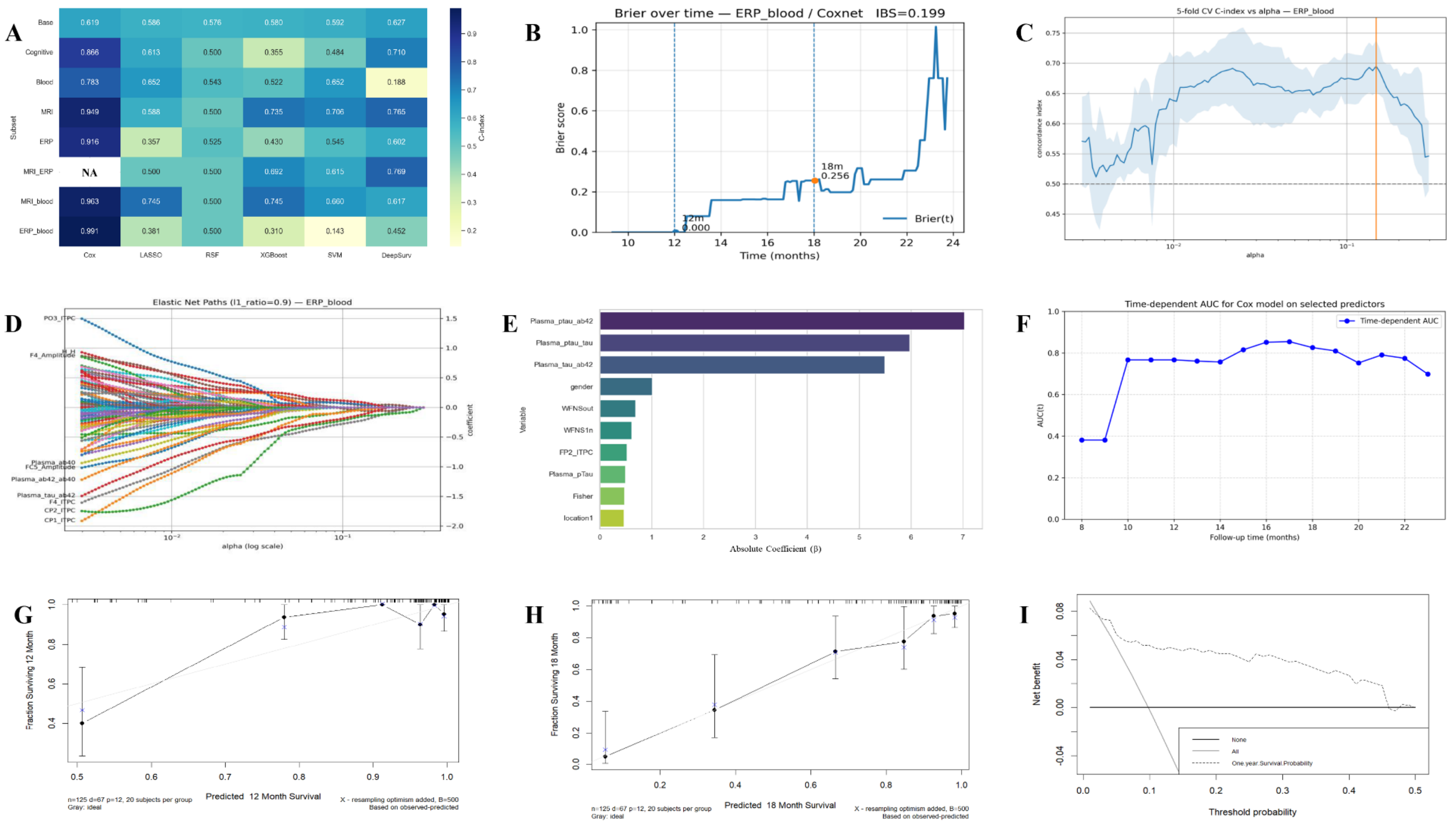

This figure summarizes the pattern-submodel survival sensitivity analysis, which assessed qualitative consistency under a time-to-detection framework. It did not contribute to primary binary model selection or final model locking. (A) C-index heatmap for all algorithms and observed modality patterns (base clinical variables only; cognitive tests; blood plasma biomarkers; CSF biomarkers; MRI; ERP; and pairwise combinations). Darker cells indicate higher discrimination. (B) Time-dependent Brier score for the ERP and plasma features in the LASSO-Cox model. (C) Cross-validated model performance across penalty strengths for the ERP and plasma features in the LASSO-Cox model. (D) The LASSO penalty selected a sparse subset of non-zero predictors in the ERP-and-plasma

SUPPLEMENTARY DATA

LASSO-Cox model. (E) Predictor importance for the final Cox model, ranked by absolute coefficient: plasma tau/amyloid ratios dominated, followed by sex, WFNS components, selected ERP features, Fisher grade, and aneurysm location. (F) Time-dependent AUC for the exploratory selected Cox submodel showed apparent discrimination peaking around 16–17 months within the same-center sensitivity analysis. Time-dependent AUC [AUC(t)] for the best Cox submodel shows discrimination rising to ~0.85 at 16–17 months and remaining ≥0.70 through ~22 months. (G) Calibration plot at 12 months. Calibration plots at 12 months demonstrate agreement between predicted and observed risk, with wider intervals at extremes. (H) Calibration plot at 18 months. Calibration plots at 18 months demonstrate agreement between predicted and observed risk, with wider intervals at extremes. (I) Decision-curve analysis at 12 months. DCA for 12-month prediction shows positive net benefit across clinically relevant threshold probabilities compared with “treat-all” and “treat-none” strategies. Abbreviations. AUC = area under the receiver-operating characteristic curve; C-index = Harrell’s concordance index; Cox = Cox proportional-hazards model; LASSO = least absolute shrinkage and selection operator (penalized Cox); RSF = random survival forest; XGBoost = extreme gradient boosting (survival variant); SVM = support vector machine (survival variant); DeepSurv = deep neural-network Cox surrogate; ERP = event-related potentials; MRI = magnetic resonance imaging; CSF = cerebrospinal fluid; WFNS = World Federation of Neurological Surgeons grade; DCA = decision curve analysis.

SUPPLEMENTARY DATA

SUPPLEMENTARY DATA

Supplemental figure 7. Time-dependent Brier scores for prediction of cognitive impairment using the Cox model in the Blood dataset.

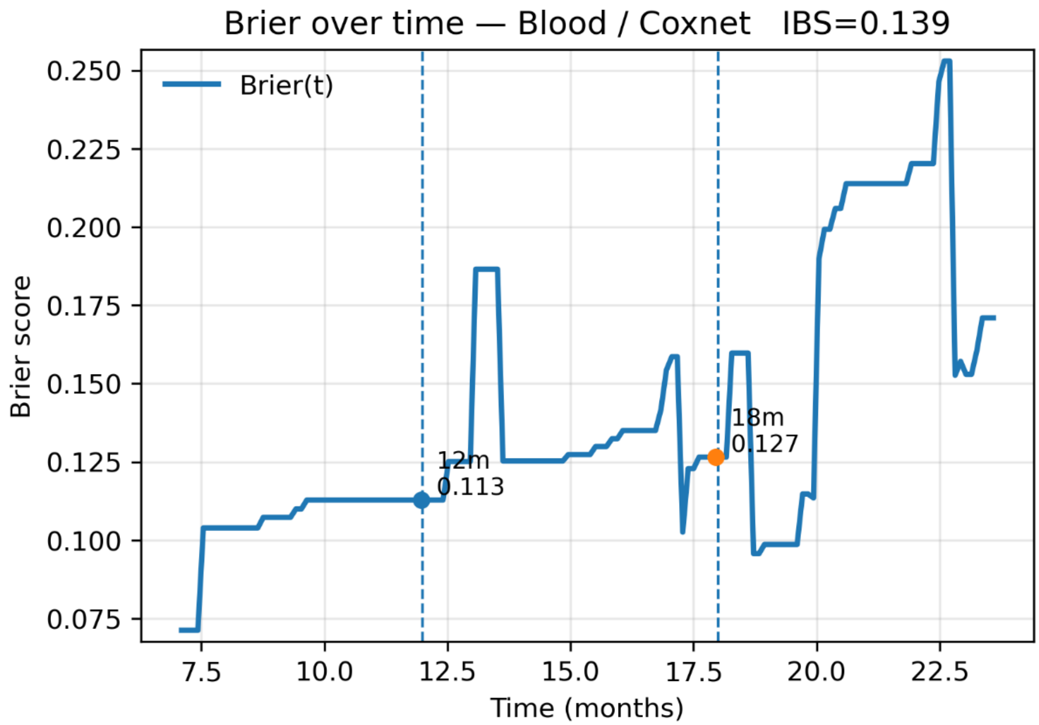

These time-dependent performance analyses were exploratory sensitivity analyses based on same-center data and should not be interpreted as external validation.

SUPPLEMENTARY DATA

Supplemental figure 8. Time-dependent Brier scores for prediction of cognitive impairment using the RSF model in the Blood dataset.

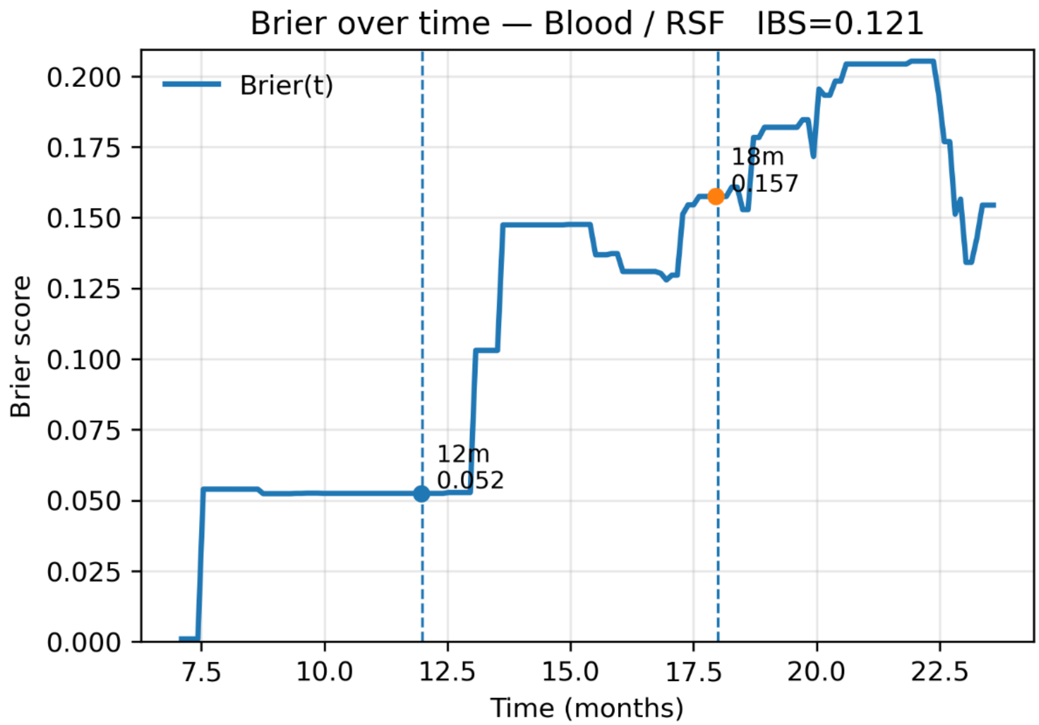

These time-dependent performance analyses were exploratory sensitivity analyses based on same-center data and should not be interpreted as external validation.

SUPPLEMENTARY DATA

Supplemental figure 9. Time-dependent Brier scores for prediction of cognitive impairment using the Cox model in the Cognitive dataset.

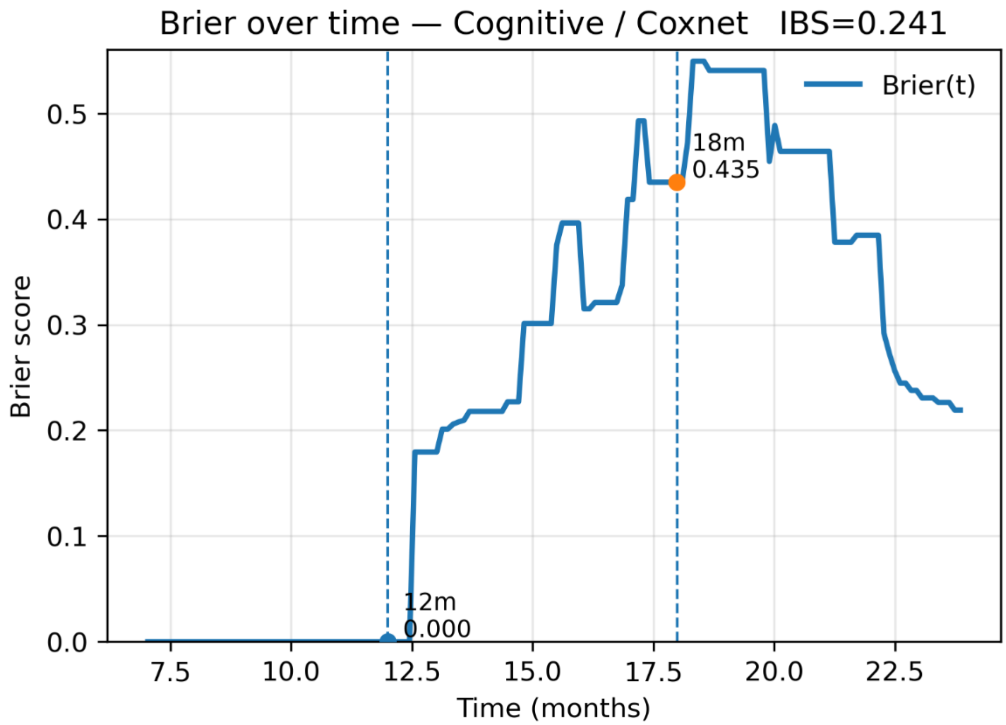

These time-dependent performance analyses were exploratory sensitivity analyses based on same-center data and should not be interpreted as external validation.

Supplemental figure 10. Time-dependent Brier scores for prediction of cognitive impairment using the RSF model in the Cognitive dataset.

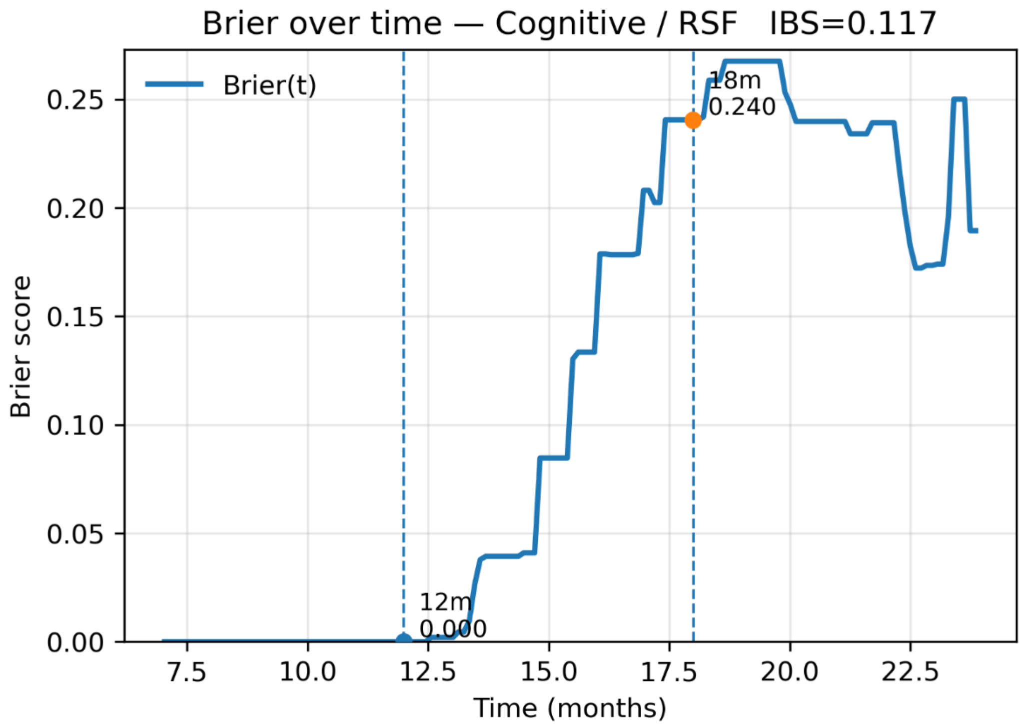

These time-dependent performance analyses were exploratory sensitivity analyses based on same-center data and should not be interpreted as external validation.

SUPPLEMENTARY DATA

Supplemental figure 11. Time-dependent Brier scores for prediction of cognitive impairment using the Cox model in the ERP and blood dataset.

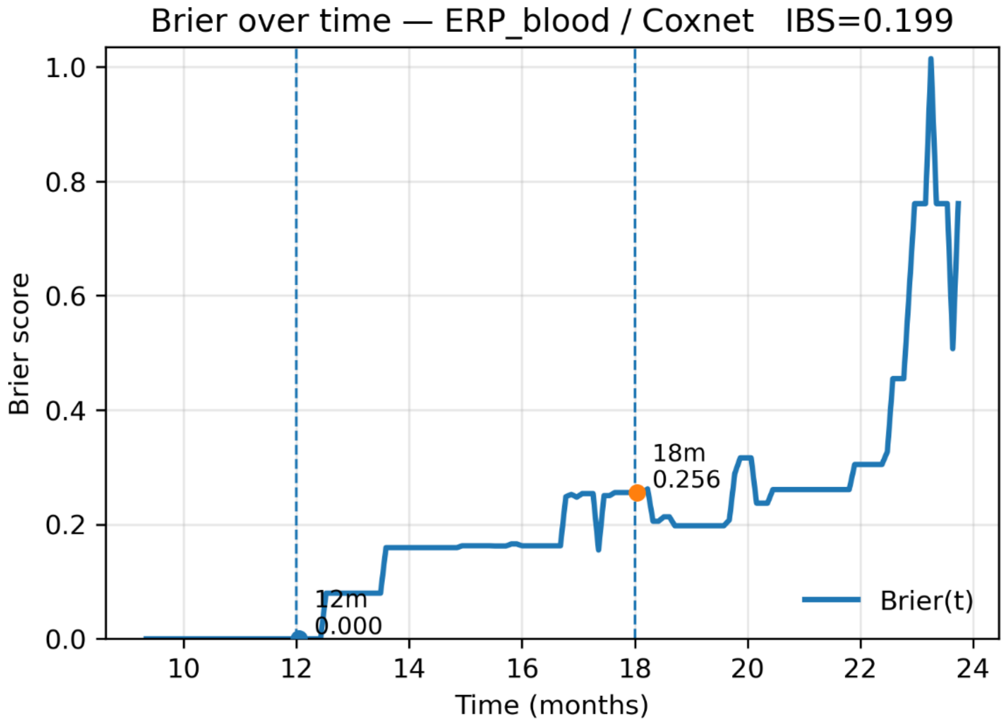

These time-dependent performance analyses were exploratory sensitivity analyses based on same-center data and should not be interpreted as external validation.

Supplemental figure 12. Time-dependent Brier scores for prediction of cognitive impairment using the RSF model in the ERP and blood dataset.

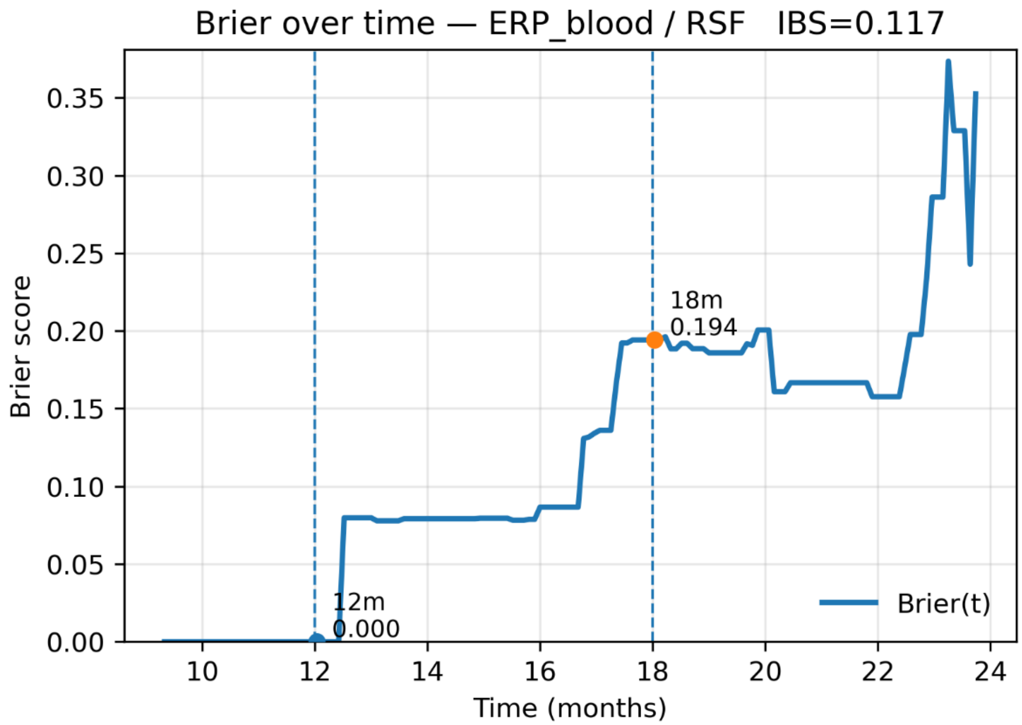

These time-dependent performance analyses were exploratory sensitivity analyses based on same-center data and should not be interpreted as external validation.

SUPPLEMENTARY DATA

Supplemental figure 13. Time-dependent Brier scores for prediction of cognitive impairment using the Cox model in the ERP dataset.

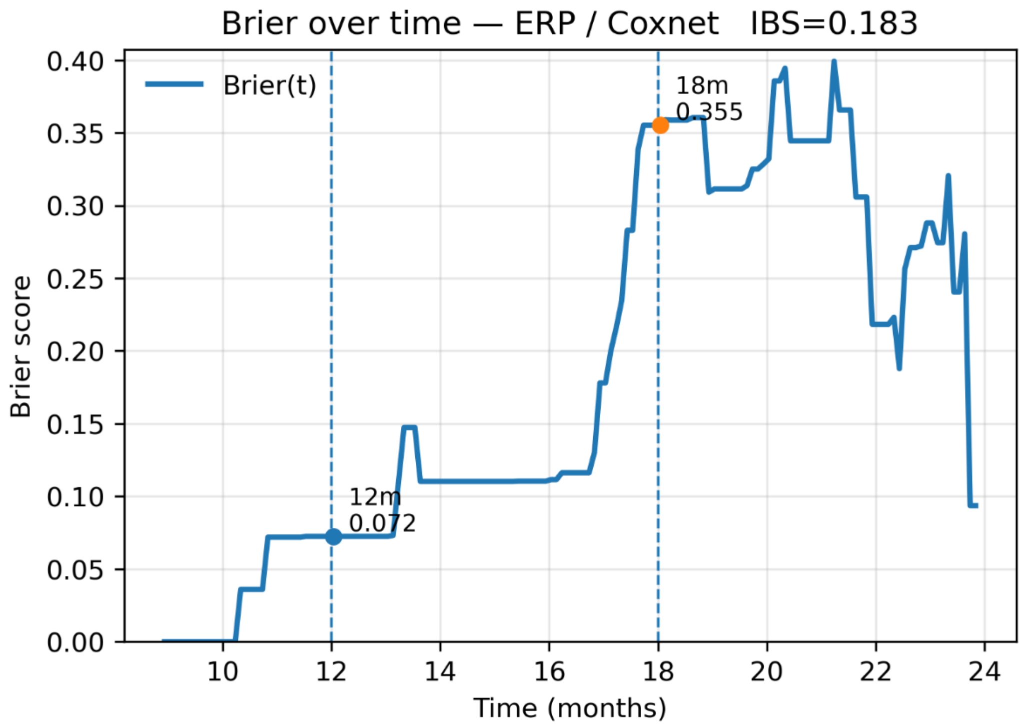

These time-dependent performance analyses were exploratory sensitivity analyses based on same-center data and should not be interpreted as external validation.

SUPPLEMENTARY DATA

Supplemental Figure 14. Time-dependent Brier scores for prediction of cognitive impairment using the RSF model in the ERP dataset.

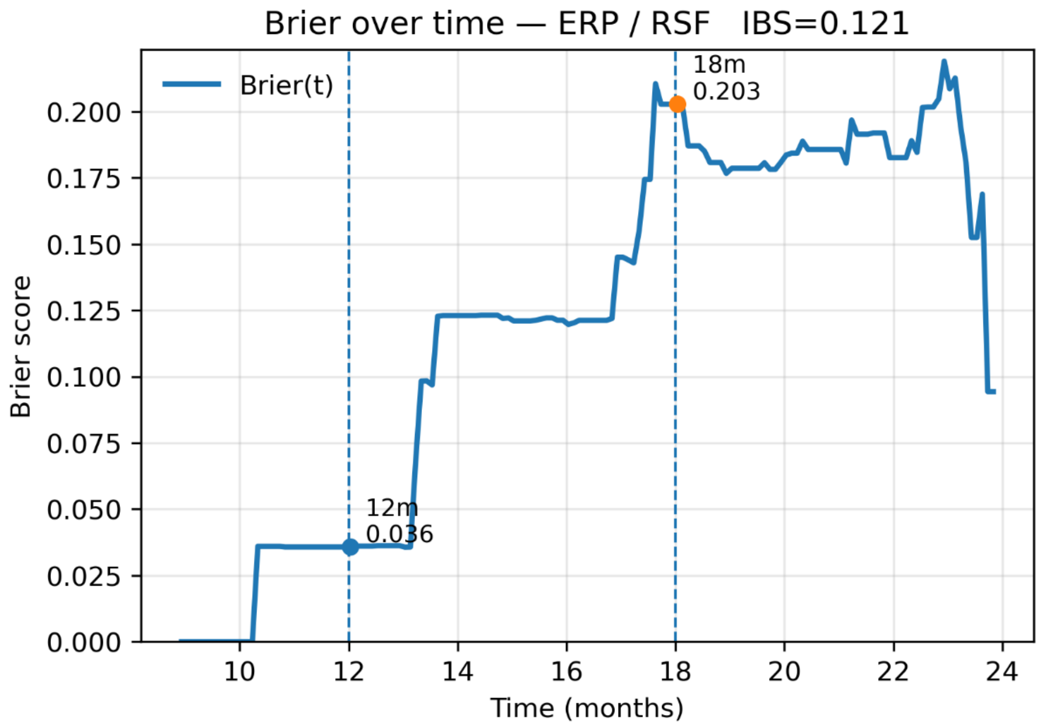

These time-dependent performance analyses were exploratory sensitivity analyses based on same-center data and should not be interpreted as external validation.

SUPPLEMENTARY DATA

Supplemental figure 15. Time-dependent Brier scores for prediction of cognitive impairment using the Cox model in the MRI and blood dataset.

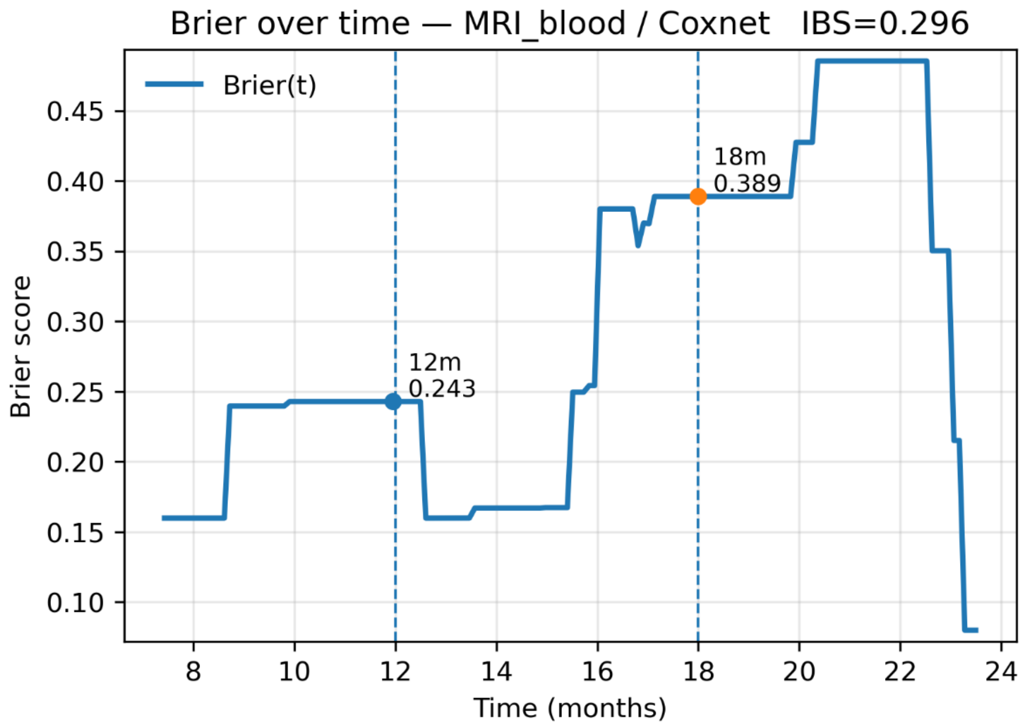

These time-dependent performance analyses were exploratory sensitivity analyses based on same-center data and should not be interpreted as external validation.

Supplemental figure 16. Time-dependent Brier scores for prediction of cognitive impairment using the RSF model in the MRI and blood dataset.

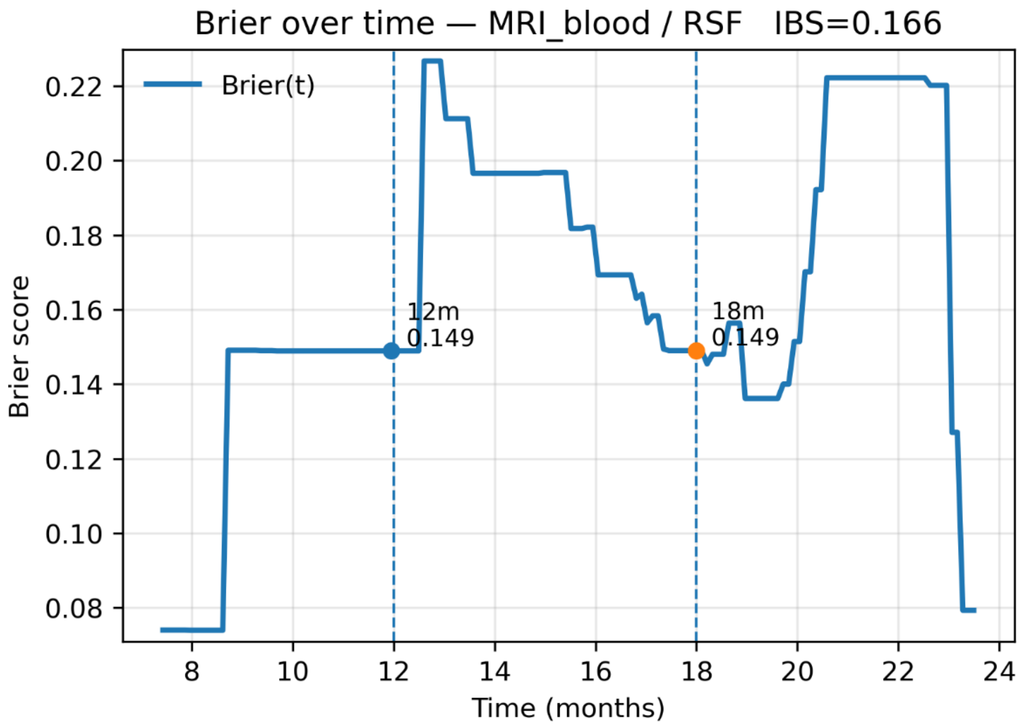

These time-dependent performance analyses were exploratory sensitivity analyses based on same-center data and should not be interpreted as external validation.

Supplemental figure 17. Time-dependent Brier scores for prediction of cognitive impairment using the Cox model in the MRI dataset.

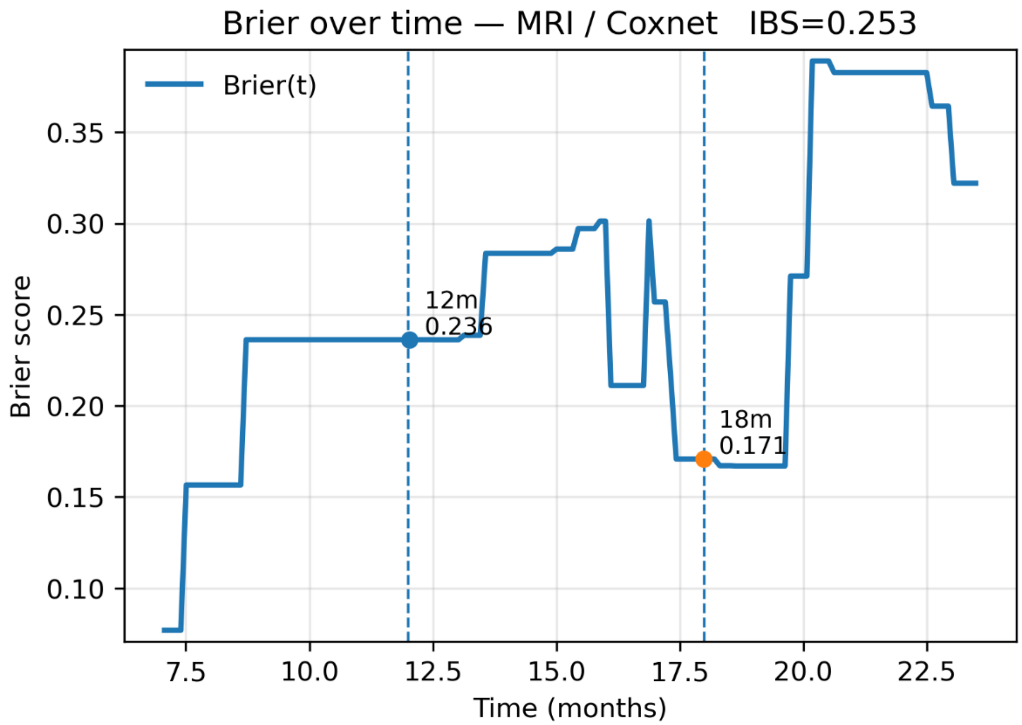

These time-dependent performance analyses were exploratory sensitivity analyses based on same-center data and should not be interpreted as external validation.

SUPPLEMENTARY DATA

Supplemental figure 18. Time-dependent Brier scores for prediction of cognitive impairment using the RSF model in the MRI dataset.

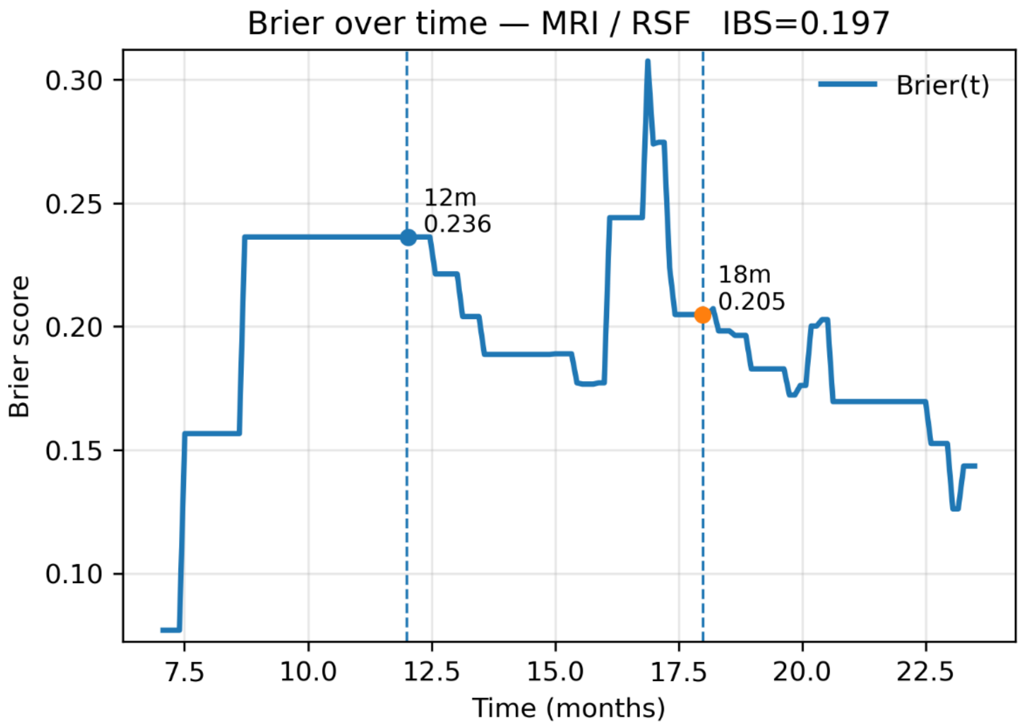

These time-dependent performance analyses were exploratory sensitivity analyses based on same-center data and should not be interpreted as external validation.

SUPPLEMENTARY DATA

Supplemental figure 19. Time-dependent Brier scores for prediction of cognitive impairment using the Cox model in the MRI and ERP dataset.

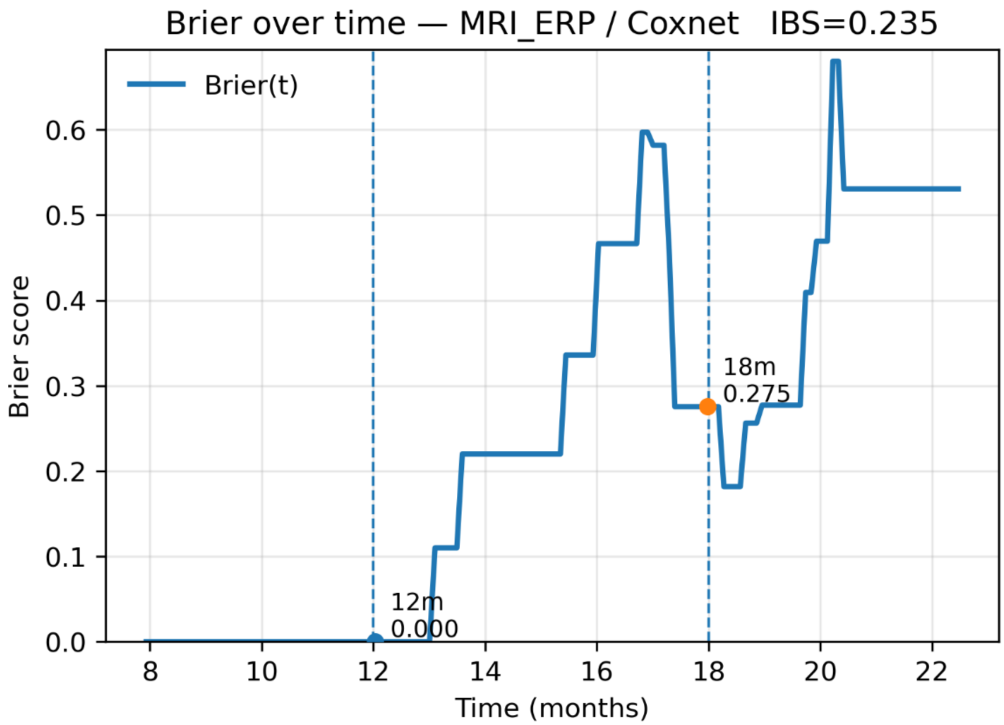

These time-dependent performance analyses were exploratory sensitivity analyses based on same-center data and should not be interpreted as external validation.

SUPPLEMENTARY DATA

Supplemental figure 20. Time-dependent Brier scores for prediction of cognitive impairment using the RSF model in the MRI and ERP dataset.

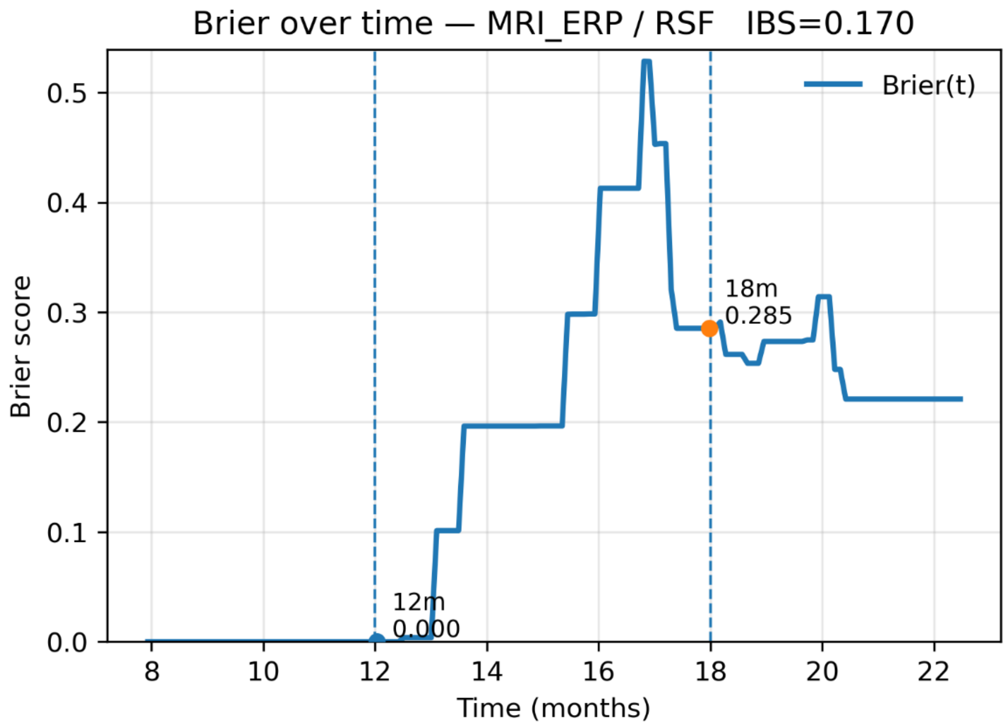

These time-dependent performance analyses were exploratory sensitivity analyses based on same-center data and should not be interpreted as external validation.

SUPPLEMENTARY DATA

Supplemental figure 21. Regularization paths of predictor coefficients in the Base dataset using LASSO-Cox models

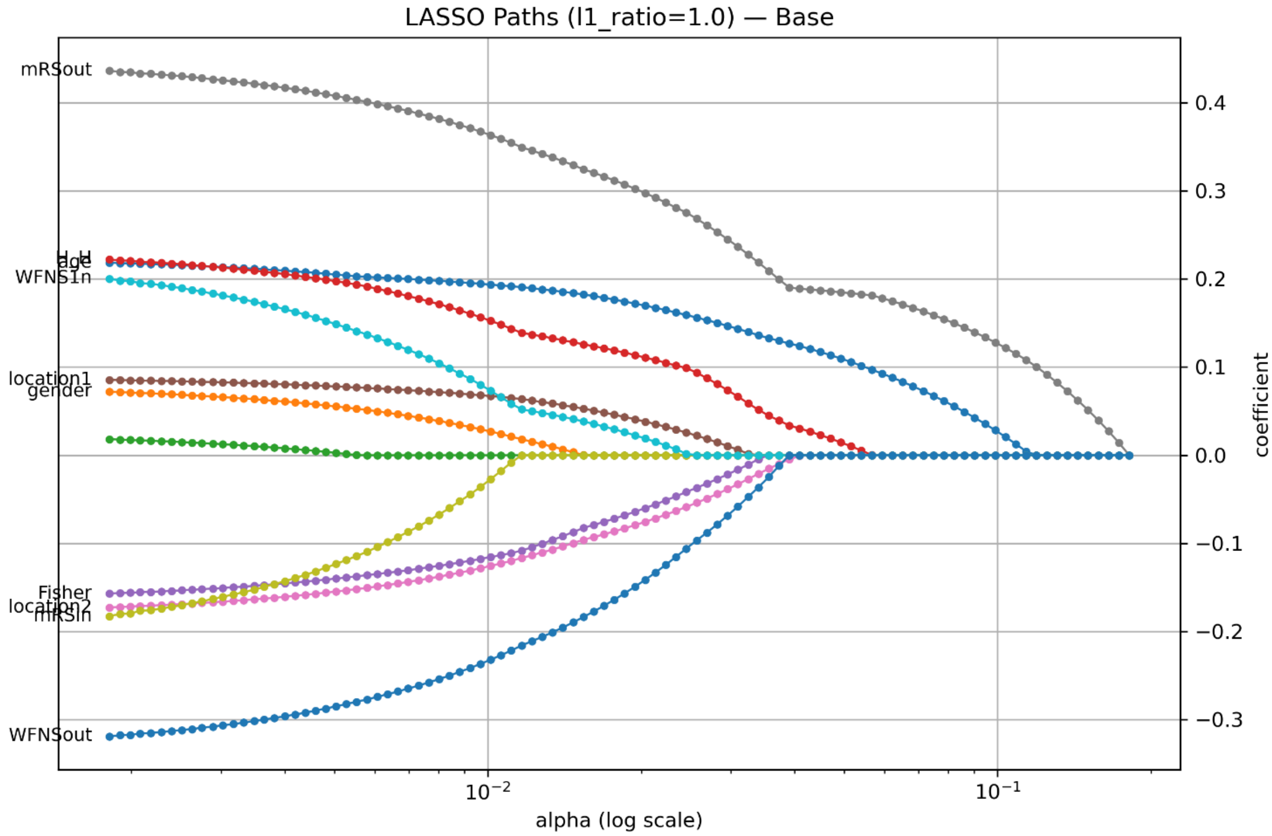

These regularization-path plots are part of the exploratory pattern-submodel survival sensitivity analysis and were not used for primary binary model selection or external validation.

SUPPLEMENTARY DATA

Supplemental figure 22. Regularization paths of predictor coefficients in the Blood dataset using LASSO-Cox models

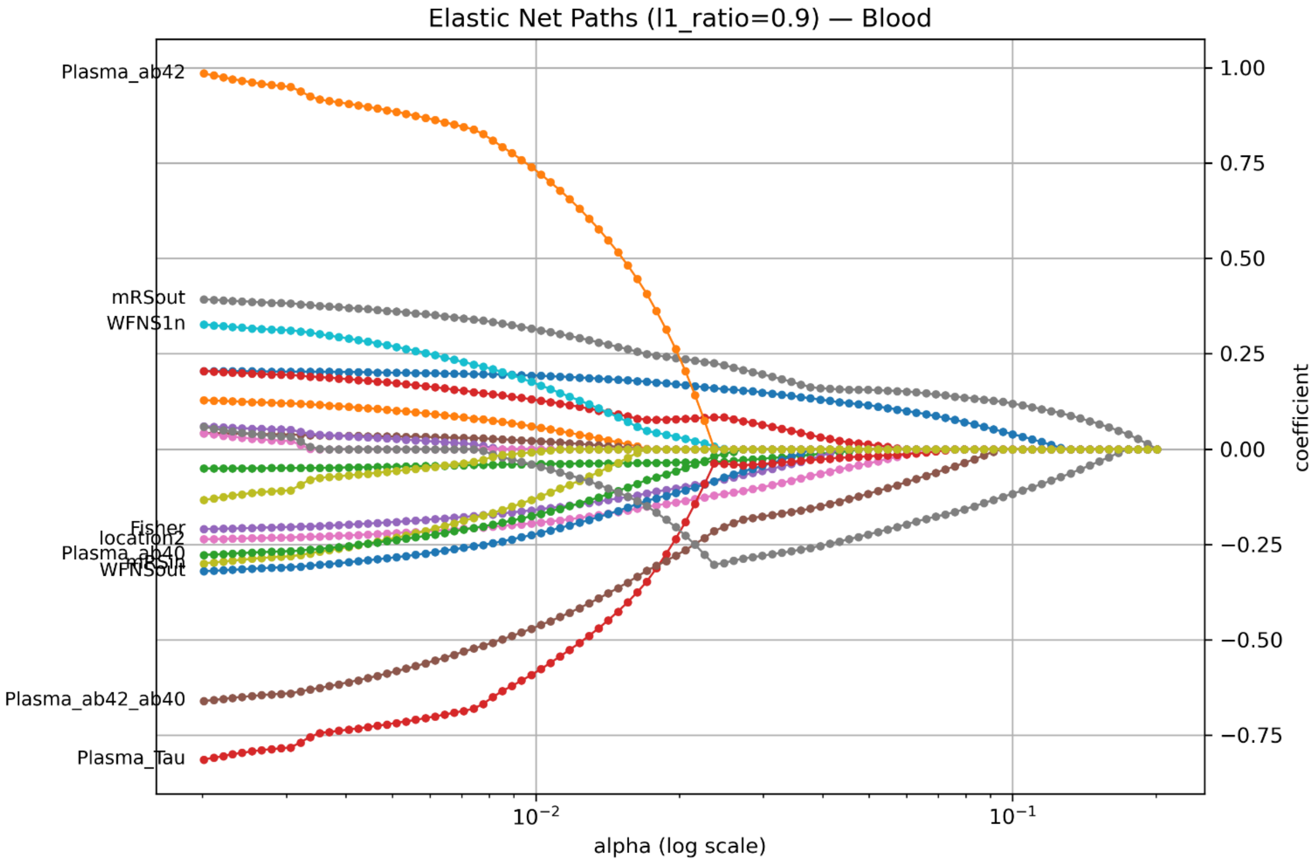

These regularization-path plots are part of the exploratory pattern-submodel survival sensitivity analysis and were not used for primary binary model selection or external validation.

SUPPLEMENTARY DATA

Supplemental Figure 23. Regularization paths of predictor coefficients in the Cognitive dataset using LASSO-Cox models

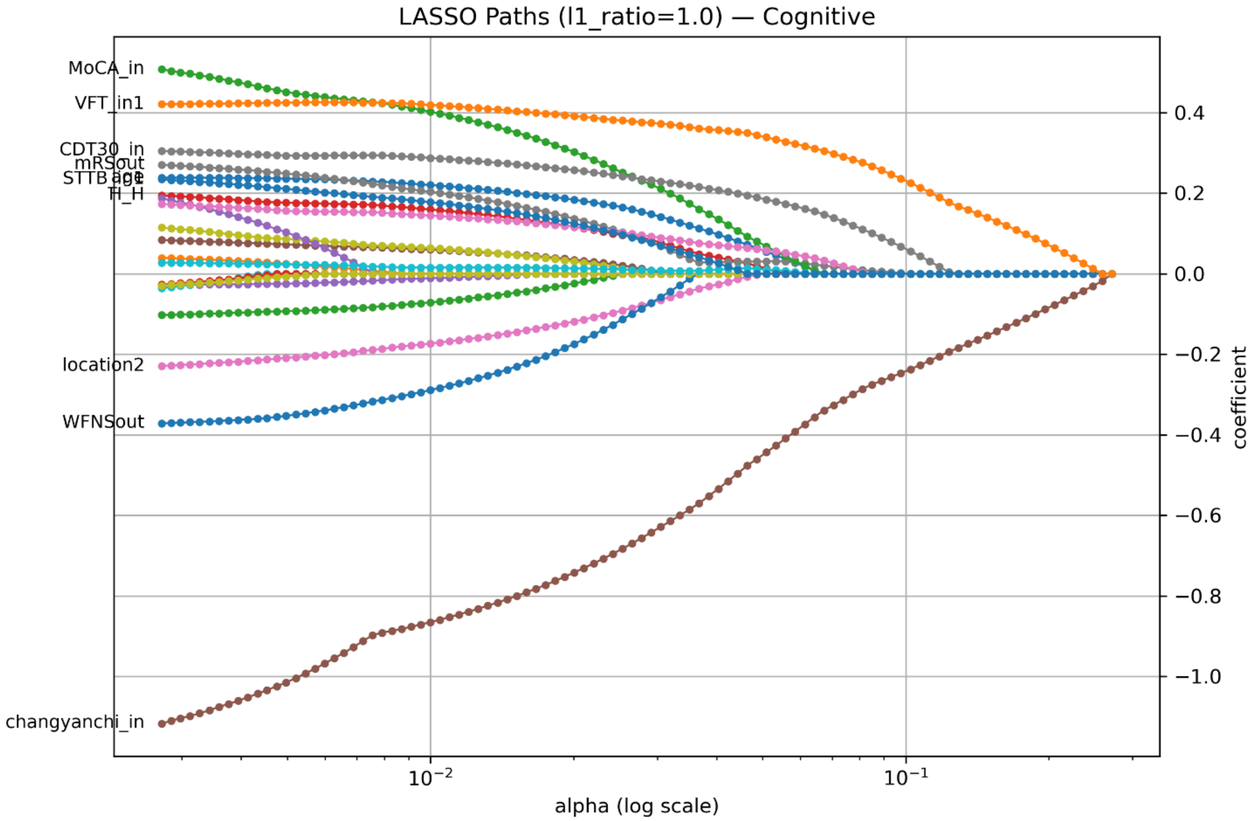

These regularization-path plots are part of the exploratory pattern-submodel survival sensitivity analysis and were not used for primary binary model selection or external validation.

Supplemental figure 24. Regularization paths of predictor coefficients in the ERP and blood dataset using LASSO-Cox models

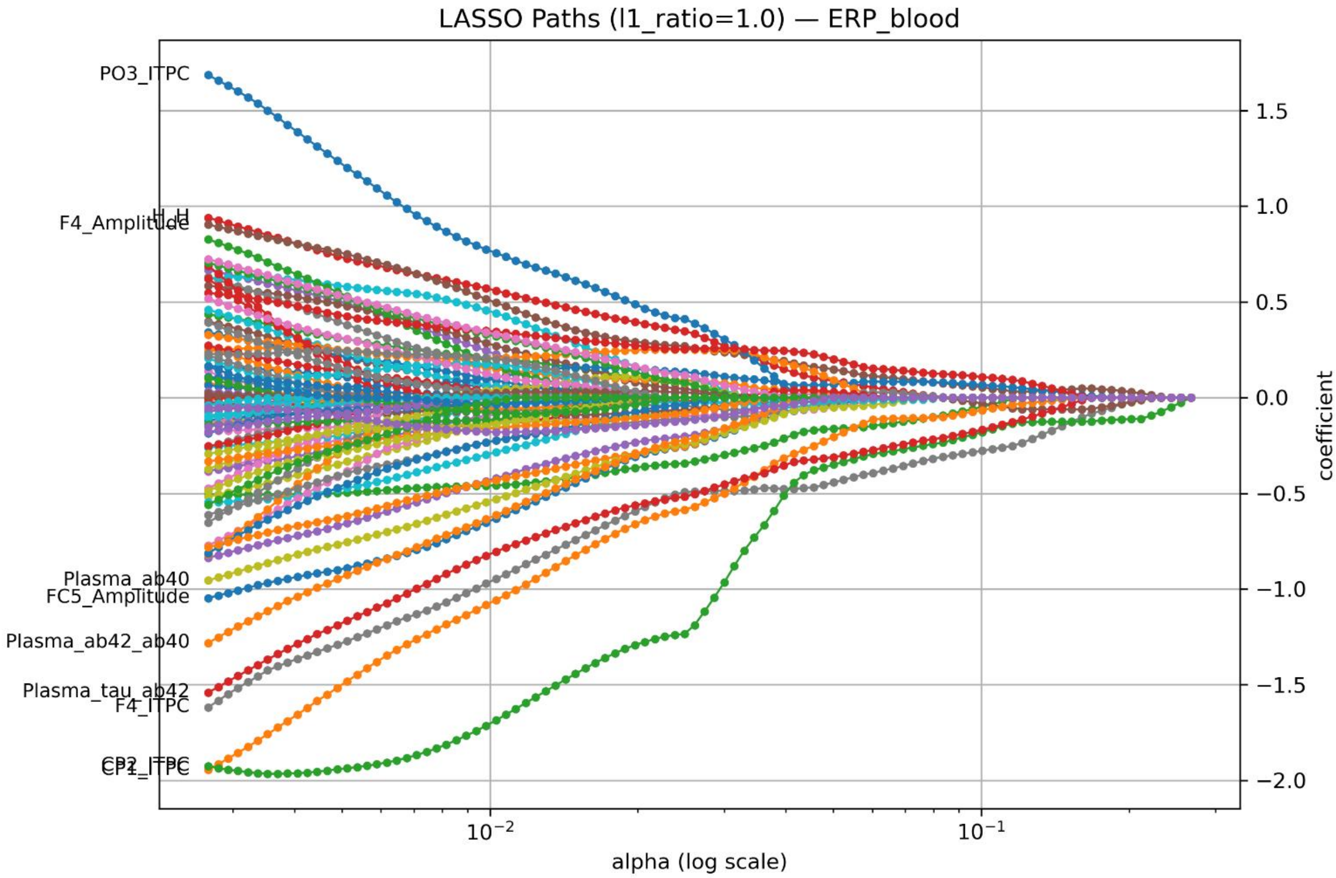

These regularization-path plots are part of the exploratory pattern-submodel survival sensitivity analysis and were not used for primary binary model selection or external validation.

SUPPLEMENTARY DATA

Supplemental figure 25. Regularization paths of predictor coefficients in the ERP dataset using LASSO-Cox models

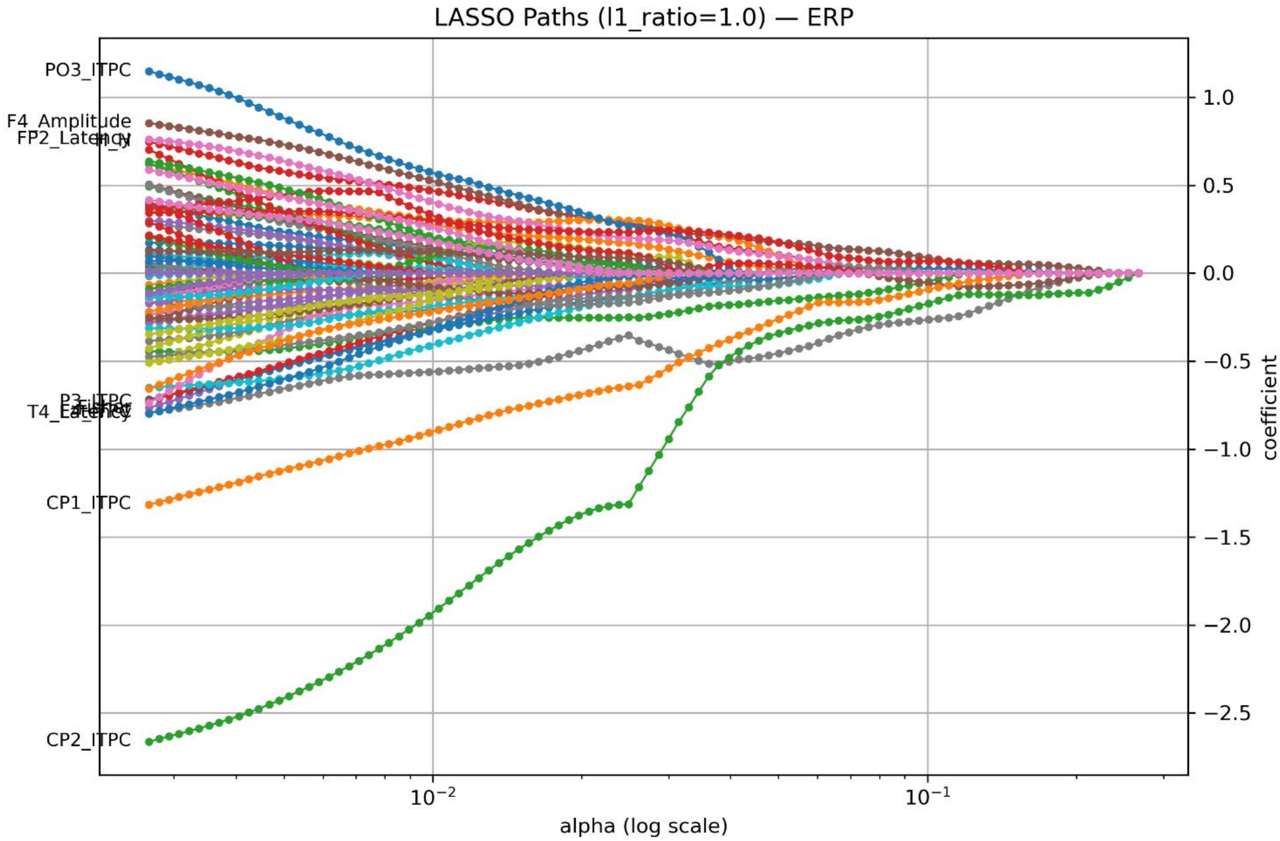

These regularization-path plots are part of the exploratory pattern-submodel survival sensitivity analysis and were not used for primary binary model selection or external validation.

SUPPLEMENTARY DATA

Supplemental figure 26. Regularization paths of predictor coefficients in the MRI and blood dataset using LASSO-Cox models

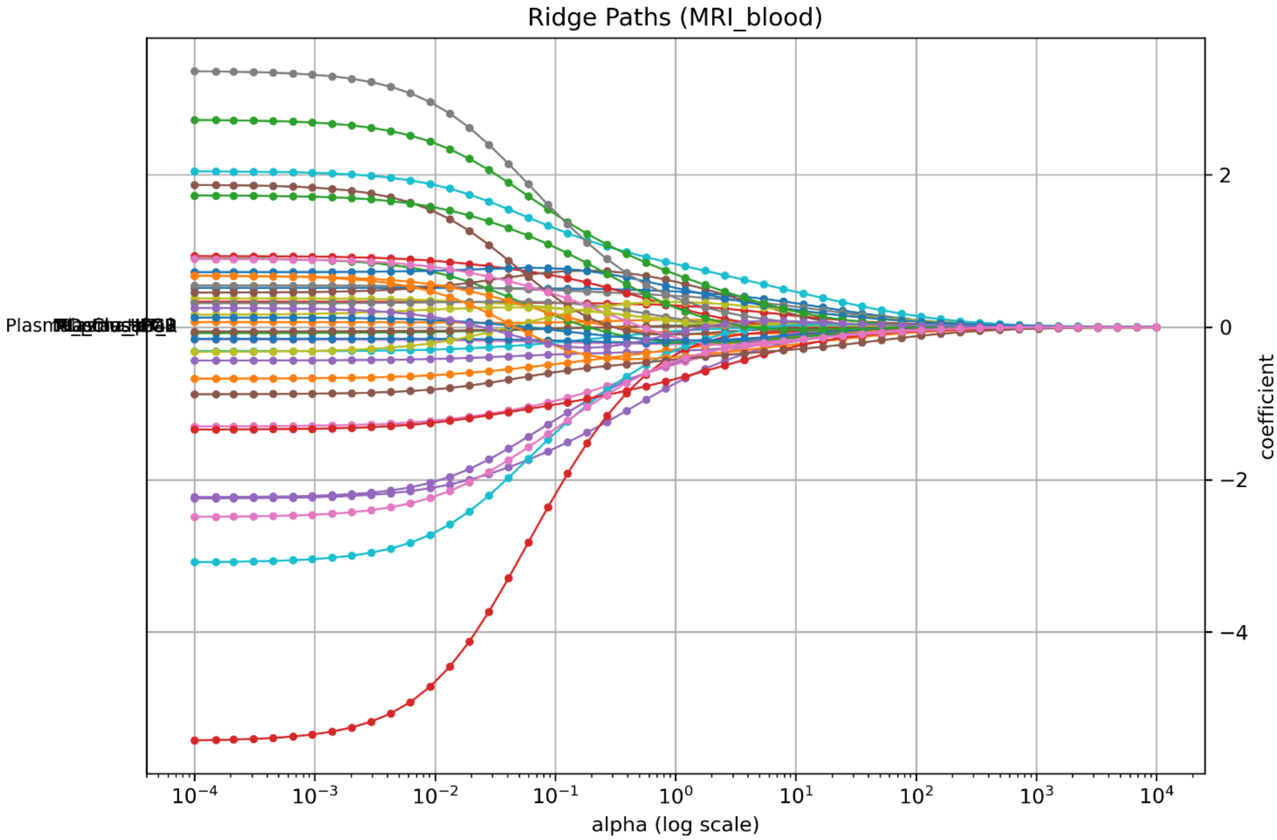

These regularization-path plots are part of the exploratory pattern-submodel survival sensitivity analysis and were not used for primary binary model selection or external validation.

SUPPLEMENTARY DATA

Supplemental figure 27. Regularization paths of predictor coefficients in the MRI and ERP dataset using LASSO-Cox models

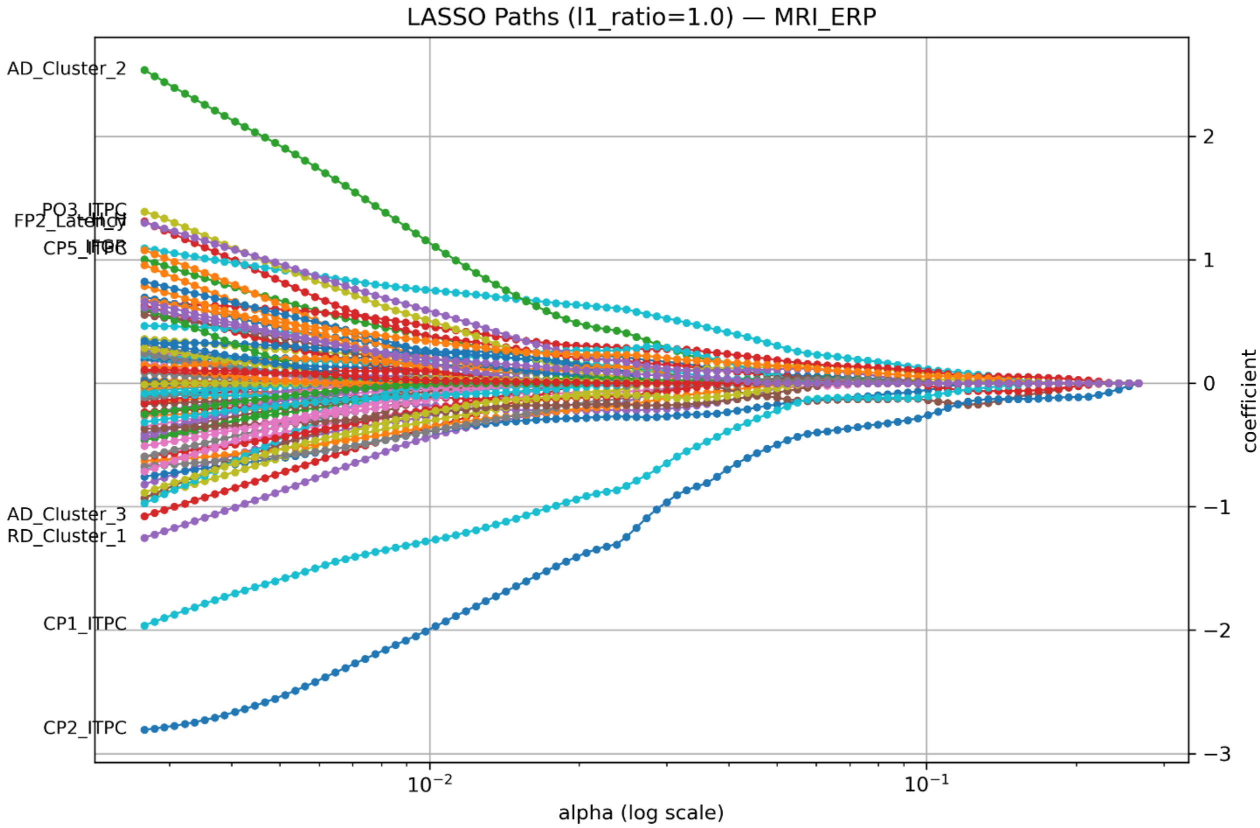

These regularization-path plots are part of the exploratory pattern-submodel survival sensitivity analysis and were not used for primary binary model selection or external validation.

SUPPLEMENTARY DATA

Supplemental figure 28. Regularization paths of predictor coefficients in the MRI dataset using LASSO-Cox models

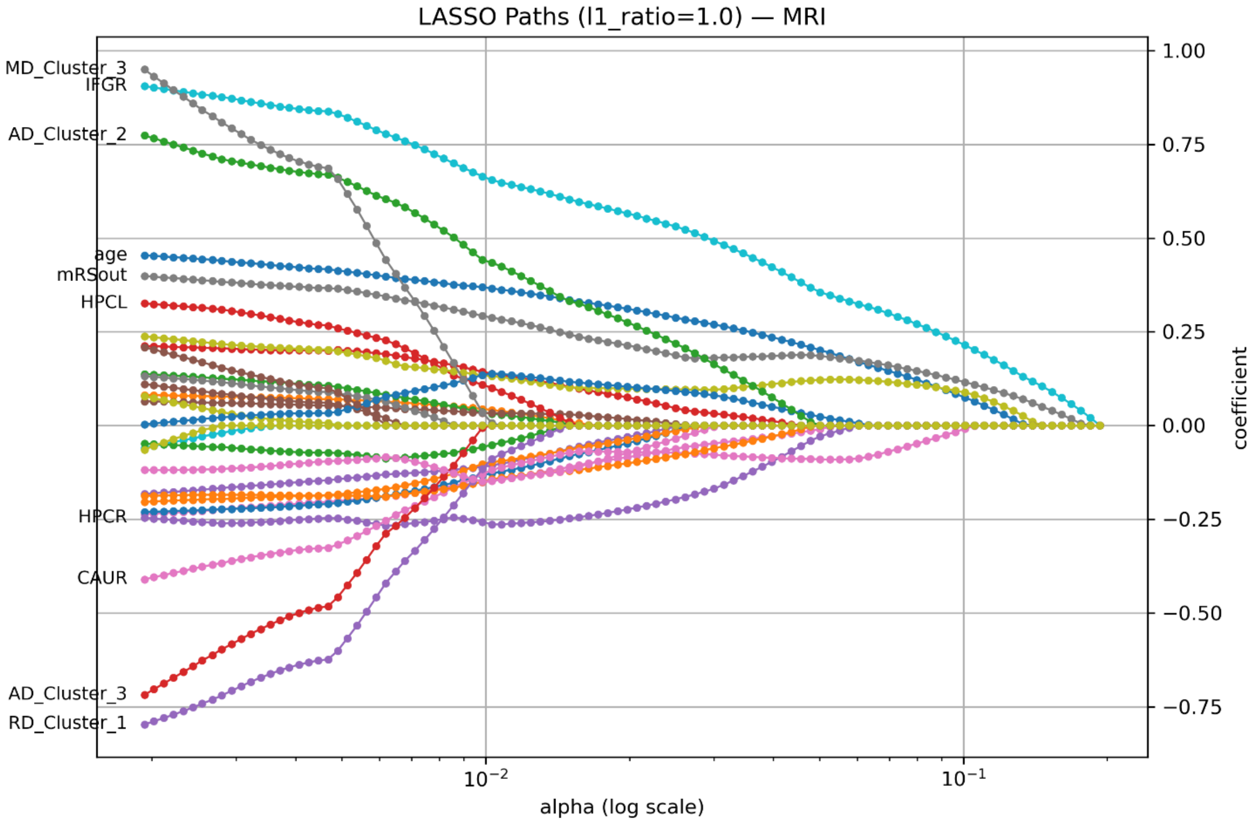

These regularization-path plots are part of the exploratory pattern-submodel survival sensitivity analysis and were not used for primary binary model selection or external validation.

Supplemental figure 29. Sensitivity analysis using the conservative endpoint of education-adjusted MoCA <23.

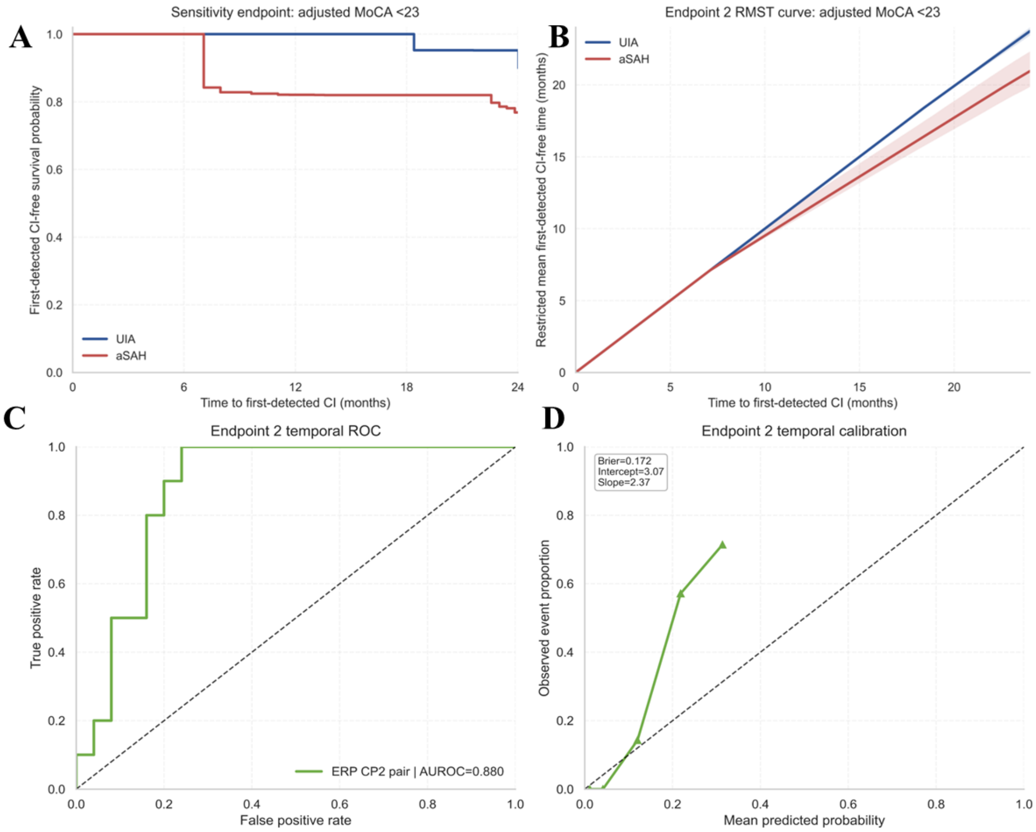

(A) Turnbull interval-censored first-detected CI-free survival curves using the conservative endpoint of education-adjusted MoCA <23. (B) Restricted mean first-detected CI-free time up to 24 months, with shaded areas representing 95% bootstrap confidence intervals from 1,000 resamples. (C) Temporal internal validation ROC curve for the prespecified ERP CP2 pair model under the conservative endpoint. (D) Grouped calibration plot for the prespecified ERP CP2 pair model under the conservative endpoint. The model structure and predictors were prespecified from the primary analysis and were re-evaluated without repeating feature selection. CI = cognitive impairment; MoCA = Montreal Cognitive Assessment; RMST = restricted mean survival time; AUROC = area under the receiver-operating-characteristic curve; ERP = event-related potential.